UNIVERSITY OF CALIFORNIA, SAN DIEGO

The Role of microRNA in Myogenesis and Rhabdomyosarcoma

A dissertation submitted in partial satisfaction of the
requirements for the degree Doctor of Philosophy

in

Biomedical Sciences

by

Shannon E. Muir

Committee in charge:

Professor Karen Arden Chair
Professor Web Cavenee, Co-Chair
Professor Frank Furnari
Professor Xiang-Dong Fu
Professor Amy Pasquinelli
Professor Eugene Yeo

2014

The Dissertation of Shannon E. Muir is approved, and it is acceptable in quality and form for publication on microfilm and electronically:

Co- Chair

Chair

University of California, San Diego

2014

DEDICATION

For Jacom Derick Larson

August 28th, 1978 - October 21st, 2008

TABLE OF CONTENTS

LIST OF FIGURES

LIST OF TABLES

ACKNOWLEDGEMENTS

Chapters 2, 3, and 4 are currently being prepared for submission as a publication. Muir, Shannon; Wilbert, Melissa; Nathanson, Jason; Yeo, Gene W.; Furnari, Frank; Cavenee, Webster; Arden, Karen C. The dissertation author was the primary investigator and author of this material.

VITA

EDUCATION

University of California, San Diego, Ludwig Institute for Cancer Research
Doctor of Philosophy, Biomedical Sciences **2014**
Dissertation: The role of microRNA in Myogenesis and Rhabdomyosarcoma
Advisors: Frank Furnari PhD, Webster Cavenee PhD, Karen Arden PhD

Tulane University School of Medicine
Master of Science, Pharmacology **2008**
Thesis: A comparison of SDF-1 Regulation of breast cancer tumorigenesis through chemokine receptors CXCR4 and CXCR7.
Advisor: Matthew Burow, PhD

University of California, Los Angeles
Bachelor of Science, Psychobiology **2004**

AWARDS

UC Student Association Advocate of the Year **2012**

Rare Diseases Science Challenge: Be HEARD Award Winner, $10,000 in donated karyotyping services **2013**

NIH Predoctoral Training Grant, Pharmacological Science **2008-2009**

EXPERIENCE

University of California, San Diego, Ludwig Institute for Cancer Research
PhD Student, Biomedical Sciences **2008-2014**

- Used high-throughput small RNA sequencing to compare miRNA profiles between cancerous and noncancerous human cell lines
- Advanced to candidacy in August, 2011
- Teaching Assistant: Compounding Pharmacology
- Rotated in Roger Tsien's lan working on phage display technology for thrombosis
- Rotated in Kenneth Kaushansky's lab studying thrombopoietin and hematopoiesis
- Biomedical Sciences representative to the UC San Diego Graduate Student Association, 2010-2011

University of California Academic Senate

Graduate Student Representative, Committee on Research Policy **2013-2014**

- Fostered, formulated, coordinated and revised general research policies and procedures, and advised the UC Office of the President on research matters affecting the University

University of California San Diego Graduate Student Association

Legislative Liaison for Local & State Affairs **2011-2013**

- Member of the Board of Directors for the University of California Student Association (UCSA)
- Chair, Graduate and Professional Student Committee, UCSA
- Legislative Committee member, UCSA
- Provided legislative analysis and authored several resolutions in support of or opposition to Senate and Assembly bills on behalf of UCSA
- Lobbied elected representatives on issues related to higher education including quality, access, and affordability
- Worked with the University of California Office of the President and the Regents of the UC to lobby the California Legislature to maintain funding for the UC during economic downturn
- Co-Chaired a 4 day conference for over 400 students to educate them about current issues facing higher education, and empower them to advocate on their own behalf
- Lead voter registration drives and voter education initiatives, as well as the Get Out the Vote campaign for UCSD Graduate Students
- Coordinated the San Diego Mayoral Debate of 2012 held at UC San Diego
- Led a state-wide, coordinated campaign across all ten UC campuses to increase student representation on the UC Board of Regents

Tulane University School of Medicine

Medical Research Specialist **2007-2008**

- Analyzed cell signaling pathways in breast cancer tumor growth and metastasis using xenograft tumors in immunocompromised mice.
- Injected mice with cells interperitoneally, subcutaneously, or via tail vein, inserted drug pellets, and took detailed measurements of tumors, followed by post-mortem dissection and analysis
- Built and maintained databases, and performed data collection, entry, and organization
- Presented a poster at the 2008 American Association for Cancer Research meeting

SRI International

Research Analyst **2004-2005**

- Investigated the link between AIDS, Alcoholism, and the central nervous system, focusing on frontal lobe and corpus callosum dysfunction
- Managed human subject HIPAA compliance
- Administered neuropsychological tests to human subjects, then scored and recorded them
- Organized and maintained databases and prepared data sets to be analyzed
- Coordinated blood draws with nurses and diagnostic interviews with staff Psychologists
- Performed MRI scans on human and rodent subjects
- Maintained a rodent population and collected dietary and behavioral data

UCLA Department of Psychology

Research Assistant **2003-2004**

- Performed psychological experiments investigating Post Traumatic Stress Disorder and Major Depression, and the biochemical links to glucose, adenosine, and cytokine responses
- In charge of the systematic and precise drug injection of rats using either tail or interperitoneal injections, or stereotaxic infusions directly into the hippocampus

PUBLICATIONS

- Glyceollins as a novel targeted therapeutic for the treatment of triple-negative breast cancer. Rhodes LV, Tilghman SL, Boue SM, Wang S, Khalili H, **Muir SE**, Bratton MR, Zhang Q, Wang G, Burow ME, Collins-Burow BM. Oncology Letters 2012 Jan;3(1):163-171.
- Effects of SDF-1-CXCR4 signaling on microRNA expression and tumorigenesis in estrogen receptor-alpha (ER-α)-positive breast cancer cells. Rhodes LV, Bratton MR, Zhu Y, Tilghman SL, **Muir SE**, Salvo VA, Tate CR, Elliott S, Nephew KP, Collins-Burow BM, Burow ME. Exp Cell Res. 2011 Nov 1;317(18):2573-81.
- Cytokine receptor CXCR4 mediates estrogen-independent tumorigenesis, metastasis, and resistance to endocrine therapy in human breast cancer. Rhodes LV, Short SP, Neel NF, Salvo VA, Zhu Y, Elliott S, Wei Y, Yu D, Sun M, **Muir SE**, Fonseca JP, Bratton MR, Segar C, Tilghman SL, Sobolik-Delmaire T, Horton LW, Zaja-Milatovic S, Collins-Burow BM, Wadsworth S, Beckman BS, Wood CE, Fuqua SA, Nephew KP, Dent P, Worthylake RA, Curiel TJ, Hung MC, Richmond A, Burow ME. Cancer Res. 2011 Jan 15;71(2):603-13.Erratum in: Cancer Res. 2011 May 1;71(9):3432.
- Effects of human mesenchymal stem cells on ER-positive human breast carcinoma cells mediated through ER-SDF-1/CXCR4 crosstalk. Rhodes LV, Antoon JW, **Muir SE**, Elliott S, Beckman BS, Burow ME. Mol Cancer. 2010 Nov 18;9:295.
- Antiestrogenic effects of the novel sphingosine kinase-2 inhibitor ABC294640. Antoon JW, White MD, Meacham WD, Slaughter EM, **Muir SE**, Elliott S, Rhodes

LV, Ashe HB, Wiese TE, Smith CD, Burow ME, Beckman BS. Endocrinology. 2010 Nov;151(11):5124-35.

- Adult human mesenchymal stem cells enhance breast tumorigenesis and promote hormone independence. Rhodes LV, **Muir SE**, Elliott S, Guillot LM, Antoon JW, Penfornis P, Tilghman SL, Salvo VA, Fonseca JP, Lacey MR, Beckman BS, McLachlan JA, Rowan BG, Pochampally R, Burow ME. Breast Cancer Res Treat. 2010 Jun;121(2):293-300.
- Human uterine smooth muscle and leiomyoma cells differ in their rapid 17beta-estradiol signaling: implications for proliferation. Nierth-Simpson EN, Martin MM, Chiang TC, Melnik LI, Rhodes LV, **Muir SE**, Burow ME, McLachlan JA. Endocrinology. 2009 May;150(5):2436-45. Epub 2009 Jan 29.

POSTERS

- The role of microRNA in PA3FOXO1A positive rhabdomyosarcoma. **Muir SE**, Nathanson J, Wilbert M, Yeo G, Furnari F, Cavenee W, Arden KC. American Association for Cancer Research Annual Meeting 2014, San Diego, Ca.
- Adult human mesenchymal stem cells enhance breast cancer tumorigenesis and promote hormone independence. Rhodes LV, **Muir SE**, Elliott S, Guillot LM, Antoon JW, Penfornis P, Tighlman SL, McLachlan JA, Rowan BG, Pochampallil R, Burow ME. American Association for Cancer Research Annual Meeting 2008, San Diego, Ca.
- Inhibition of p38 mitogen-activated protein kinase signaling suppresses estrogen receptor-positive breast cancer tumorigenesis. Guillot M, Bratton M, Fonseca JP, **Muir SE**, Rhodes LV, Salvo VA, Elliott S, Rowan BG, McLachlan JA, Beckman BS, Wadsworth S, Curiel TJ, Burow ME. American Association for Cancer Research Annual Meeting 2008, San Diego, Ca.
- The Chemokine receptor CXCR7 mediates estrogen-stimulated breast cancer tumorigenesis. **Muir SE**, Rhodes LV, Zhu Y, , Salvo VA, Elliott S, Guillot LM, Fonseca JP, McLachlan JA, Barnett B, Beckman BS, Curiel TJ, Burow ME. American Association for Cancer Research Annual Meeting 2008, San Diego, Ca.
- Effect of Novel Sphingosine Kinase Inhibitors on Estrogen Receptor in Endocrine Sensitive and Endocrine Resistant Breast Cancer. Meacham WD, Antoon JW, Burow ME, Smith CD, Slaughter EM, Rhodes LV, **Muir SE**, Guillot LM, Bratton MR, Beckman BS. Tulane University Health Sciences Center Research Days, March 2008.
- Glyceollins (I-III), novel anti-estrogenic phytochemicals isolated from soy. Collins-Burow BM, Boue, SM, **Muir SE**, Rhodes LV, Guillot LM, Zimmermann MC, Salvo, VA, Fonseca JP, Elliott S, Payton FL, Shih BY, Carter-Wientjes C, Wood C, Beckman BS, McLachlan JA, Cleveland TE, Burow ME. Southern Societies Regional Meeting, New Orleans, LA February 23rd, 2008.
- Contribution of the corpus callosum to visual conjunction search: influence of age and sex. E.M. Muller-Oehring EM, Schulte T, McCloskey C, **Muir SE**, Pfefferbaum A, Sullivan EV. Neuroscience Conference, Oct. 2006.

VOLUNTEER WORK

Ostional Turtle Refuge, Guanacaste, Costa Rica **2013**

- Worked as a volunteer team leader with biologists and trained personnel to help conserve endangered Olive Ridley and Leatherback turtles, and conducted esearch related to sand microbial populations and turtle hatching success

MEMBERSHIPS

American Society of Human Genetics **2013-current**

American Association of Cancer Research **2014-current**

ABSTRACT OF THE DISSERTATION

The role of microRNA in Myogenesis and Rhabdomyosarcoma

by

Shannon E. Muir

Doctor of Philosophy in Biomedical Sciences

University of California, San Diego, 2014

Professor Karen Arden, Chair
Professor Webster Cavenee, Co-Chair

Rhabdomyosarcoma is the most commonly diagnosed pediatric soft tissue carcinoma and involves cells in the skeletal muscle lineage. The disease is classified into

two main subtypes: embryonal rhabdomyosarcoma (ERMS) which is associated with a more favorable clinical outcome, and the less common alveolar rhabdomyosarcoma (ARMS) which has higher rates of metastasis, drug resistance, recurrence, mortality, and an overall poorer prognosis. Most ARMS tumors are characterized by a t(2;13)(q35;q14) chromosomal translocation that produces a fusion protein from the embryogenesis-associated gene PAX3 and FOXO1a. The chimeric protein PAX3-FOXO1a acts as a transcription factor capable of inhibiting myoblast differentiation, however, the complexity of myogenesis suggests multigenic regulation.

The present goal is to determine the role of miRNAs in the etiology of rhabdomyosarcoma and the regulation of myogenesis by taking a more comprehensive approach. In this study, we use RNA-sequencing-based technology to assess the miRNA expression profiles of rhabdomyosarcoma cell lines (RD and Rh30) that are either positive or negative for the PAX3-FOXO1a fusion protein, and compare the profiles to those of undifferentiated and differentiated primary skeletal muscle cells. Additionally, we define the impact PAX3-FOXO1a has on expression of specific miRNAs by modulating fusion protein levels in tumor cell lines.

CHAPTER 1- INTRODUCTION

Rhabdomyosarcoma (RMS) is unique in that, unlike other cancers, it can arise almost anywhere in the body (Ries, et al, 1999b). The unifying characteristic of the tumors is that they express molecular markers in a pattern similar to that of undifferentiated skeletal muscle cells (Wachtel, et al, 2006). In an effort to shed light on the mechanisms of rhabdomyosarcoma, we will compare RMS cells to those of normal skeletal muscle cells. A review of normal skeletal muscle differentiation will provide background information necessary for an in-depth discussion. RMS is also unique in that some tumors harbor a chromosomal translocation that yields the novel protein PAX3-FOXO1a. As of yet, no one has examined the effect of fusion protein expression on non-coding regulatory miRNAs. This chapter will serve an introduction to some of the key concepts and players presented throughout the dissertation.

MYOGENESIS

Myogenesis is the process by which undifferentiated cells become differentiated, functional muscle (Figure 1). Human embryonic myogenesis occurs when cells in the gastrula split into the exoderm, which gives rise to the central nervous system and outer skin; the endoderm, which forms the gastrointestinal and respiratory systems; and the mesoderm, from which the circulatory system, bones, muscles, and gonads will arise. From that point, the mesoderm further differentiates into the notochord (a transient, embryological structure), and the somites. Somites are the progenitors of the excretory system, sex organs, skeletal muscles, and the smooth muscles that line the digestive tract. Specific cells in the somites, collectively called

the dermomyotome, contain muscle precursor cells, or myoblasts, which are committed to the skeletal muscle cell lineage with few exceptions (For review, see (Solnica-Krezel and Sepich, 2012).

Morphologically, over the course of myogenesis myoblasts transform from an archetypal cellular shape to long, multinucleated, mature muscle cells (Figure 1). Embryonic myoblasts proliferate to generate sufficient numbers of cells, then exit the proliferative cycle and form myotubes by fusing together. The myotubes align and mature into myocytes, also called myofibers or muscle fibers. The myocytes are composed of several myofibrils, which in turn contain bundles of filaments, which are responsible for canonical skeletal muscle contraction (For review, see (Bentzinger, et al, 2012).

Maturation of myoblasts into functioning muscle cells depends on complex and timely coordination of several growth factors and regulators, both from the myoblasts themselves, and extracellular influences. Chief among the intrinsic factors are a family of transcription factors that all contain a basic-helix-loop-helix (bHLH) motif, which facilitates DNA binding. These myogenic bHLH proteins, MyoD, Myogenin (or Myf4), Myf5, and Mrf4 (or Myf6), form heterodimers with E-proteins and bind to E-box sequences in regulatory sites of genes, initiating transcription of muscle-specific genes such as those needed for contraction (Santoro, et al, 1991,Braun and Arnold, 1991).

Although the details of myogenesis vary according to skeletal muscle region, it can generally be stated that myogenic regulatory factors are themselves regulated by

each other and by transcription factors like PAX3 which induces MyoD expression, and PAX7 (Figure 2) (Bober, et al, 1994). PAX3 directly targets *Myf5* (Bajard, et al, 2006), but PAX3 and PAX7 seem to indirectly control expression of the other myogenic proteins (Tajbakhsh, et al, 1997). MyoD is also upregulated by Mrf4 and Myf5 (Kassar-Duchossoy, et al, 2004), (Tajbakhsh, et al, 1997). MyoD promotes its own transcription in a feedback loop, as well as Mrf4 and Myogenin, which is also upregulated by Myf5. Mrf4 acts as a feedback inhibitor on Myogenin, acting in both lineage specification events and again in the final stages of differentiation (Kassar-Duchossoy, et al, 2004).

RHABDOMYOSARCOMA

Overview

Rhabdomyosarcoma is the most common pediatric soft tissue cancer, responsible for approximately 50% of soft tissue tumor diagnoses (Pastore, et al, 2006,Ries, et al, 1999a). The five-year survival rate depends on subtype, metastatic and lymph node involvement, tumor site, and age at diagnosis, but in general is about 60%, making it one of the most lethal pediatric cancers. Unlike most cancers that develop within in a primary organ or tissue, rhabdomyosarcoma tumors can arise in diverse locations. The location can act as a prognostic indicator; favorable prognostic sites include the head and neck, orbit, and genitourinary tract, whereas tumors that develop in the extremities and trunk are deemed more likely to be unfavorable (Crist, et al, 1995). Despite their various locations, rhabdomyosarcoma tumors resemble

undifferentiated skeletal muscle cells, and skeletal muscle markers like MyoD are used in diagnosis (Wachtel, et al, 2006).

Treatment

Until the 1970s, treatment for rhabdomyosarcoma relied on resection alone, resulting in a cure rate lower than 20% (Sutow, et al, 1970). Implementation of chemotherapeutics dramatically increased the survival to approximately 60%, but since then, the survival rate has only marginally increased, due mostly to better diagnostic tools and novel combinations of older drugs, as opposed to novel therapies (Punyko, et al, 2005).

The current standard of care includes initial biopsy and/or complete resection, depending on tumor location, then neoadjuvant or adjuvant chemotherapy and radiation (Maurer, et al, 1993). The suggested chemotherapeutic regime includes vincristine and dactinomycin, with cyclophosphamide added in cases with a poor prognosis. Vincristine works by binding tubulin and arresting cells in metaphase (PALMER, et al, 1963), and dactinomyicin inhibits transcription by binding DNA at initiation sites (KERSTEN, et al, 1960), (PALMER, et al, 1963). Both these drugs target cells that are actively proliferating, and subsequently can cause alopecia, and gastrointestinal upset. Other possible side effects of this regiment include bone marrow suppression, mouth ulcers, fatigue, and peripheral neuropathy (BOHANNON, et al, 1963,PHILIPS, et al, 1960). Cyclophosphamide causes DNA crosslinking that leads to apoptosis (Friedman and Seligman, 1954), but can lead to the induction of

secondary neoplasms, sterility, infections, and hemorrhagic cystitis (Kenney, et al, 2001),(Heyn, et al, 1993)(Green, et al, 2010). Radiation therapy is recommended in the majority of cases, and side effects depend on the irradiated site, but may include sterility, secondary neoplasms, and cardiac toxicity (Chemaitilly, et al, 2006), (Spunt, et al, 2005,Sudour, et al, 2010), (van Dalen, et al, 2006).

For patients with high-risk disease, the five-year, event-free survival is about 30%, and there is currently no standard therapy. High-risk patients are encouraged to enroll in available clinical trials, or use the standard regiment as palliative care (Raney, et al, 2001).

Current therapeutic regiments often result in permanent sequelae, including growth inhibition, facial asymmetry, impaired vision and hearing, learning disabilities, and hypogonadism (Kenney, et al, 2001)(Raney, et al, 1999)(Paulino, et al, 2000,Krasin, et al, 2012,Paulino, 2004), (Raney, et al, 2000). Given the failure rate of standard of care, especially among high-risk patients, and the lack of any substantial advances in treatment in over thirty years. it is imperative that new therapeutics are developed that not only combat the disease more effectively, but also have fewer devastating side effects.

Associated Syndromes

Although most cases of rhabdomyosarcoma have no known etiology, a few germline diseases have been associated with rhabdomyosarcoma.

Li-Fraumeni syndrome arises due to mutations in the tumor suppressor gene *TP53*, or the gene of one of its regulating proteins, *CHEK2*. p53 is involved in DNA repair mechanisms, so mutations in the p53 pathway predispose cells to high rates of mutation, and therefore cancer. Breast, brain, and adrenal cancer also frequently occur in patients with Li-Fraumeni syndrome. Ionizing radiation may be contraindicated in these patients because of the high possibility of secondary neoplasms (Dagher and Helman, 1999).

Beckwith-Wiedermann syndrome is caused by overexpression of genes on chromosome 11 that control fetal development. Patients with the syndrome are at a higher risk of rhabdomyosarcoma and Wilm's tumor, but also present with macroglossia, hemihyperplasia, and visceromegaly (Smith, et al, 2001).

Costello Syndrome, or faciocutaneal skeletal syndrome, is caused by constitutively activating mutations in *HRAS*, which is located on Chromosome 11. Patients have about 20% chance of developing a solid tumor, and those with the disease are encouraged to have regular screenings for rhabdomyosarcoma, as well as bladder cancer and neuroblastoma (Gripp, et al, 2002). Other symptoms of the syndrome are delayed development and unusually flexible joints.

Diagnosis

Historically, rhabdomyosarcomas tumors were diagnosed histologically in that they stain blue with hematoxylin and eosin, much like other pediatric bone and soft tissue cancers including Ewing sarcoma, osteosarcoma, and lymphoma. Additionally,

tumor cells displayed markers of the skeletal muscle lineage, such as cross-striations. Immunochemical staining for muscle specific proteins like desmin greatly enhanced the ability of physicians to make correct diagnosis, and even to delineate between different subtypes of rhabdomyosarcoma (Wachtel, et al, 2006), (Dias, et al, 2000,Heerema-McKenney, et al, 2008).

Using histology, two major subtypes of rhabdomyosarcoma were identified. The first is embryonal rhabdomyosarcoma (ERMS), which can have botryoid and spindle cell variants. Botryoid tumors grow in grape-like cluster and usually develop in the bladder and vagina of infants, and spindle cell tumors usually present as paratesticular cancer in young men. The second major subtype of rhabdomyosarcoma is alveolar rhabdomyosarcoma, or ARMS. These tumors derive their name from the pattern of widely dispersed cells these tumors demonstrate histologically, which mimics pulmonary alveoli.

Modern subtype classification schemas use genetic analysis to diagnose rhabdomyosarcomas. ERMS is most often defined by loss of heterozygosity on the short arm of chromosome 11(Scrable, et al, 1987), which contains the imprinted gene *IGF-II* (insulin growth factor II). Loss of imprinting may lead to increased expression of IGF-II and subsequent aberrant growth signals (El-Badry, et al, 1990), (Zhan, et al, 1994). ERMS has an overall more favorable prognosis, and generally occurs in more favorable sites (Punyko, et al, 2005). In contrast, ARMS is characterized by a chromosomal translocation between chromosome 13 and either chromosome 1 or 2 (Shapiro, et al, 1993), (Galili, et al, 1993)(Davis, et al, 1994). These translocations

lead to fusion genes, *PAX3-FOXO1*a or *PAX7-FOXO1a*, respectively. The *PAX3-FOXO1a* translocation occurs more than twice as often as its *PAX7* counterpart (Ries, et al, 1999b). ARMS is clinically much more dire than other RMS subtypes (Sorensen, et al, 2002). The tumors occur more often in unfavorable sites, and are more likely to recur, metastasize, and become drug resistant, and patients are usually classified as high risk (Ries, et al, 1999b).

THE FUSION PROTEIN

The identification of chromosomal translocations in rhabdomyosarcoma spurred investigation into the fusion proteins, as well as conjectures about their mechanism of disease. It was evident that the majority of ARMS tumors had the chromosomal translocations, but the role of the mutation in tumorigenesis remained unclear.

The fusion proteins created by the chromosomal translocations contain the DNA binding portion of the PAX3 or PAX7 protein combined with the strong FOXO1a transactivation domain, creating a novel fusion transcription factor (Shapiro, et al, 1993,Galili, et al, 1993)(Bennicelli, et al, 1996).

PAX3

Normal PAX protein family members are transcription factors that regulate the development of the nervous system and skeletal muscle system during embryogenesis. They all contain an N-terminal paired (or paired box) DNA binding domain, which was a motif originally found in the Drosophila segmentation gene *paired* (*prd*) (Bopp,

et al, 1986). The paired domain has two subunits, PAI and RED, with each containing three α-helices. DNA binding is achieved by the third helix in PAI. PAX3 also contains a homeodomain consisting of a helix-turn-helix that binds DNA in the major groove. Mutations in either of the DNA binding domains can inhibit the ability of the other to bind (Fortin, et al, 1997). The two DNA binding domains are separated by the octapeptide motif HSIDGILG, which controls homodimerization (Chalepakis, et al, 1994). The C-terminal transactivation domain is rich in serine and threonine amino acids (Gruss and Walther, 1992).

In humans, hemizygous mutations in PAX3 lead to Waardenburg syndrome types I and III, which confers to congenital deafness, pigmentary disturbances in the skin, eyes and hair, and wide-set eyes. Type III is also known as Klein-Waardenburg syndrome, and can manifest in malformation of the upper limbs. In mice, mutation of the PAX3 homolog *splotch* yields the Splotch phenotype, characterized by perinatal death, and defects in both the neural tube and limb musculature (Franz, 1993).

Exogenous expression of PAX3 in mouse pluripotent stem cells is enough to induce myogenesis, as measured by expression of MyoD and myogenin (Ridgeway and Skerjanc, 2001). PAX3's target binding sequence is TCGTCACRCTTHM (Chalepakis and Gruss, 1995). PAX3 direct target genes include MET (Epstein, et al, 1996), BCL2L1 (Margue, et al, 2000), Myf5 (Bajard, et al, 2006) and MyoD (Goldhamer, et al, 1995), as previously mentioned.

FOXO1a

FOXO1a is a member of the FOXO family of transcription factors that in turn belong to a wider group of *FOX* genes. The first known member of the *FOX* genealogy was originally named *forkhead* (*FKHR*) after its ability to cause fork-like projections on the head of Drosophila when mutated. The group is also referred to as "winged helices" because the crystallographic DNA structure resembles butterfly wings. The *FOX* family is now known to consist of *FOXA* through *FOXR*, which are grouped by sequence homology. The *FOXO* group has four members (1, 3, 4, and 6) which are all regulated by insulin/PI3K/Akt signaling. FOXO proteins are involved in a wide variety of cell functions such as apoptosis (Tothova, et al, 2007), oxidative stress response (Berry, et al, 2008), differentiation (Nakae, et al, 2003), inflammation (Ouyang, et al, 2012), skeletal muscle mass (Kamei, et al, 2004), aging (Demontis and Perrimon, 2010), and energy homeostasis (Ren, et al, 2012).

FOXO factors were first classified in humans as the genes in the chromosomal translocations in alveolar rhabdomyosarcoma and AML, and *FOXO1a* was at first named *ALV* because of this association (Shapiro, et al, 1993). *FOXO1a* is distinguished from a pseudogene *FOXO1b* (or *FKHRP1*) that is located on chromosome 5 (Anderson, et al, 1998).

Structurally, the FOXO1a protein contains three α-helices, three β strands that form a sheet, and two large loops. The third helix acts as the most prominent DNA recognition site by binding target sequences in the major groove (Clark, et al, 1993). The FKHR domain acts as the DNA binding moiety. The protein also contains a

nuclear localization signal, a nuclear export sequence, and a transactivation domain. FOXO1a contains three AKT phosphorylation sites (Rena, et al, 1999), (Arden and Biggs, 2002); the sites near the N-terminus and in the nuclear export sequence both become 14-3-3 binding sites when engaged (Rena, et al, 2001). CDK1 and CDK2 are also able to phosphorylate FOXO1a, which shuttles FOXO1a to the cytoplasm where it can no longer promote transcription of its target genes (Liu, et al, 2008), (Huang, et al, 2006). A few of the FOXO1a gene targets are *SOX2* (Zhang, et al, 2011), *OCT4* (Zhang, et al, 2011), *INFG* (Ouyang, et al, 2012), and *RUNX2* (Teixeira, et al, 2010).

PAX3-FOXO1a

As mentioned earlier, *PAX3-FOXO1a* chromosomal translocations are de novo, although they may be accompanied by mutations that contribute to general genetic destabilization (see Li-Fraumeni Syndrome). Recently, a study by Yuan et al showed the presence of *PAX3-FOXO1a* mRNA in non cancerous, translocation negative mesenchymal stem cells, suggesting that fusion protein mRNA may have a role in normal myogenesis (Yuan, et al, 2013).

Clinically, it is known that the *PAX3-FOXO1a* translocation is unique to the alveolar subtype of rhabdomyosarcoma, and that alveolar patients fare worse than their embryonal counterparts, but the exact mechanism of PAX3-FOXO1a's role in disease initiation and progression remains unclear. Indeed, an in-depth, retrospective examination of the histological characteristics of alveolar tumors found no correlation

with fusion status (Parham, et al, 2007), despite the fact that their presence has a proven effect on clinical outcome.

PAX3-FOXO1a contains the DNA binding domain of PAX3, so it would be tempting to assume that PAX3-FOXO1a causes disease simply by initiating anachronistic expression of normal PAX3 targets, which are usually only expressed during embryogenesis. The fact that the phenotype of PAX3 deficient mice is mostly rescued by *PAX3-FXO1a* knock in lends credence to this hypothesis (Relaix, et al, 2003), however, the reality seems to be much more complicated. First, PAX3-FOXO1a induces transcription more than normal PAX3 (Fredericks, et al, 1995)(Bennicelli, et al, 1996), demonstrating the fusion protein's stronger transactivation domain. Secondly, several association experiments have been conducted to determine specific and consensus targets for PAX3 and PAX3-FOXO1a, but only a few studies have demonstrated direct binding and activation of target genes. PAX3-FOXO1a and PAX3 do have some direct targets in common, including *CNR1* (Begum, et al, 2005), but only PAX3-FOXO1a binds and activates *JARID2* (Walters, et al, 2014), and *MYCN* (Mercado, et al, 2008). PAX3 binding to DNA can be inhibited by Daxx, but Daxx cannot inhibit the binding of PAX3-FOXO1a (Hollenbach, et al, 1999). Furthermore, although PAX3 is able to induce mesenchymal/epithelial transitions (Wiggan, et al, 2002), PAX3-FOXO1a does so in a more robust manner (Begum, et al, 2005).

In vivo, transgenic mice expressing *PAX3-FOXO1a* do not have a phenotype that would be predicted by overexpression of normal PAX3 targets. Instead, the mice

more closely resemble PAX3 knockout mice, demonstrating that PAX3-FOXO1a functionally competes with PAX3 (Anderson, et al, 2001b), (Finckenstein, et al, 2006).

PAX3-FOXO1a has additional tumorigenic capabilities that do not seem to stem from its similarity to wild type PAX3. When introduced to chick fibroblasts, PAX3-FOXO1a was able to confer anchorage-independent growth (Scheidler, et al, 1996), but interestingly, Lam et al found that transformation was independent of the paired box DNA binding domain (Lam, et al, 1999). When stably transfected into ERMS cell line RD, PAX3-FOXO1a increased proliferation in vivo, and made xenograft tumors larger and more invasive (Anderson, et al, 2001a). However, transgenic PAX3-FOXO1a knock in mice do not develop tumors (Lagutina, et al, 2002), (Anderson, et al, 2001b).

From a mechanistic standpoint, PAX3-FOXO1a can act independently of its canonical role as a transcription factor. Roeb et al showed that PAX3-FOXO1a contributes to tumor development by binding and destabilizing EGR1, thus interrupting activation of anti-oncogenic p57Kip2 (Roeb, et al, 2007). PAX3-FOXO1a can also promote a cancer phenotype by evading immune detection. Nabarro et al demonstrated the ability of PAX3-FOXO1a to inhibit inflammatory response by binding directly to STAT (Nabarro, et al, 2005).

Limited work has been done on PAX3-FOXO1a's reciprocal fusion protein FOXO1a-PAX3 (Hu, et al, 2013), but FOXO1a-PAX3 remains predominantly in the cytoplasm, and does not seem to function as a transcription factor.

Pediatric vs. adult rhabdomyosarcoma

Adult rhabdomyosarcoma is much more rare than its pediatric counterpart, but the prognosis is worse (Ferrari, et al, 2003,Sultan, et al, 2009). At presentation, tumors are more likely to be of the pleomorphic and not otherwise specified subtypes, which is unusual in children, and adults are much more likely to succumb to the disease within five years of diagnosis. Unlike pediatric RMS, the alveolar subtype has no predictive value in adults, nor does tumor site. The differences in etiology between pediatric and adult RMS are largely unknown. Adult rhabdomyosarcoma, though rare, is exceedingly deadly, and further investigation into the disease is warranted.

MICRORNA

MicroRNAs, or miRNAs, are a class of small, highly conserved, non-coding RNAs that regulate the ability of mRNAs to be translated, and are fundamental to several normal cellular functions.

miRNAs were first experimentally observed in petunias in 1990 (Napoli, et al, 1990), but first described in the nematode *Caenorhabditis elegans* in 1993 (Lee, et al, 1993). miRNAs were shown to be cleaved from a longer precursor RNA by the ribonuclease Dicer (Hutvagner, et al, 2001). Dicer was already known to be central in RNAi, or RNA interference, a mechanism by which RNAs can inhibit production of proteins (Bernstein, et al, 2001), but the notion of RNA being inhibited by antisense RNA oligonucleotides originated much earlier (Tomizawa and Itoh, 1981).

miRNAs genes can be located in the introns of coding genes, and in both the introns and exons of non-coding genes (which may change with alternative splicing) (Rodriguez, et al, 2004). miRNAs within genes are usually transcribed along with their host genes. However, miRNA genes can also be found in intergenic space, or in intragenic space but with antisense orientation. Several miRNAs can be encoded by the same primary transcript, which is then cut to yield individual miRNAs.

miRNAs are initially transcribed from genes by RNA polymerase II(Lee, et al, 2004) or RNA polymerase III (Faller and Guo, 2008). This RNA strand is referred to as primary miRNA, or pri-miRNA, and has a 5’ guanosine cap and a poly adenoylic tail (Cai, et al, 2004). At this point, complimentary base pairs within the pri-miRNA strand bind together creating a double strand RNA hairpin (Cai, et al, 2004). DGCR8, a double stranded RNA binding protein, and Drosha, an enzyme specific for double stranded RNA, bind and digest the pri-miRNA, releasing the hairpin structure now termed precursor miRNA or pre-miRNA (Gregory, et al, 2006). The pre-miRNA leaves the nucleus via direct binding to Exportin-5 (Yi, et al, 2003). In the cytoplasm, the RNAse Dicer cuts the loop from the two stem strands, creating double stranded RNA (Bernstein, et al, 2001). The RNA-induced silencing complex, also known as RISC, contains several proteins that aid miRNA processing (Tomari, et al, 2004). One of these proteins, Argonaute (AGO), selects which complimentary RNA strand becomes mature miRNA; the other strand will eventually be degraded (Schwarz, et al, 2003). The mature miRNA and RISC complex then regulate translation by binding to target mRNA.

Human miRNAs most often regulate transcription by imperfectly binding, via base-pairing, to the 3’ untranslated end of mRNA, effectively halting translation. miRNAs can also degrade mRNA by initiating the binding of GW182 proteins which recruit a deadenylase complex that acts on the target mRNA. The stabilizing 5’guanosine cap on the mRNA is subsequently removed via a decapping complex, followed by degradation via exonuclase activity (Behm-Ansmant, et al, 2006,Eulalio, et al, 2007,Eulalio, et al, 2009).

MicroRNA in Myogenesis

In 2007 O’Rourke et al found that miRNAs were essential to skeletal muscle development; when the miRNA-processing enzyme Dicer was conditionally knocked out in mouse embryos, the mice had decreased skeletal muscle mass, abnormal myofiber morphology, and died perinatally (O'Rourke, et al, 2007). In the years since, four muscle specific myomirs have been identified. miR-1, miR-206, miR-133a and 133b are almost exclusively found in striated muscle, with miR-206 being found only in skeletal muscle (as opposed to cardiac) (McCarthy, 2008)(Chen, et al, 2006). miR-1 and mir-133 overexpression during embryogenesis leads to disorganized muscle tissue and cardiac morphology, and expression of miR-206 is enough to induce differentiation in mouse myoblasts (Rao, et al, 2010)(Lagos-Quintana, et al, 2002).

Myomirs target several different players in the myogenesis pathway. miR-1 and miR-206 cause eventual downregulation of PAX3, halting further PAX3 induced cell migration (Goljanek-Whysall, et al, 2011). miR-206 and miR-486 act in concert to

inhibit PAX7, which not only halts cell proliferation, but eventually induces differentiation through increased expression of MyoD (Dey, et al, 2011). miR-206 also inhibits known differentiation repressors, including *POLα*, *MyoR*, *Id1-3* (Kim, et al, 2006), and *HDAC4* (Chen, et al, 2006). Additionally, miR-206 and miR-1 aid the cellular synchronization and fusion of individual myocytes into myotubes (Anderson, et al, 2006), (Sun, et al, 2010). miR-133 provides negative feedback inhibition of differentiation by targeting the IGF-1 receptor that is activated via P13K/Akt signaling during myogenesis (Huang, et al, 2011).

In addition to the four myomirs, several other miRs also work to regulate myogenesis. miR-27 acts early to inhibit myogenic repressor *MSTN* (the gene for myostatin) (Huang, et al, 2011), and miR-214 inhibits *N-RAS* resulting in the de-repression of p21 and cell cycle arrest (Liu, et al, 2010). miR-24 (Sun, et al, 2008), mir-26a (Ciarapica, et al, 2009,Wong and Tellam, 2008), and mir-181(Naguibneva, et al, 2006) are also known to induce the early stages of cellular differentiation.

Other miRNAs are inhibitors of myogenesis. miR-125b inhibits both *LIN-28* and *IGF2*, which both promote myocyte formation (Ge, et al, 2011). miR-121 and miR-122 both target *p27*, an inducer of cell cycle arrest (Cardinali, et al, 2009) and miR-23a inhibits myosin heavy chain (Wang, et al, 2012). miR-669a and miR-669q are expressed in cardiac muscle in order to prevent skeletal muscle development by inhibiting MyoD (Crippa, et al, 2011).

MicroRNA in Cancer

Given their critical role in cell behavior, it is not surprising that dysregulation of miRNAs can lead to myriad disorders and diseases. miRNAs can act as both tumor suppressors (Cimmino, et al, 2005) and oncongenes (or oncomirs) (Metzler, et al, 2004,Kluiver, et al, 2005), and miRNA levels may be used to diagnose malignancies(Lu, et al, 2005), assign prognosis (Calin, et al, 2005), stratify treatment groups (Pardini, et al, 2013) and evaluate treatment response (Andreoli, et al, 2014).

With the advent of high throughput technology, several studies have been done comparing the miRNA profiles of tumors and tumor cells to their cells and tissues of origin (Landgraf, et al, 2007,Lui, et al, 2007,Wang, et al, 2008b,Sun, et al, 2009,Bearfoot, et al, 2008), (Pallante, et al, 2006,Fulci, et al, 2007). The resulting data has been useful both as a starting point for investigation into individual miRNAs, and to indentify miRNAs that are dysregulated in several types of cancer. For example, the miR-29 family has been found to be down regulated in CLL, AML, lung cancer, and cholangiocarcinoma (Calin, et al, 2005,Iorio, et al, 2005,Yanaihara, et al, 2006,Garzon, et al, 2008b,Fabbri, et al, 2007,Pekarsky, et al, 2006,Mott, et al, 2007). Conversely, miR-21 has been found to be overexpressed in many cancers including breast, colon, pancreas, lung, prostate, liver, stomach, and glioblastoma (Calin, et al, 2005,Garzon, et al, 2008b,Calin, et al, 2004,Garzon, et al, 2008a,Ciafre, et al, 2005,Meng, et al, 2007,Meng, et al, 2007,Chan, et al, 2005,Frankel, et al, 2008,Zhu, et al, 2007), suggesting it acts as an oncomir.

One must be careful in designating a miRNA as either tumor suppressive or oncongenic; miRNAs that are upregulated in one cancer or have been found to be downregulated in others. miR-29, mentioned previously as tumor suppressor, has also been found to promote metastasis and epithelial to mesenchymal transition in breast cancer cells and patient samples (Gebeshuber, et al, 2009). Similarly, miR-26a promotes metastasis in lung cancer cells (Liu, et al, 2012) and is amplified in glioma (Huse, et al, 2009), but it is downregulated in hepatocellular cancer (Kota, et al, 2009).

Dysregulation of a miRNA can be caused by a variety of reasons including deletions (Calin, et al, 2002), mutations (Calin, et al, 2005), copy number alterations (Ota, et al, 2004,Volinia, et al, 2006,Venturini, et al, 2007), epigenetic changes (He, et al, 2007,Raver-Shapira, et al, 2007,Chang, et al, 2007), and dysfunction of miRNA processing machinery (Nakamura, et al, 2007).

miRNAs make attractive therapeutic targets due to their promiscuous inhibitory capabilities. Repairing the expression of one miRNA could affect targets in several dysregulated pathways. Treatment of disease by either overexpression or inhibition of miRNAs is currently in Preclinical, Phase 1 and Phase 2 clinical trials(Rayner, et al, 2011,Trang, et al, 2011,Hullinger, et al, 2012)(Janssen, et al, 2013).

MicroRNA in Rhabdomyosarcoma

A handful of studies have examined the role of the four muscle specific myomirs in rhabdomyosarcoma, and the data sometimes conflict. In 2008, Wang et al

reported that although miR-1 is expressed at a lower rate in RMS tumors compared to skeletal muscle tissue, there is no pattern with miR-206 (Wang, et al, 2008). However, Yan et al later found that miR-1 and miR-206 expression were low in all tested tumor samples compared to normal tissue (Yan, et al, 2009). Rao et al also observed decreased expression of all four myomirs in two RMS cell lines compared to skeletal muscle tissue (Rao, et al, 2010).

Exogenously increasing expression of myomirs in RMS cells can induce a differentiation phenotype. Transfection of miR-1 and miR-206 into the ERMS cell line RD decreased both cell growth and migration by targeting c-MET (Yan, et al, 2009), and overexpression of miR-206 has been found to promote myogenesis and block xenograft tumor growth (Missiaglia, et al, 2010)(Taulli, et al, 2009). Induction of miR-133a and 133b into RMS cells was able to increase differentiation, but only in the embryonal subtype and not the alveolar, suggesting a different mode of myogenic block in the two subtypes (Rao, et al, 2010).

Clinically, higher expression of miR-206 in RMS tumors correlates with higher patient survival, but only in PAX3-FOXO1a negative patients; survival of patients with ARMS could not be predicted based on miR-206 expression(Missiaglia, et al, 2010). mir-133a and miR-133b expression are able to discriminate between RMS tumors and neuroblastoma tumors; this fact could aid in difficult to diagnosis cases of RMS(Wei, et al, 2009).

Non-myomirs have also been found to be dysregulated in RMS. Amplification of 13q31 is frequent in translocation positive tumors. This amplicon contains the miR-

17-92 cluster (Gordon, et al, 2000), which codes for miR-17, miR-19a, miR-19b, miR-20a, and miR-92. Patients with the 13q31 amplification have a poorer prognosis, as do amplification negative patients that have increased expression of the miRs in the 13q31 cluster (Reichek, et al, 2011).

miR-26a is downregulated in RMS cell lines, and more so in ARMS cells than ERMS cells (Ciarapica, et al, 2009). One validated target of miR-26a is *EZH2*, which is upregulated in RMS and is negative regulator of myogenesis (Wong and Tellam, 2008), (Ciarapica, et al, 2009).

miR-29 has been identified in a faulty feedback loop that may contribute to tumorigenesis. miR-29 is negatively regulated by NF-κB, which is known to inhibit myogenesis through YY1(Wang, et al, 2007). YY1, in turn, is negatively regulated by miR-29(Wang, et al, 2008). YY1 overexpression and miR-29 downregulation have both been found in RMS, suggesting that YY1 inhibits cellular differentiation by inhibiting miR-29, therefore augmenting its own expression through lack of feedback inhibition (Wang, et al, 2008).

miR-183 has been found to be upregulated in RMS, where it targets known tumor suppressors *EGR1* and *PTEN* and promotes cell migration(Sarver, et al, 2010). mir-9* is also upregulated in RMS, and its expression is higher in AMRS tumors than in ERMS tumors (Armeanu-Ebinger, et al, 2012). In the same study, miR-200c was found to be downregulated, but was not subtype specific (Armeanu-Ebinger, et al, 2012).

miR-335-3p has been found to be upregulated in RMS. The host gene of miR-335-3p is *MEST*, or *PEG1*, which has been implicated in skeletal muscle development. Interestingly, *MEST* is a downstream target of PAX 7 andPAX3, and has also been found to be upregulated in ARMS tumors (Mayanil, et al, 2001), (Baer, et al, 2004).

Recently, Gougelet et al sought to differentiate between ERMS and ARMS tumors using miRNA microarrays (Gougelet, et al, 2011). They found ten miRs that were upregulated in both PAX3-FOXO1a and PAX7-FOXo1a positive tumors compared to EMRS tumors: miR-376a, miR-539, miR- 487b, miR- 323-3p, miR- 532-3p, miR-758, miR-410, miR-433, miR-127-3p and miR-495.

MicroRNA-495

MicroRNA-495 is located on chromosome 14 in a large cluster of non-coding RNAs called *DKL1-DIO3*. Evidence exists that it shares a primary transcript with several of the other miRNAs in the cluster, but this has yet to be experimentally confirmed (Chien, et al, 2011).

The role of miR-495 in cancer appears to be highly dependent on cancer type. It has been demonstrated that the miRNA can act in both pro-tumorigenic and anti-tumorigenic capacities. miR-495 has been shown to be downregulated in MLL rearranged leukemia, where it inhibits apoptosis by directly targeting *PBX3* and *MEIS1* (Jiang, et al, 2012), and in glioma cells, where it inhibits growth of tumor cells by suppressing expression of CDK6(Chen, et al, 2013a). Downregulation of miR-495 has also been associated with metastatic pancreatic cancer cells, and it is predicative of

lymph node invasion (Formosa, et al, 2013). miR-495 has also been found to be downregulated in drug resistant lung cancer cells, and is thought to target *MDR1*, a multi drug resistant gene (Xu, et al, 2013). Similarly, miR-495 has been shown to increase drug sensitivity in drug-resistant small cell lung cancer cells (Guo, et al, 2010), and inhibit lung cancer cell proliferation and migration (Chu, et al, 2014). Additionally, miR-495 was able to induce differentiation of pancreatic acinar cells, therefore preventing metaplasia (Prevot, et al, 2013).

There are, however, several instances in which miR-495 has been associated with a cancerous phenotype. miR-495 has been found to be upregulated in breast cancer and is able to promote tumorigenesis in vivo, and other markers of cancer in vitro(Hwang-Verslues, et al, 2011). mir-495 is upregulated in KRAS positive adenocarcinomas (Dacic, et al, 2010), and also in hepatocellular carcinoma, where it has been shown to increase tumor growth, metastasis and invasion(Yang, et al, 2013). The microRNA also inhibits differentiation of hMSCs by directly targeting *SOX9* (Lee, et al, 2014). Clearly, the role or miR-495 in cancer is complex and highly context-dependent.

The mature sequence of mir-495 is AAACAAACAUGGUGCACUUCUU. It shares its seed targeting sequence with miR-5688, miR-3065-5p, mir-7-1-3p, and miR 7-2-3p. It is reported to target mRNAs that contain the sequence GUUUGUU (Lee, et al, 2014)

Direct targets of miR-495 include *E-cadherin* and *REDD*1 (Hwang-Verslues, et al, 2011).

HIGH-THROUGHPUT SEQUENCING

The advent of high-throughput sequencing allows for whole genome and transcriptome analysis that would previously have been unreasonable. During the Human Genome project of the late 1990s and early 2000s, it became clear that the state of the art was too slow and too expensive to produce the quantity of data for which researchers were looking.

The mid 2000s saw the launch of a few commercially available platforms for sequencing large amounts of DNA in days rather than years. These included 454 sequencing (later dubbed GS FLX after acquisition by Roche) (Margulies, et al, 2005), the SOLiD (Supported Oligonucleotide Ligation and Detection) platform from Applied Biosystems, and the Illumina Genome Analyzer, originally developed by Solexa as Solexa 1G. These three technologies brought the cost of sequencing down drastically, and increased quality by eliminating the need to clone DNA in bacteria.

The three platforms had similarities, differences, strengths, and weaknesses. In all cases, DNA fragments were ligated to adapters on solid supports, either beads (Roche and Applied Biosystems(Dressman, et al, 2003)) or a flow cell (Illumina) (Fedurco, et al, 2006). With beads, PCR was performed in an oil and water emulsion(Dressman, et al, 2003), whereas in the flow cell, PCR is performed via bridge amplification that creates clusters of cloned DNA (Adessi, et al, 2000), (Fedurco, et al, 2006). The Roche system detected base pairs via pyrosequencing, in which the addition of each sequential base triggered a luciferase reaction unique to

each base (Ronaghi, et al, 1996). Illumina used four different fluorescently labeled bases, and excited the bases with a laser at each additional round of incorporation (Turcatti, et al, 2008). Instead of four probes, the Applied Biosystems platform uses 16 different fluorescent octomers, each with a unique pair of nucleotides flanked by 3 universal bases (Shendure, et al, 2005). Each round of oligonucleotide excitation is followed by removal of the last two universal bases and subsequent addition of another octomer (Ng, et al, 2005). At the end of the DNA template, the octomers are all removed, and the process is begins again at a different start site, and this process repeats itself until all bases are read (Housby and Southern, 1998). The octomers have an advantage over the four probe systems in that their dinucleotide discretion makes the reads more reliable (McKernan, et al, 2011). 454 sequencing produced 1.25 million reads in a day. In comparison, Illumina's Genome Analyzer and Applied Biosystems' SOLiD produced up to 120 million reads, but processing took between 2 and 4 days.

Overall, 454 could sequence longer reads in a shorter amount of time, but had trouble sequencing long homopolymers and repetitive regions, which resulted in insertion and deletion errors. Illumina was cheaper and processed more samples, but had a higher probability of substitution errors. Applied Biosystems was also cheap and high throughput, but had negative biases for GC rich regions. Roche proved better for de novo sequencing, while Illumina was better at mapping reads back to a sequence, which gave it an advantage in transcriptomics research (For review see (Shendure and Ji,)).

Even now, the next generation sequencing technologies are being replaced by next-next-generation platforms that produce more data of a higher quality in a shorter amount of time, and at a lower cost.

small RNA-seq

Regular mRNA-seq requires more than 80 million reads in order to achieve a sample size large enough to be reliable(Cloonan, et al, 2008), and even this number of reads does not have the power to analyze alternative splicing. This is due to the incredibly large number of RNA transcripts that are possible targets. However, there are very few small RNAs by comparison, meaning the same statistical reliability can be achieved with as few as 1 million reads. Even if there are hundreds of miRNAs yet to be discovered, the magnitude is nowhere near as large as that of total RNA, making small RNA-seq much easier and less expensive than normal RNA-seq.

In the Illumina TruSeq small RNA protocol, amplified cDNA is separated by PAGE, and bands corresponding to the size of primer-ligated miRNAs are excised from the gel and purified.

SUMMARY

Rhabdomyosarcoma is among the most deadly of pediatric cancers. Current therapeutics are limited in their ability to treat advanced disease, and result in devastating side effects that can be permanent. The relatively recent discovery of miRNA provides a new avenue to investigate the causes of rhabdomyosarcoma and identify possible therapeutic targets. The biological discovery of miRNA coupled with

advances in high throughput sequencing have made global profiling of rhabdomyosarcoma miRNA transcriptomes a reality, which may provide clues to the etiology of this terrible disease.

FIGURES

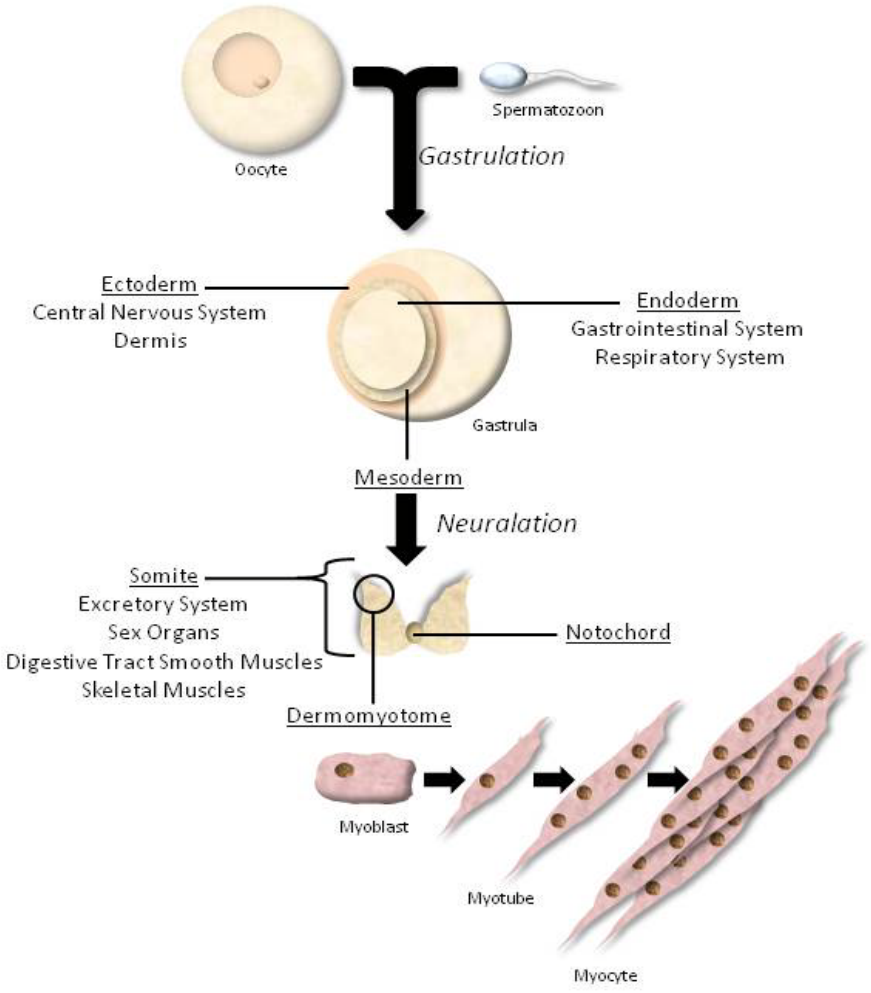

Figure 1. Embryonic myogenesis
A zygote differentiates into a morula first, followed by a blastula. The blastula further differentiates in to three separate layers, which form the gastrula.. Somites develop from the mesoderm during neuralation. The dermomyotome contains myoblasts, which fuse to form myotubes. Myotubes align to form myocytes.

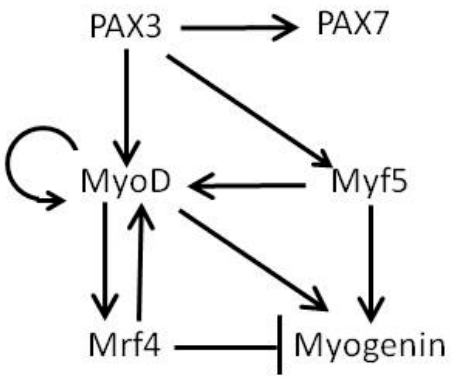

Figure 2. Molecular regulation of embryonic myogenesis.
MyoD is induced by PAX3, Myf5, Myogenin, Mrf4, and itself. Several intertwining circuits allow for tight control of the myogenic program.

CHAPTER 2 - SKELETAL MUSCLE CELLS HAVE DIFFERENT MICRORNA TRANSCRIPTOMES THAN THOSE OF RHABODOMYOSARCOMA CELLS

INTRODUCTION

Rhabdomyosarcoma tumors express markers known to exist in undifferentiated skeletal muscle tissue, but RMS tumors and normal skeletal muscle cells result in different phenotypes. During normal myogenesis, mono-nucleated myoblasts will divide without differentiating due to the continued presence of fibroblast growth factors. Upon depletion of the growth factors, the myoblasts exit the cell cycle, and wild-type PAX3 induces the transcription of muscle-specific transcription factors in the MyoD family (Myf5, myogenin, Myf6). This in turn activates genes that promote terminal differentiation.

It has been shown that non-coding short RNAs called miRNAs are indispensible in embryonic myogenesis. Conditional blockade of miRNA processing in mice lead to decreased skeletal muscle mass, abnormal myofiber morphology, and death(O'Rourke, et al, 2007). Specifically, miR-1 and miR-133 control muscle cell organization, and miR-206 is sufficient to induce differentiation (Rao, et al, 2010,Dey, et al, 2011,Kim, et al, 2006).Together, miR-1, miR-133a and miR-133b, and miR-206 make up the group of four myomirs, or miRs that are expressed specifically in muscle tissue. These miRs function in a number of different capacities, including inhibition of migratory signaling via PAX3, halting proliferation by inhibiting PAX7, and inhibiting differentiation repressors(Goljanek-Whysall, et al, 2011,Dey, et al,

2011,Kim, et al, 2006) In addition to myomirs, several other miRS also have regulatory capacities in myogenesis.(Huang, et al, 2011,Ciarapica, et al, 2009,Wong and Tellam, 2008,Naguibneva, et al, 2006,Ge, et al, 2011,Cardinali, et al, 2009,Crippa, et al, 2011)

A few studies have also linked miRNA dysregulation with rhabdomyosarcoma. Myomirs have been found to be downregulated in RMS tumors compared to normal tissue (Rao, et al, 2010,Wang, et al, 2008,Yan, et al, 2009), and exogenously expressing myomirs in RMS cells leads to differentiation(Rao, et al, 2010,Yan, et al, 2009,Missiaglia, et al, 2010,Taulli, et al, 2009). Other non-myomirs have also been found to be dysregulated in RMS, including upregulation of miR-183, miR-9* , miR-335-3p, and miRs in the miR-17-92 cluster, and down regulation of miR-26a and miR-29(Ciarapica, et al, 2009,Wong and Tellam, 2008,Reichek, et al, 2011), (Wang, et al, 2008), (Sarver, et al, 2010,Armeanu-Ebinger, et al, 2012),(Baer, et al, 2004).

By comparing the miRNA transcriptome of both differentiated and undifferentiated cultured primary skeletal muscle cells (SKMCs) to those of RMS cell lines, we can indentify cancer specific miRNAs in cells along the myogenic spectrum. Additionally, we can compare myomir expression levels between the normal cell lines and cancer cell lines in order to gauge the cancer cells' myogenic state.

The comparison of the undifferentiated and differentiated cells also served as a proof of principal experiment by demonstrating that data from small-RNA seq is able to delineate between cell types. Before we could start investigating new associations

between cell types and miRNA profiles, it also necessary to demonstrate that the sequencing data we produced was consistent with known literature.

Using small RNA-seq we show that differentiated and undifferentiated cultured primary muscle cells have different miRNA transcriptomes, which also differ from the transcriptomes of both ERMS cells and ARMS cells. Furthermore, ARMS and ERMS cell lines have their own unique miRNA profiles. Small RNA-seq data were validated using qPCR.

RESULTS

Small RNA-seq identifies miRNAs known to be differentially expressed between differentiated and undifferentiated primary skeletal muscle cells

In order to assess the microRNA profiles in both differentiated and undifferentiated primary skeletal muscle cells, primary muscle cells were differentiated using horse serum (Figure 3a). An increase in myosin, indicative of differentiation, can be seen in differentiated cells compared to undifferentiated cells for two biological replicates (Figure 3b). Small RNA-seq performed using the same samples showed increases in all four muscle specific miRNAs, also called myomirs, in both of the differentiated samples compared to undifferentiated samples (Figure 3c, Table 1). miRNA levels were validated via qPCR, and mirror the results of the high-throughput sequencing (Figure 3d).

Differentiated and undifferentiated skeletal muscle cells have unique miRNA signatures

Small RNA-seq was able to identify known myomirs, but we were interested in identifying possible novel miRNAs that may be associated with skeletal muscle differentiation. Data analysis showed significant differences in 56 microRNAs upon differentiation (Figure 4a, Table 2). One of the most significantly different miRNAs was miRNA-143, with a z score of -2.386 and a p value of 0.0066 (Figure 4b). qPCR data mirrors the sequencing results (Figure 4c). miRNA-143 has a well-characterized role in smooth muscle and cardiomyocyte differentiation, but as of yet it has not been linked to skeletal muscle myogenesis(Deacon, et al, 2010).

Of the 56 significantly different microRNAs, six of them had high number miRNA names. miR-3065, miR-3676, miR-3681, miR-3912, miR-4682, and miR-5683 were all significantly downregulated in differentiated cells compared to undifferentiated cells (Table 2). miRNA nomenclature assigns numbers to miRNAs in the order in which they are discovered, therefore the high values of the six aforementioned miRNAs indicated their recent discovery, and the possibility that little research may have been done on them. A literature search shows that miR-3065 is differentially expressed between clear cell renal cell carcinoma and normal tissue, and that the miR targets NRP2, which functions in VEGF signaling and has been linked to cancer(Nasarre, et al, 2013), and FLT1, a member of the VEGFR signaling family(Muller and Nowak, 2014)(). FLT1 functions in angiogenesis and has been implicated in cancer recurrence (Suspitsin, et al, 2013). miR-3065 is more highly

expressed in differentiated cells than undifferentiated cells. The fact that it has two targets in the VEGF pathway that are known to be detrimental in cancer suggests it inhibits a growth phenotype, consistent with its increased expression in differentiated skeletal muscle cells.

There are no publications about the other high-numbered miRNAs at the time of this writing. Further experimentation is required to confirm the specific roles of these miRNAs in skeletal muscle differentiation.

Normal skeletal muscle cells and rhabdomyosarcoma cells reflect differential miRNA expression

RMS tumors are thought to be myogenic cells that cannot complete terminal differentiation. Identification of an RMS specific miRNA signature could lead to new therapeutic targets, as well as a better understanding of RMS etiology. First, we compared the expression of myomirs in the differentiated and undifferentiated primary skeletal muscle cells in Figure 3 with the miRNA profiles of two RMS cell lines: ERMS cell line RD, and ARMS cell line Rh30. The RNA-seq data showed that all four myomirs, miR-1, miR-206, miR-133a, and miR-133b, had higher reads per million (RPM) in the differentiated cells compared to either the undifferentiated cells or any of the cancer cell lines (Figure 5a). qPCR validation of the RNA-seq results showed relative decreased expression of all four myomirs in the differentiated skeletal muscle biological replicate 2 sample (Figure 5b). qPCR data showed no

discernible pattern in myomir expression between undifferentiated skeletal muscle cells and the rhabdomyosarcoma cell lines.

To investigate expression of miRNAs other than myomirs, we compared the miRNA transcription profiles of the same 8 cell lines from Figure 3. Hierarchical clustering of all miRNAs analyzed showed that the normal skeletal muscle cells, both undifferentiated and differentiated, cluster apart from the cancer cells, with one exception (Figure 6). Undifferentiated skeletal muscle biological replicate 2 clusters most closely with alveolar rhabdomyosarcoma cell line Rh30. Whether these data represent sample contamination, mislabeling, or actual biological variation between the cells is unknown. Further study is needed to determine the absolute similarities and differences in the miRNA transcriptomes of these cells.

Between RD cells and undifferentiated skeletal muscle cells, there were 71 miRNAs that were differentially regulated (Figure 7, Table 3). Rh30 cells also had 71 differentially regulated miRNAs compared to undifferentiated skeletal muscle cells (Table 4). Between them, 42 of those were consensus miRNAs, overlapping in both comparisons (Table 5).

When compared to the differentiated skeletal muscle cells, RD cells had 81 differentially regulated miRNAs, and Rh30 had 130, with 40 consensus miRNAs (Table 6, Table 7, Table 8). Between the 42 consensus miRNA that were significantly different when comparing both RMS cell lines to undifferentiated skeletal muscle cells, and the 40 consensus miRNAs that were significantly different when comparing

RMS cell lines to differentiated skeletal muscle cells, four consensus miRNAs were identified, miR-146a, miR-204, let-7f, and let-7i (Figure 7, Figure 8a, Table 9).

let-7 family members have been implicated in other tumor types. let-7f and let-7i are known to be downregulated in many cancers compared to normal tissue, including lung, breast, liver, and neural tissue, however this is the first time that downregulation of let-7 miRNAs has been associated with RMS(Fassina, et al, 2011,Yan, et al, 2008,Ge, et al, 2014,Lee, et al, 2011). let-7 acts as a tumor suppressor by targeting the well characterized RAS family oncogenes and HMGA2, which regulates chromatin architecture and is associated with a cancer phenotype(Kumar, et al, 2008), (Shell, et al, 2007).Downregulation of the let-7 miRNAs was validated by qPCR (Figure 8b.).

miR-146a was also found to be downregulated in cancer cells compared to skeletal muscle cells. miR-146a is well studied, and has been linked to cancer on numerous occasions, but can act as both an oncogene or a tumor suppressor. miR-146a has been found to be downregulated in lung cancer (Cornett and Lutz, 2014), triple negative breast cancer(Berber, et al, 2014), colorectal cancer(Bao, et al, 2014) and hepatocellular carcinoma(Huang, et al, 2014). miR-146a has a reciprocal relationship with MyD88, which is associated with ovarian tumors(d'Adhemar, et al, 2014). These studies correlate with ours in that miR-146a expression is lower in cancer tissue than normal tissue. However, miR-146a has been found to be upregulated in basal-like breast cancer cells, and leads to cancer cell proliferation in vitro(Sandhu, et al, 2014). Furthermore, miR-146a has been found to delay

differentiation of mouse myoblasts by inhibiting Numb(Kuang, et al, 2009). Additionally, a recent publication showed that HMOX1, which inhibits myoblast differentiation by downregulating myomirs, induces expression of miR-146a (Kozakowska, et al, 2012), suggesting that miR-146a is associated with a less differentiated phenotype. The situation is complicated by the fact that miR-146a contains a G>C polymorphism, which may change patients' susceptibility to some cancers (Fan and Wu, 2014). miR-146a has not previously been tied to rhabdomyosarcoma.

miR-204 can also act as either an oncogene or tumor suppressor. miR-204 is downregulated in buccal cancer(De Sarkar, et al, 2014) clear cell renal cell carcinoma(Munari, et al, 2014), and melanoma(Kozubek, et al, 2013). Clinically, lower expression correlates with a poor prognosis in breast cancer(Li, et al, 2014), and downregulation increases invasion of nasopharyngeal carcinoma cells(Ma, et al, 2014). Similarly, miR-204 has been shown to cause pancreatic cell death (Chen, et al, 2013b) , inhibit invasion of gastric cells(Zhang, et al, 2013)

and inhibit epithelial to mesenchymal transition in intrahepatic cholangiocarcinoma cells(Qiu, et al, 2013). Mechanistically, miR-204 targets SOX4 to promote proliferation and invasion (Zhou, et al, 2014). However, miR-204 can also contribute to invasion, proliferation, and tumor growth of endometrial cells, and high expression is associated with lymph node metastasis (Bao, et al, 2013). Additionally, the miRNA is significantly upregulated in serum of endometrial cancer patients compared to healthy controls (Jia, et al, 2013).

ERMS cells and ARMS cells have unique miRNA transcriptomes

Another goal of this study was to identify the possible differences in miRNA expression between the two major subtypes of RMS, embryonal and alveolar. One theory about rhabdomyosarcoma suggests that the more aggressive alveolar subtype is in a less differentiated state than the embryonal subtype (Begum, et al, 2005). Upon comparing the ERMS cell line RD to the ARMS cell line Rh30, RNA-seq data shows expression levels of miR-1 to be higher in RD cells than in Rh30 cells, but for the other three myomirs (miR-133a and b, and miR-206), the alveolar subtype has more reads per million (Figure 9a). qPCR data also showed higher miR-1 expression in embryonal cells compared to alveolar cells, but the other three myomirs showed no significant pattern (Figure 9b).

The next step was to look for non-myomirs that were differentially regulated between the two cell lines. RNA-seq analysis revealed 94 miRNAs that were differentially regulated (Figure 10, Table 10). Among those were six members of the let-7 family of miRNAs (Figure 11). In every case, the reads per million for each let-7 family member were higher in the alveolar subtype than in the embryonal cell line.

Additionally, and quite strikingly, almost 40% (37 of 94) of the differentially regulated miRNAs came from one chromosome, chromosome 14. This phenomenon will be discussed further in the following chapter.

DISCUSSION

Before we could investigate the differences between normal cells and cancer cells, it was necessary to establish the landscape of miRNA expression in normal

skeletal muscle cells, both differentiated and undifferentiated. The four muscle specific myomirs were all upregulated in differentiated cells compared to undifferentiated cells, including myomirs 133a and 133b. There is currently debate as to whether miR-133a and b act as inhibitors or promoters of myogenesis (Chen, et al, 2006), (Rao, et al, 2010), but the data presented here support the expression of miR-133a and 133b in a more differentiated phenotype. In all instances, the undifferentiated skeletal muscle cell line 2 has lower relative qPCR expression than would be predicted by the corresponding RPM values, which could be due to artificially high RNA-seq read, but is more likely a consequence of sample degradation between the RNA-seq and qPCR experiments.

In order to identify miRNAs associated with a cancer phenotype, we compared miRNA profiles of RMS cell lines to the profiles of normal skeletal muscle cells. Because RMS cells have markers of undifferentiated skeletal muscle cells, we expected myomir levels in RMS cell lines to more closely resemble undifferentiated cells than differentiated cells. However, qPCR analysis of myomir levels in skeletal muscle cells and RMS cell lines only showed correlation in miR-1. This could indicated that the mechanism by which RMS blocks terminal differentiation is downstream or otherwise unrelated to myomir function.

In the RMS field, it has been proposed that ARMS tumors are less differentiated than their ERMS counterparts(Begum, et al, 2005). It would therefore be expected that expression of myomirs would be higher in ERMS cell lines than ARMS cell lines. This was the case for miRNA-1, but for miRNA-206 and 133a and b, the

ARMS cells had higher myomir expression (Figure 5a and b, Figure 9a and b). The theory that ARMS cells are less differentiated than ERMS cells is based on phenotypic data, which may not correlate molecularly with myogenic state. The applicability of our data is limited here, but it can be stated that ARMS cells do not necessarily express lower levels of myomirs than their ERMS counterparts.

In the case of both let-7i and let-7f, there is a significant difference not only between the differentiated and undifferentiated skeletal muscle cells, but also between the skeletal muscle cells and the cancer cell lines, with the differentiating cells having the highest expression, followed by the undifferentiated cells, and lowest of all, the cancer cells (Figure 8). Low levels of let-7i and let-7f may prove to be useful biomarkers of RMS.

Several let-7 miRNAs were also differentially regulated between the ERMS cell line RD and the ARMS cell line Rh30, and in all cases the miRNA levels were higher in ARMS cell line Rh30 (Figure 11). While direct comparison between two cultured lines provides limited information, the non-myomir miRNAs that were downregulated in cancer cells were not necessarily more down regulated in the more aggressive ARMS cell lines. This suggests that these miRNAs correlate with RMS in general, and do not necessarily distinguish between subtypes. miRNA profiling on a larger sample of cell lines and tumors needs to be examined to understand how the expression of these miRNAs relates to RMS subtype.

METHODS

Cell culture of primary cells and cell lines

Human primary skeletal muscle cells from the abdominal oblique of a 48-year-old female were purchased from Zen Bio, Inc. Cells were expanded using Zen Bio Skeletal Muscle Cell Growth Medium. RD, Rh30, Rh28 and Rh18 cells were grown in DMEM supplemented with 10% FBS, amphotericin, penicillin, streptomycin, and L-glutamine. RD. All cells were maintained at 37° C, 5% CO_2.

Generation of differentiation primary skeletal muscle cells

Primary muscle cells were plated in Skeletal Muscle Growth Medium until they were 80-90% confluent. Cells were then changed to Skeletal Muscle Cell Differentiation Medium (Zen Bio). Medium was changed every other day. Differentiated cells were harvested 6 days later.

Western blot analysis

Cells were lysed directly in the dish by washing twice with PBS then adding RIPA buffer supplemented with Roshe's EDTA-free protease inhibitor cocktail. Cells were incubated at 4° C for 10 minutes. Plates were scraped and lysates was transferred to microtube, then centrifuged at 4° for 10 minutes, 10,000 RPM to remove cell debris. Protein concentration was determined by running a BCA assay (Thermo Pierce). 20ug of protein were run on a 4-12% NuPage Bis-Tris gel (Life Technologies) in NuPage MOPS SDS Running Buffer (Life Technologies). Gels were transferred to

nitrocellulose membranes in NuPage transfer buffer (both from Life Technologies) at, 150 mV for 1.5 hours. Blots were blocked with 4% milk for 1 hour. Antibodies were used as follows: β-actin, 1/10,000 (Santa Cruz), and Myosin, 1/1000 (MF20, Upstate) β-actin was incubated at room temperature for one hour, and Myosin incubated at 4° C overnight. After washing, the Myosin blot was incubated with a mouse secondary antibody (Dako Corporation) for one hour at room temperature. Blots were developed with West Femto (Thermo Scientific) using either photo-sensitive film (Kodak) or Bio-Rad's ChemiDoc MP Imaging System.

RNA harvesting and extraction, and sample preparation

RNA was harvested and isolated using a standard TRIzol (Life Technologies)-chloroform protocol, and concentration and purity were tested by 260/280 optical density using a Nanodrop. Samples were prepped for sequencing using Illumina's Truseq Small RNA protocol, adapted from Lu et al, 2009. Briefly, 3' and 5' adapters were ligated to 10ug total RNA, then underwent reverse transcription and PCR amplification for 16 cycles. Unique. bar-coded PCR primers were used to identify individual samples. Small cDNAs were purified using acrylamide gel separation, and cleaned using Gel Breaker tubes and filtration.

High throughput sequencing

After the barcoded samples were quality control checked using Agilnet Technology's chip-based capillary electrophoresis, multiplexed and sequenced for 36

cycles using the Illumina Genome Anlayzer II, available at the UCSD sequencing core.

Processing small RNA-seq data

After standard processing through Illumina software, sequenced reads were returned in FASTA format. Linker sequences were removed from raw reads, leaving 18-25 base pair sequences that were mapped to the human genome (NCBI BUILD 36/HG18) using the algorithm Bowtie v.0.12.2 (Langmead et al). Sequences with up to two mismatches were included for miRNA expression level analysis. Reads that map to genomic repeats or more than 20 loci in the genome were excluded from the dataset.

Analysis of small RNA-seq data

For analysis, reads per million (RPM) were mapped for each miRNA; those with <1 RPM were discarded. The RPM for every miRNA was calculated for each cell line and averaged between the two paired lines. Average RPM for each paired line was compared to the average RPM of other paired lines. miRNAs with a z score of >1.96 or <-1.96, or with t test values >.05 were labeled as significantly different.

Reverse Transcription PCR and Quantitative Real-Time PCR

RNA was harvested and isolated using a standard TRIzol (Life Technologies)-chloroform protocol, quantified via Nanodrop (Thermo Scientific), and DNAse treated (Invitrogen). Reverse Transcription was performed using Applied Biosystems'

TaqMan miRNA Reverse Transcription Kit, and quantified on BioRad's CFX96 Real Time Thermocycler using Applied Biosystems' TaqMan miRNA Assays. RNU6B was used as an endogenous control. U6, an evolutionarily conserved, ubiquitous component of the spliceosome, will be used as a control for RNA loading.

Hierarchical clustering

A modified version of the matlab clustergram function was utilized to calculate the linkage between tissue-culture samples based on their small RNA expression profiles as determined via small RNA-Seq, described herein. The distance between sample datasets, and between small RNAs, was computed using a Euclidean distance metric to perform unsupervised hierarchical clustering. The resulting dendograms and corresponding heatmap are displayed along with the RPM expression range.

ACKNOWLEDGEMENTS

Data from this Chapter are currently being prepared for submission as a publication. Muir, Shannon; Wilbert, Melissa; Nathanson, Jason; Yeo, Gene W.; Furnari, Frank; Cavenee, Webster; Arden, Karen C. The dissertation author was the primary investigator and author of this material.

FIGURES

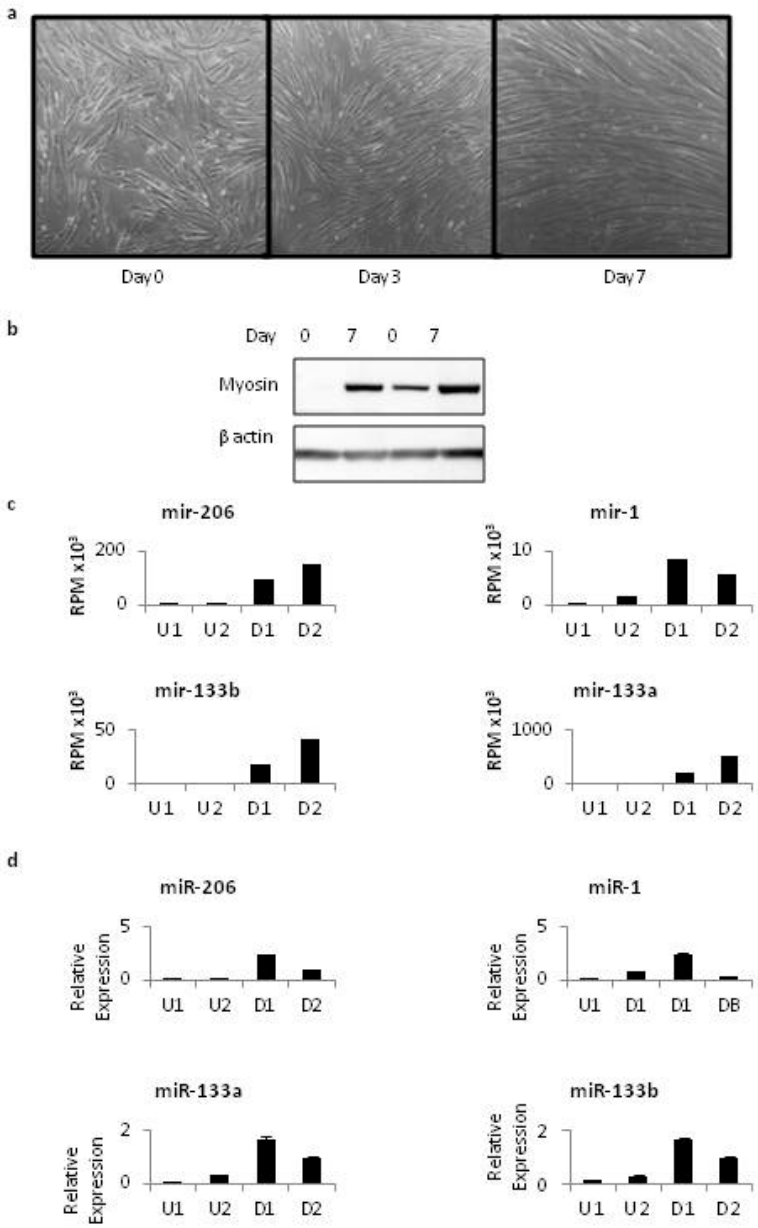

Figure 3. Differentiation and myomir analysis in cultured primary SKMCs
a. Primary skeletal muscle cells were cultured in differentiation media for seven days and brightfield images were taken at days 0, 3, and 7. b. Western blot analysis of relative expression of myosin heavy chain, a marker of terminal muscle cell differentiation. c. Small RNA-seq data displayed as reads per million (RPM). d. qPCR validation of small RNA-seq results. Error bars = standard error of the mean of three technical replicates. U 1= undifferentiated primary skeletal muscle cell biological replicate 1;U-2 = biological replicate 2; D 1= differentiated primary skeletal muscle cell biological replicate 1; D 2 = biological replicate 2.

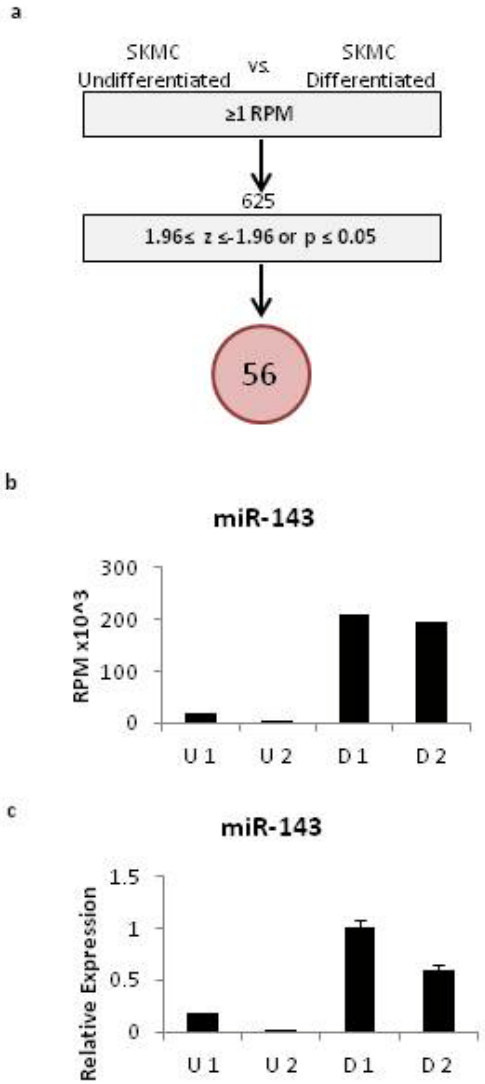

Figure 4.Differential expression of miRs in differentiated and undifferentiated SKMCs
a. After removing miRs with fewer than one read per million (RPM) from analysis, 625 unique miRNAs were compared for their expression in differentiated and undifferentiated skeletal muscle cells. miRNAs with a z score of ≥ 1.96 or ≤=1.96, or miRNAs with a p value of ≤ 0.05 were considered significant. b. Small RNA-seq data showing two significantly differentially regulated miRNAs displayed in reads per million (RPM) c. qPCR data validating the results from b. Error bars represent standard error of the mean of three technical replicates.

.

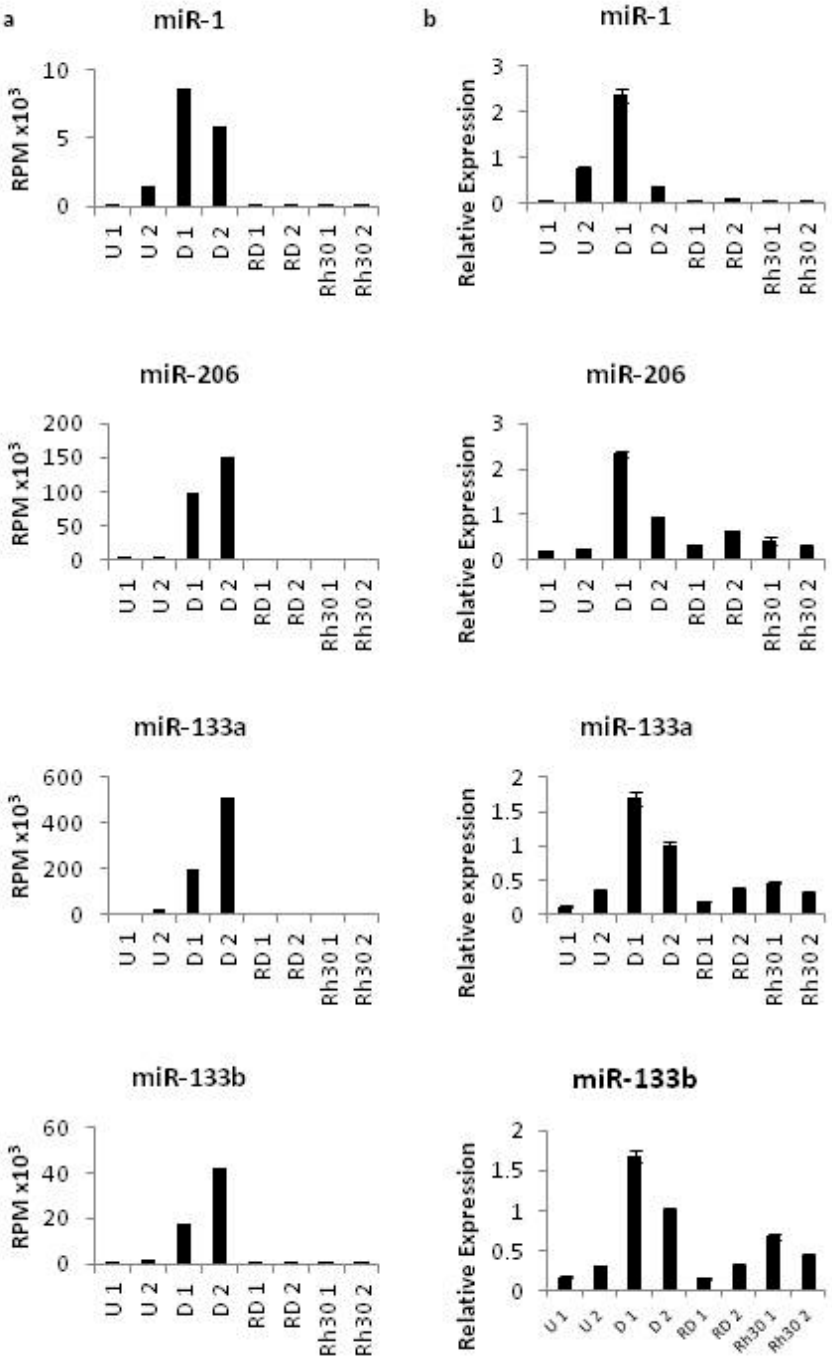

Figure 5. Comparison of myomir expression in normal SKMCs and RMS cell lines
a. Myomir expression as measured by reads per million (RPM). b. qPCR data on the same samples from a. Error bars represent standard error of the mean for three technical replicates

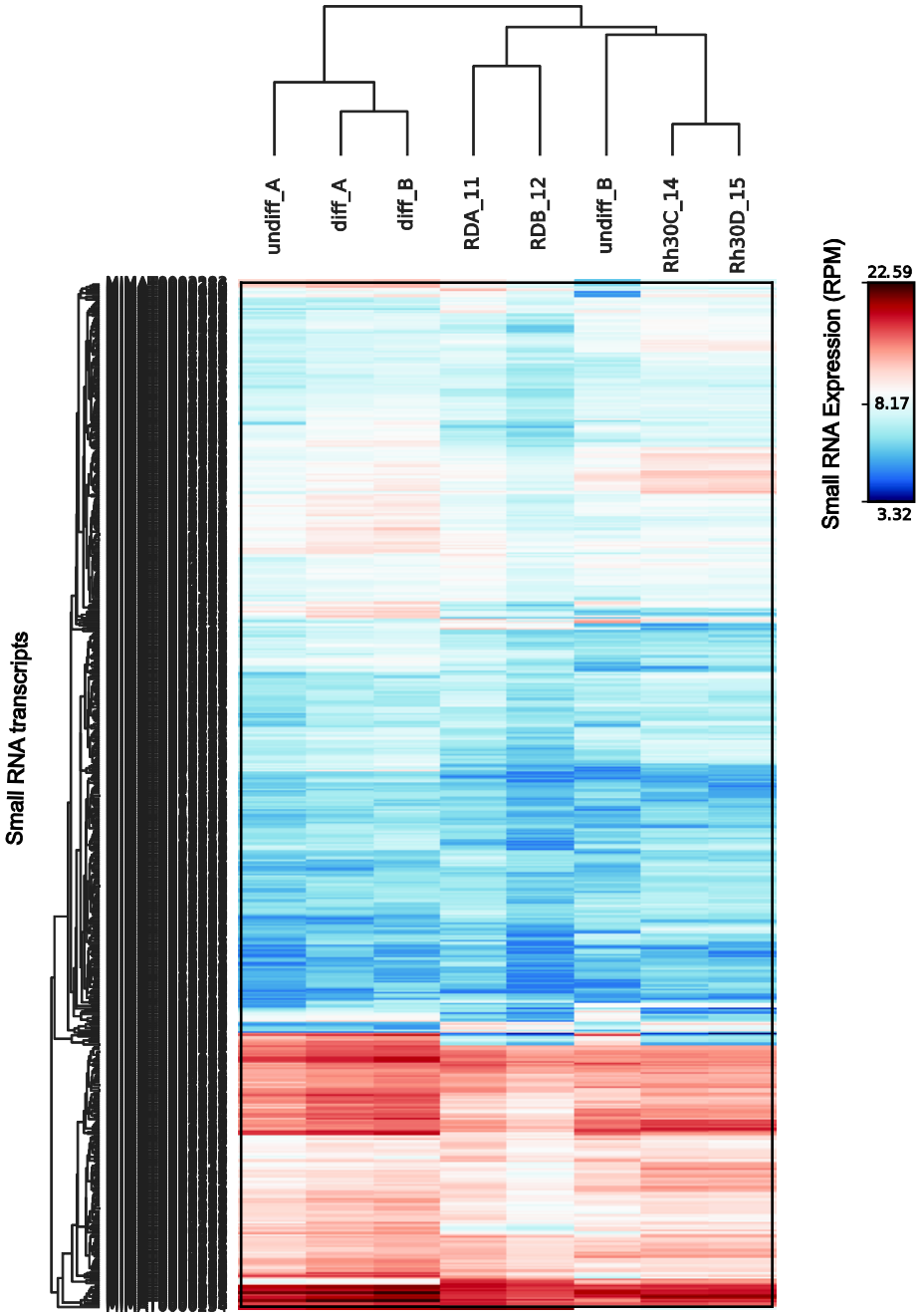

Figure 6. Hierarchical clustering of SKMCs and RMS cells based on miRNA expression profiles

Unsupervised hierarchical clustering was used to group datasets based on their small RNA-seq gene expression profiles. The relative distance of related datasets is measured by the dendograph and small-RNA expression levels (RPM) scale given to the right.

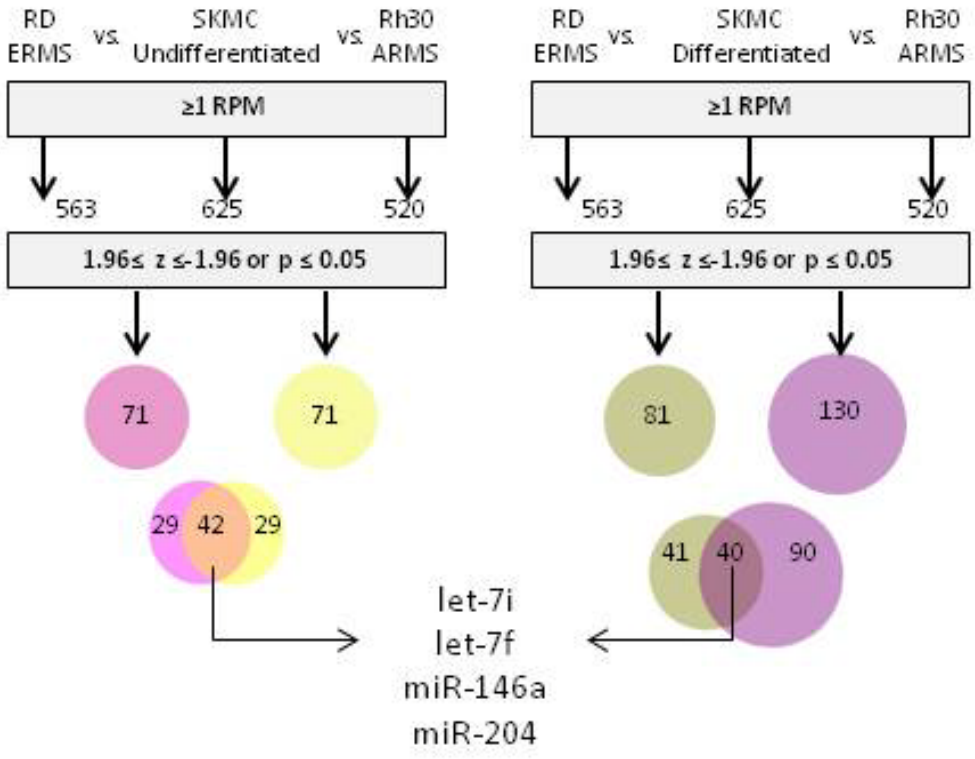

Figure 7. Schematic of comparison between differentiated and undifferentiated SKMCs to ERMS and ARMS cells

miRs with fewer than 1 RPM were excluded from analysis. miRNAs with a z score of≥ 1.96 or ≤ -1.96, or miRNAs with a p value of ≤ 0.05 were considered significant.

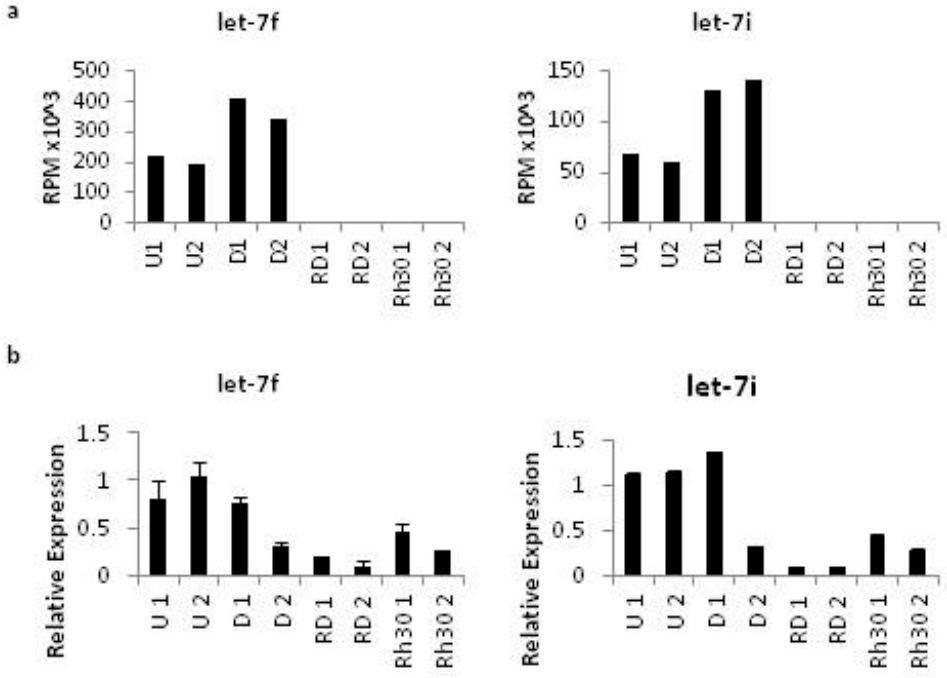

Figure 8. miRNAs differentially expressed between normal cells and RMS cell lines.
a. RNA-seq data for two significantly differently expressed miRNAs in RPM. b. qPCR data from the same samples as a. Error bars represent standard error of the mean over three technical replicates.

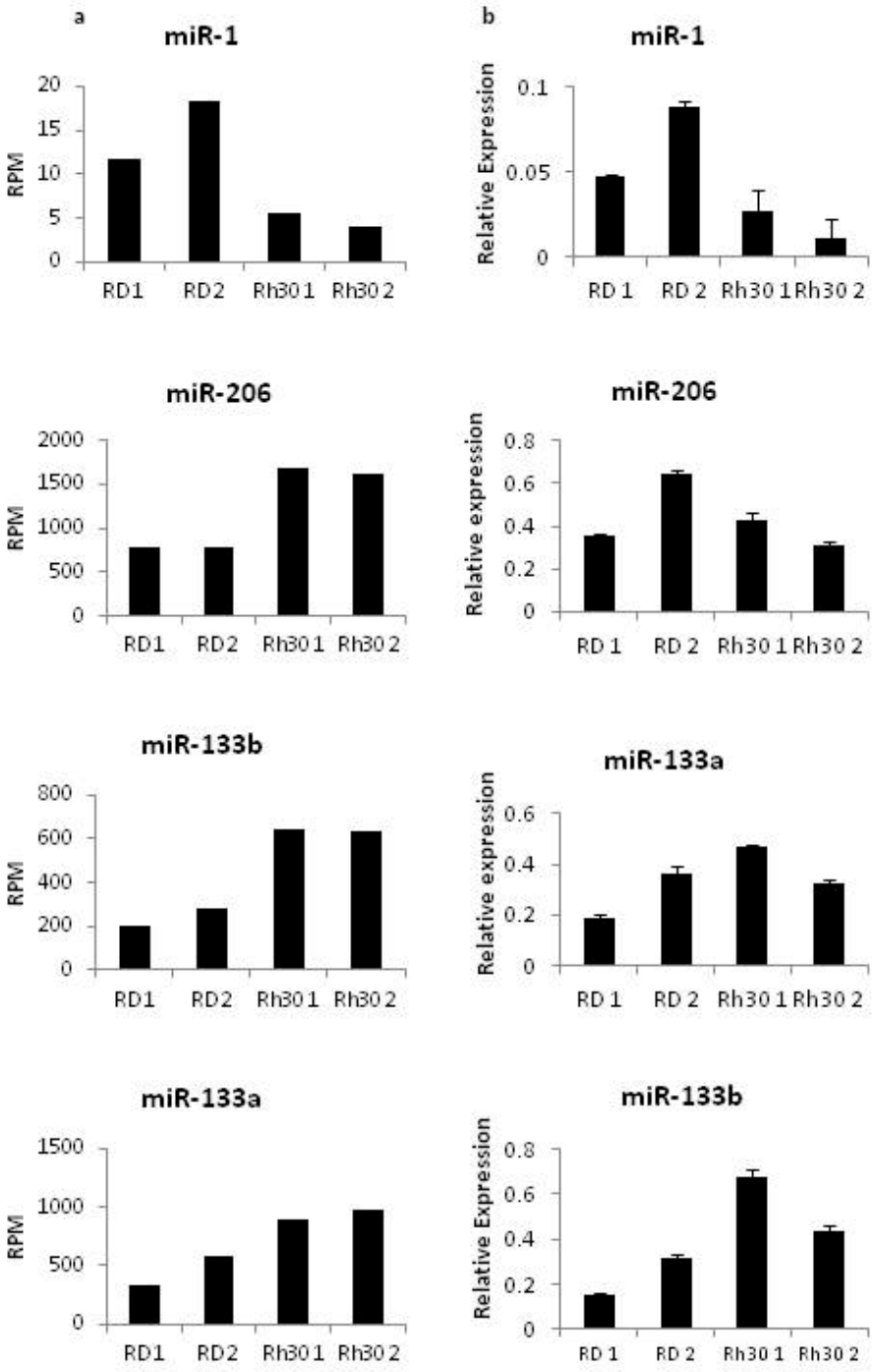

Figure 9. Myomir expression in ERMS cell line RD vs. ARMS cell line Rh30
a. RNA-seq data measuring expression in RPM. b. qPCR validation of samples in a.

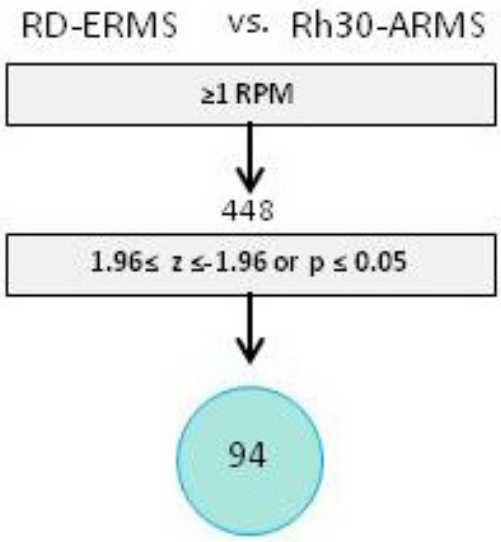

Figure 10. Schematic of RD vs. Rh30 miRNA expression

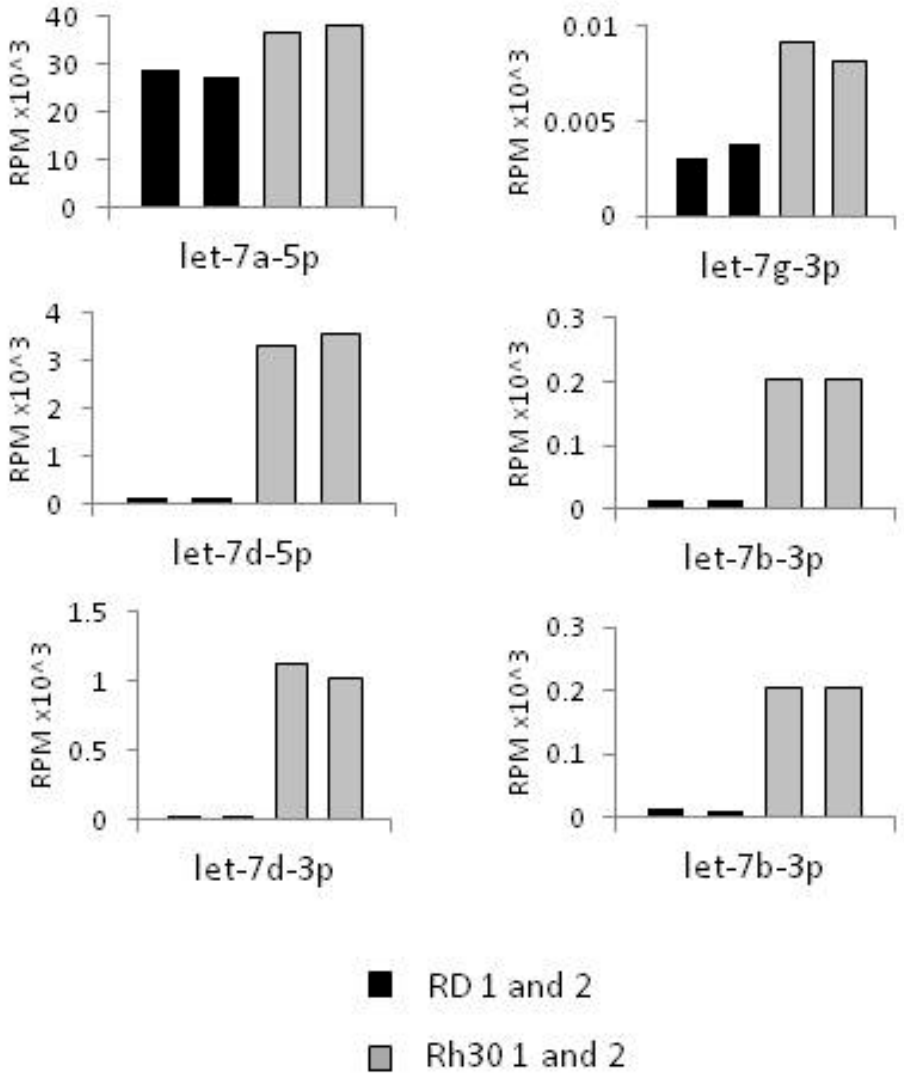

Figure 11. Differentially regulated miRNAs in ERMS vs. ARMS
RNA-seq data of six let-7 family members that had differential expression between ERMS and ARMS cell lines, as RPM.

TABLES

Table 1. Undifferentiated vs. Differentiated Skeletal Muscle Cells: myomirs

miRNA	U 1	U 2	D 1	D 2	ln(avg/avg)	z score	t test
miR-1	231	1513	8561	5881	-2.114	-1.523	0.088
miR-133a	7885	24297	196388	509649	-3.088	-2.476	0.276
miR-133b	954	1591	17799	42020	-3.157	-2.543	0.255
miR-206	4828	5671	97406	150643	-3.162	-2.548	0.140

Table 2. Undifferentiated vs. Differentiated Skeletal Muscle Cells

miRNA	U 1	U 2	D 1	D 2	ln(avg/avg)	z score	t test
let-7i-5p	67528	60477	131817	141237	-0.758	-0.197	0.009
miR-107	4009	2530	7815	8929	-0.940	-0.375	0.037
miR-1237	7	7	19	18	-0.957	-0.392	0.005
miR-1247-3p	38	27	4	10	1.572	2.081	0.087
miR-1266	6	143	14	9	1.868	2.371	0.526
miR-133a	7885	24297	196388	509649	-3.088	-2.476	0.276
miR-133b	954	1591	17799	42020	-3.157	-2.543	0.255
miR-139-5p	12	103	554	1455	-2.860	-2.253	0.280
miR-140-3p	148	122	339	358	-0.947	-0.382	0.008
miR-143-3p	19745	473	208664	196032	-2.997	-2.386	0.007
miR-145-5p	153	1	1617	2401	-3.263	-2.646	0.117
miR-146b-5p	1387	78	4711	5559	-1.947	-1.360	0.042
miR-148b-5p	146	122	387	382	-1.054	-0.487	0.024
miR-181d	552	619	1637	1652	-1.033	-0.466	0.015
miR-182-5p	3002	41258	3752	4032	1.738	2.244	0.515
miR-183-3p	4	65	5	2	2.281	2.775	0.495
miR-183-5p	304	8423	560	649	1.977	2.477	0.524
miR-184	156	7	2926	4814	-3.860	-3.231	0.154
miR-185-5p	267	157	992	795	-1.438	-0.862	0.045
miR-18a-3p	50	546	46	85	1.519	2.030	0.520
miR-18a-5p	37	1693	207	78	1.804	2.308	0.543
miR-1910	15	174	19	17	1.669	2.176	0.513
miR-194-3p	3	1	14	18	-2.079	-1.489	0.049
miR-206	4828	5671	97406	150643	-3.162	-2.548	0.140
miR-208b	28	72	3113	2448	-4.018	-3.385	0.076
miR-22-5p	616	26	1766	2246	-1.832	-1.247	0.051
miR-3065-3p	111	98	216	223	-0.745	-0.185	0.009
miR-30b-3p	151	175	260	244	-0.436	0.118	0.036
miR-30e-5p	239	285	678	614	-0.902	-0.338	0.014
miR-3180-3p	86	19	606	1067	-2.773	-2.168	0.176
miR-335-3p	532	63041	1040	1097	3.393	3.862	0.506
miR-335-5p	70	5273	206	59	3.006	3.483	0.508
miR-34a-5p	4333	2748	12762	10534	-1.191	-0.620	0.034
miR-3676-3p	7	4	41	42	-2.019	-1.430	0.018
miR-3681-5p	2	1	66	80	-3.885	-3.255	0.061
miR-374a-5p	426	394	1444	1392	-1.240	-0.668	0.003
miR-375	73	24101	52	113	4.987	5.421	0.500
miR-376a-5p	59	45	116	107	-0.768	-0.206	0.033
miR-3912	7	6	11	10	-0.480	0.075	0.030

Table 2. Undifferentiated vs. Differentiated Skeletal Muscle Cells, Continued

miRNA	U 1	U 2	D 1	D 2	ln(avg/avg)	z score	t test
miR-421	2234	1554	7330	7353	-1.355	-0.781	0.039
miR-449a	33	34	48	51	-0.385	0.167	0.028
miR-4682	6	1	32	39	-2.303	-1.707	0.024
miR-4741	6	3	37	38	-2.120	-1.529	0.017
miR-509-3p	2	790	13	54	2.456	2.945	0.527
miR-542-5p	191	87	855	1006	-1.901	-1.315	0.019
miR-548ar-3p	6	18	2	1	2.058	2.557	0.324
miR-5683	13	5	94	75	-2.240	-1.646	0.048
miR-577	3	532	39	32	2.029	2.529	0.541
miR-652-5p	2	45	1	5	2.058	2.557	0.514
miR-767-5p	1	49	1	2	2.813	3.295	0.507
miR-769-3p	69	83	251	264	-1.226	-0.655	0.003
miR-769-5p	13948	8991	27248	32550	-0.958	-0.393	0.037
miR-937	41	36	132	147	-1.294	-0.721	0.028
miR-9-5p	18	17097	66	76	4.791	5.229	0.502
miR-96-5p	14	138	11	2	2.459	2.949	0.463
miR-99a-3p	53	26	161	169	-1.428	-0.852	0.049

Table 3. RD ERMS vs. Undifferentiated Skeletal Muscle Cells

miRNA	U 1	U 2	RD 1	RD 2	ln(avg/avg)	z score	t test
let-7a-3p	678	590	50	31	2.753	0.344	0.039
let-7b-3p	9191	3570	15	13	6.128	2.950	0.265
let-7b-5p	196411	84308	309	260	6.201	3.006	0.242
let-7d-3p	3522	4237	29	28	4.912	2.011	0.059
let-7d-5p	27369	40928	156	150	5.411	2.396	0.125
let-7f-5p	220549	194851	2895	1407	4.570	1.747	0.039
let-7i-3p	237	252	1	2	5.046	2.115	0.019
let-7i-5p	67528	60477	890	499	4.523	1.711	0.035
miR-101-3p	3472	3745	461	119	2.522	0.165	0.005
miR-10b-5p	442370	827	271226	405526	-0.423	-2.109	0.691
miR-1227	18	17	3	2	1.908	-0.309	0.009
miR-1254	57	56	11	8	1.733	-0.444	0.011
miR-1260a	510	536	23	15	3.325	0.786	0.009
miR-126-5p	634	156	1635	559	-1.021	-2.571	0.399
miR-1271-5p	400	385	4	5	4.508	1.699	0.012
miR-127-3p	421941	462503	21985	23358	2.971	0.512	0.031
miR-140-5p	152	171	16	2	2.900	0.457	0.009
miR-146a-5p	906	19	3	3	5.077	2.138	0.489
miR-148b-5p	146	122	30	15	1.774	-0.412	0.025
miR-154-5p	129	149	5	4	3.478	0.903	0.046
miR-15a-5p	724	668	75	19	2.692	0.297	0.004
miR-16-5p	35543	38833	6545	2801	2.074	-0.181	0.006
miR-181d	552	619	43	27	2.817	0.393	0.031
miR-182-5p	3002	41258	63604	46643	-0.913	-2.487	0.307
miR-183-3p	4	65	114	65	-0.960	-2.524	0.296
miR-183-5p	304	8423	25577	26393	-1.784	-3.160	0.115
miR-196b-5p	310	76	627	261	-0.833	-2.426	0.385
miR-199b-5p	115	107	3	1	3.841	1.184	0.015
miR-204-5p	17168	569	29	27	5.766	2.671	0.480
miR-23a-5p	1564	197	7	4	5.098	2.154	0.422
miR-3065-3p	111	98	33	15	1.468	-0.649	0.022
miR-3065-5p	9	10	4	3	1.143	-0.900	0.012
miR-30b-3p	151	175	6	3	3.596	0.995	0.047
miR-30c-5p	17122	16324	1659	1174	2.468	0.124	0.003
miR-30d-3p	410	502	77	45	2.013	-0.227	0.050
miR-30e-3p	4485	4577	806	456	1.971	-0.260	0.020
miR-3130-5p	8	6	1	2	1.539	-0.594	0.050
miR-376a-5p	59	45	116	107	-0.768	-0.206	0.033
miR-3158-3p	401	429	32	16	2.835	0.407	0.005

Table 3. RD ERMS vs. Undifferentiated Skeletal Muscle Cells, Continued

miRNA	U 1	U 2	RD 1	RD 2	ln(avg/avg)	z score	t test
miR-31-5p	30126	313	152	79	4.882	1.988	0.496
miR-320b	196	214	66	55	1.221	-0.839	0.011
miR-330-3p	66	58	9	7	2.066	-0.187	0.030
miR-338-3p	9	10	4	3	1.143	-0.900	0.012
miR-339-3p	1161	1315	181	118	2.116	-0.148	0.023
miR-340-3p	222	235	53	29	1.721	-0.453	0.014
miR-342-3p	967	821	88	118	2.162	-0.113	0.050
miR-3661	112	117	4	3	3.592	0.992	0.012
miR-3681-5p	2	1	41	22	-3.038	-4.129	0.197
miR-374a-5p	426	394	115	54	1.583	-0.560	0.025
miR-3938	3	3	12	8	-1.236	-2.737	0.160
miR-3939	9	5	12	8	-0.352	-2.054	0.420
miR-450b-5p	832	871	99	44	2.476	0.130	0.003
miR-4677-3p	340	318	24	8	3.048	0.572	0.003
miR-4741	6	3	11	16	-1.113	-2.642	0.112
miR-4786-5p	13	6	20	10	-0.448	-2.128	0.495
miR-5001-3p	10	9	4	5	0.736	-1.214	0.049
miR-504	41	29	144	162	-1.482	-2.927	0.014
miR-509-3p	2	790	3	2	5.033	2.104	0.500
miR-542-3p	493	438	54	14	2.616	0.238	0.008
miR-548e	34	44	12	3	1.667	-0.495	0.044
miR-550a-3p	123	127	17	10	2.220	-0.068	0.002
miR-550b-2-5	82	85	11	7	2.201	-0.083	0.003
miR-576-5p	103	95	6	3	3.197	0.687	0.014
miR-584-5p	234	1462	4	1	5.817	2.710	0.400
miR-744-3p	171	162	14	11	2.593	0.220	0.011
miR-767-5p	1	49	743	482	-3.199	-4.253	0.130
miR-769-3p	69	83	23	8	1.596	-0.550	0.027
miR-873-3p	115	544	877	665	-0.850	-2.439	0.251
miR-873-5p	8	111	122	37	-0.289	-2.005	0.794
miR-9-5p	18	17097	45	17	5.631	2.566	0.500
miR-96-5p	14	138	336	239	-1.331	-2.810	0.122

Table 4. Rh30 ARMS vs. Undifferentiated Skeletal Muscle Cells

miRNA	U 1	U 2	RD 1	RD 2	ln(avg/avg)	z score	t test
let-7a-3p	678	590	31	28	3.059	0.863	0.046
let-7f-1-3p	456	501	38	38	2.540	0.445	0.033
let-7f-5p	220549	194851	12550	8018	3.006	0.819	0.036
let-7i-3p	237	252	11	14	2.988	0.805	0.017
let-7i-5p	67528	60477	2577	2504	3.227	0.997	0.036
miR-1	231	1513	6	4	5.202	2.586	0.405
miR-100-5p	923695	5886	3108	4308	4.831	2.288	0.498
miR-101-3p	3472	3745	351	235	2.513	0.423	0.011
miR-10b-5p	442370	827	24	40	8.832	5.506	0.499
miR-1226-3p	102	101	20	17	1.689	-0.240	0.009
miR-1227	18	17	6	8	0.882	-0.888	0.022
miR-1254	57	56	22	21	0.978	-0.811	0.000
miR-1260a	510	536	83	78	1.875	-0.090	0.015
miR-1271-5p	400	385	27	17	2.892	0.728	0.001
miR-127-3p	421941	462503	185532	171252	0.908	-0.868	0.030
miR-140-5p	152	171	7	4	3.395	1.132	0.036
miR-143-3p	19745	473	81	70	4.895	2.339	0.487
miR-146a-5p	906	19	2	1	5.550	2.865	0.488
miR-146b-5p	1387	78	3	6	5.098	2.502	0.466
miR-149-5p	1156	1342	1935	2042	-0.465	-1.972	0.036
miR-152	4877	146	17	30	4.667	2.156	0.484
miR-15a-5p	724	668	41	24	3.066	0.868	0.017
miR-16-5p	35543	38833	3397	2065	2.611	0.502	0.014
miR-181d	552	619	58	40	2.487	0.402	0.029
miR-184	156	7	135	134	-0.501	-2.001	0.607
miR-196a-5p	2145	21	13	12	4.485	2.009	0.497
miR-204-5p	17168	569	4	2	8.007	4.842	0.479
miR-20b-5p	7	11	48	21	-1.346	-2.680	0.310
miR-221-3p	265289	187	488	860	5.283	2.651	0.501
miR-221-5p	3906	5	5	10	5.568	2.880	0.500
miR-29a-3p	65487	301	271	423	4.552	2.063	0.500
miR-3065-3p	111	98	29	39	1.117	-0.700	0.015
miR-3065-5p	9	10	5	4	0.712	-1.026	0.029
miR-30b-3p	151	175	21	15	2.201	0.172	0.042
miR-30c-5p	17122	16324	1322	1265	2.559	0.461	0.016
miR-30d-3p	410	502	61	28	2.332	0.278	0.046
miR-30e-3p	4485	4577	472	389	2.353	0.294	0.000
miR-376a-5p	59	45	116	107	-0.768	-0.206	0.033
miR-3158-3p	401	429	75	76	1.700	-0.230	0.026

Table 4. Rh30 ARMS vs. Undifferentiated Skeletal Muscle Cells, Continued

miRNA	U 1	U 2	RD 1	RD 2	ln(avg/avg)	z score	t test
miR-3173-5p	6	5	1	1	1.468	-0.417	0.045
miR-320b	196	214	25	35	1.937	-0.040	0.009
miR-330-3p	66	58	17	20	1.209	-0.625	0.028
miR-338-3p	9	10	5	4	0.712	-1.026	0.029
miR-339-3p	1161	1315	82	89	2.670	0.550	0.042
miR-340-3p	222	235	27	19	2.309	0.259	0.003
miR-342-3p	967	821	103	154	1.939	-0.038	0.039
miR-34c-5p	1510	365	3	3	5.724	3.005	0.350
miR-3661	112	117	19	15	1.881	-0.085	0.002
miR-374a-5p	426	394	49	19	2.488	0.403	0.003
miR-374b-3p	78	86	11	9	2.120	0.107	0.024
miR-375	73	24101	6	8	7.496	4.431	0.498
miR-3944-3p	9	8	2	3	1.188	-0.643	0.014
miR-433	120	496	528	507	-0.521	-2.017	0.464
miR-4473	15	14	1	1	2.396	0.329	0.023
miR-449a	33	34	4	2	2.393	0.327	0.004
miR-450b-5p	832	871	157	59	2.068	0.066	0.022
miR-4677-3p	340	318	14	13	3.159	0.942	0.022
miR-4728-3p	35	33	2	4	2.343	0.287	0.003
miR-4741	6	3	21	18	-1.472	-2.782	0.018
miR-497-5p	569	1644	1	2	6.582	3.696	0.288
miR-5001-3p	10	9	2	1	1.947	-0.032	0.040
miR-542-3p	493	438	77	46	2.020	0.027	0.014
miR-548al	18	19	1	1	2.673	0.552	0.021
miR-550a-3p	123	127	28	31	1.437	-0.442	0.001
miR-550b-2-5	82	85	19	21	1.439	-0.441	0.001
miR-576-5p	103	95	8	6	2.698	0.572	0.021
miR-625-5p	23	19	3	4	1.884	-0.082	0.047
miR-708-3p	245	664	4	2	5.027	2.445	0.276
miR-708-5p	272	740	2	3	5.349	2.704	0.277
miR-744-3p	171	162	26	23	1.912	-0.060	0.014
miR-943	10	10	2	2	1.688	-0.240	0.003

Table 5. Undifferentiated Skeletal Muscle Cells vs RD and vs Rh30 consensus miRNAs

let-7a-3p	miR-127-3p	miR-30c-5p	miR-3661
let-7f-5p	miR-140-5p	miR-30d-3p	miR-374a-5p
let-7i-3p	miR-146a-5p	miR-30e-3p	miR-450b-5p
let-7i-5p	miR-15a-5p	miR-3157-5p	miR-4677-3p
miR-101-3p	miR-16-5p	miR-3158-3p	miR-4741
miR-10b-5p	miR-181d	miR-320b	miR-5001-3p
miR-1227	miR-204-5p	miR-330-3p	miR-542-3p
miR-1254	miR-3065-3p	miR-338-3p	miR-550a-3p
miR-1260a	miR-3065-5p	miR-339-3p	miR-550b-2-5
miR-1271-5p	miR-30b-3p	miR-340-3p	miR-576-5p
			miR-744-3p

Table 6. Differentiated Skeletal Muscle Cells vs RD Cells

miRNA	DA	DB	RD 1	RD 2	ln(avg/avg)	z score	t test
let-7b-3p	11515	28377	148	66	5.230	2.622	0.256
let-7b-5p	301179	605790	2992	1364	5.338	2.687	0.207
let-7f-1-3p	813	1044	11	5	4.786	2.357	0.079
let-7f-5p	408361	340052	28002	7382	3.052	1.321	0.044
let-7g-5p	99307	115281	11243	3461	2.681	1.099	0.022
let-7i-3p	627	828	12	10	4.192	2.002	0.089
let-7i-5p	131817	141237	8613	2621	3.191	1.404	0.004
miR-1	8561	5881	113	96	4.236	2.028	0.118
miR-10a-3p	913	919	123	24	2.523	1.004	0.037
miR-1185-5p	75	79	4	1	3.426	1.544	0.001
miR-1237	19	18	7	7	0.981	0.083	0.018
miR-125a-3p	1252	1586	526	182	1.389	0.327	0.047
miR-1271-5p	471	430	39	24	2.657	1.085	0.016
miR-1306-5p	73	87	36	20	1.056	0.128	0.043
miR-132-5p	250	234	73	40	1.458	0.368	0.024
miR-133a	196388	509649	3158	3031	4.737	2.327	0.268
miR-143-3p	208664	196032	7573	2252	3.718	1.719	0.008
miR-145-5p	1617	2401	10	8	5.408	2.728	0.123
miR-146a-5p	1549	2599	27	16	4.575	2.231	0.159
miR-146b-3p	255	748	7	6	4.385	2.117	0.294
miR-146b-5p	4711	5559	109	47	4.194	2.003	0.052
miR-152	14298	13746	341	111	4.129	1.964	0.004
miR-181c-5p	7748	8732	359	128	3.521	1.601	0.030
miR-182-5p	3752	4032	615305	244774	-4.705	-3.314	0.261
miR-183-3p	5	2	1100	342	-5.328	-3.686	0.309
miR-183-5p	560	649	247435	138505	-5.766	-3.948	0.176
miR-184	2926	4814	8	9	6.121	3.154	0.153
miR-185-5p	992	795	199	49	1.976	0.678	0.029
miR-1908	743	644	35	25	3.132	1.368	0.046
miR-1910	19	17	622	221	-3.168	-2.395	0.293
miR-195-5p	1027	1002	19	3	4.540	2.210	0.001
miR-199b-5p	215	243	33	7	2.431	0.950	0.008
miR-204-5p	13429	26360	278	141	4.555	2.219	0.202
miR-212-3p	206	238	47	29	1.763	0.550	0.021
miR-21-3p	98924	105891	10388	2271	2.784	1.160	0.003
miR-222-3p	9683	10700	1331	303	2.524	1.005	0.006
miR-22-3p	5467852	6330421	252076	66829	3.611	1.655	0.039
miR-2355-5p	252	247	27	8	2.648	1.079	0.019
miR-376a-5p	59	45	116	107	-0.768	-0.206	0.033

Table 6. Differentiated Skeletal Muscle Cells vs RD Cells, Continued

miRNA	DA	DB	RD 1	RD 2	ln(avg/avg)	z score	t test
miR-24-2-5p	973	859	52	21	3.222	1.423	0.030
miR-24-3p	3	4	70	22	-2.651	-2.087	0.324
miR-24-3p	79451	85215	7415	3182	2.743	1.136	0.003
miR-2682-5p	345	422	3	1	5.257	2.638	0.064
miR-26a-5p	948742	1122636	185542	62631	2.122	0.765	0.018
miR-27b-3p	1700326	1894849	515061	178804	1.645	0.480	0.031
miR-28-5p	7596	9245	1451	356	2.233	0.831	0.025
miR-29b-1-5p	459	556	96	14	2.227	0.828	0.020
miR-3065-5p	3	8	108	33	-2.547	-2.025	0.331
miR-3074-5p	23560	23244	2526	1245	2.519	1.002	0.013
miR-30a-5p	116002	102285	6507	1608	3.292	1.464	0.024
miR-30b-3p	260	244	53	18	1.955	0.666	0.026
miR-30b-5p	10156	12267	2700	865	1.839	0.596	0.022
miR-30e-5p	678	614	158	53	1.808	0.577	0.022
miR-3126-5p	97	87	19	1	2.218	0.822	0.033
miR-31-5p	28055	31341	1472	413	3.451	1.559	0.023
miR-330-3p	204	256	87	35	1.329	0.291	0.045
miR-335-3p-3p	1040	1097	147706	41448	-4.483	-3.181	0.329
miR-335-3p-5p	206	59	8634	1854	-3.680	-2.702	0.373
miR-337-3p	731	874	222	69	1.707	0.517	0.025
miR-337-5p	374	327	59	14	2.269	0.853	0.010
miR-34c-5p	4599	4145	8	1	6.879	3.607	0.033
miR-365b-5p	292	327	107	39	1.445	0.361	0.046
miR-3661	138	162	35	14	1.812	0.580	0.017
miR-3676-3p	41	42	10	10	1.413	0.341	0.006
miR-375	52	113	1849	2486	-3.268	-2.456	0.094
miR-376a-5p	116	107	23	8	1.973	0.676	0.017
miR-381	67605	80996	15844	4845	1.972	0.675	0.020
miR-424-5p	6241	5446	1427	516	1.794	0.569	0.016
miR-4745-5p	11	32	896	170	-3.210	-2.421	0.393
miR-4746-5p	71	68	1256	381	-2.466	-1.976	0.336
miR-4749-3p	7	8	2	1	1.576	0.439	0.024
miR-4775	275	228	74	11	1.778	0.559	0.040
miR-497-5p	716	937	5	9	4.771	2.348	0.085
miR-497-5p	716	937	5	9	4.771	2.348	0.085
miR-503	2195	2656	263	134	2.503	0.993	0.050
miR-542-5p	855	1006	44	14	3.468	1.570	0.045
miR-5683	94	75	20	1	2.085	0.743	0.031
miR-376a-5p	59	45	116	107	-0.768	-0.206	0.033

Table 6. Differentiated Skeletal Muscle Cells vs RD Cells, Continued

miRNA	U 1	U 2	D 1	D 2	ln(avg/avg)	z score	t test
miR-767-5p	1	2	7192	2529	-8.083	-5.332	0.285
miR-873-3p	175	272	8480	3490	-3.288	-2.467	0.260
miR-873-5p	24	21	1177	196	-3.413	-2.542	0.405

Table 7. Differentiated Skeletal Muscle Cells vs. Rh30 Cells

miRNA	U 1	U 2	RD 1	RD 2	ln(avg/avg)	z score	t test
let-7f-5p	408361	340052	119414	75457	1.346	0.502	0.031
let-7g-5p	99307	115281	29435	22383	1.421	0.546	0.033
let-7i-5p	131817	141237	24519	23567	1.737	0.727	0.025
miR-1	8561	5881	53	38	5.067	2.641	0.118
miR-103a-3p	109932	111127	28936	30163	1.319	0.487	0.000
miR-103b	109932	111127	28936	30163	1.319	0.487	0.000
miR-107	7815	8929	1344	1252	1.864	0.800	0.049
miR-10a-3p	913	919	72	58	2.646	1.249	0.001
miR-10b-5p	843529	1134407	231	380	8.082	4.374	0.093
miR-1185-1-3	410	561	5044	4961	-2.333	-1.612	0.002
miR-125b-1-3	26632	24926	2755	1896	2.406	1.111	0.007
miR-126-3p	304	347	207	173	0.538	0.038	0.043
miR-1287	519	577	114	122	1.536	0.611	0.039
miR-132-5p	250	234	17	31	2.310	1.056	0.003
miR-134	3618	4685	10674	10838	-0.952	-0.818	0.047
miR-140-5p	444	371	63	40	2.073	0.920	0.046
miR-143-3p	208664	196032	773	659	5.643	2.973	0.020
miR-145-5p	1617	2401	9	5	5.660	2.982	0.123
miR-146a-5p	1549	2599	21	13	4.802	2.489	0.159
miR-146b-5p	4711	5559	29	56	4.799	2.487	0.053
miR-148b-5p	387	382	85	96	1.447	0.560	0.003
miR-149-3p	2	13	43	50	-1.836	-1.327	0.038
miR-151a-3p	124234	139518	46484	32237	1.209	0.424	0.013
miR-152	14298	13746	162	284	4.141	2.109	0.009
miR-154-3p	10	3	69	86	-2.472	-1.692	0.046
miR-17-5p	6155	5155	2979	2160	0.789	0.182	0.044
miR-181c-5p	7748	8732	1199	1857	1.685	0.697	0.012
miR-181d	1637	1652	550	372	1.271	0.459	0.046
miR-182-5p	3752	4032	88208	91227	-3.138	-2.075	0.011
miR-183-3p	5	2	382	382	-4.693	-2.969	0.002
miR-183-5p	560	649	23202	21628	-3.613	-2.348	0.023
miR-186-5p	120721	125506	35591	27960	1.354	0.507	0.005
miR-18a-3p	46	85	354	349	-1.685	-1.240	0.039
miR-1908	743	644	273	194	1.090	0.355	0.021
miR-193a-3p	1043	996	85	62	2.630	1.241	0.004
miR-195-3p	201	349	1	2	5.211	2.724	0.168
miR-196a-5p	3313	3515	122	109	3.385	1.674	0.019
miR-196b-5p	653	739	99	69	2.117	0.945	0.027
miR-376a-5p	59	45	116	107	-0.768	-0.206	0.033

Table 7 Differentiated Skeletal Muscle cells vs. Rh30 Cells, Continued

miRNA	U 1	U 2	D 1	D 2	ln(avg/avg)	z score	t test
miR-204-5p	13429	26360	34	22	6.566	3.503	0.200
miR-208b	3113	2448	10	5	5.915	3.129	0.076
miR-20b-5p	10	8	461	196	-3.560	-2.317	0.250
miR-212-3p	206	238	24	11	2.541	1.189	0.026
miR-21-3p	98924	105891	28211	30331	1.252	0.449	0.019
miR-218-5p	426	439	7	10	3.959	2.004	0.007
miR-221-3p	268843	396794	4644	8094	3.956	2.003	0.123
miR-221-5p	5601	7113	44	97	4.502	2.316	0.076
miR-222-3p	9683	10700	560	749	2.745	1.307	0.029
miR-22-3p	5467852	6330421	346482	301704	2.902	1.397	0.049
miR-2277-5p	323	342	188	218	0.493	0.012	0.029
miR-2355-5p	252	247	37	30	2.020	0.890	0.001
miR-23a-5p	2147	2077	743	691	1.080	0.350	0.001
miR-24-2-5p	973	859	84	70	2.474	1.151	0.041
miR-24-3p	79451	85215	6293	5620	2.626	1.238	0.022
miR-25-5p	28	73	301	351	-1.865	-1.343	0.015
miR-27b-3p	1700326	1894849	254677	225726	2.013	0.886	0.036
miR-296-5p	224	606	3	12	4.048	2.055	0.278
miR-299-3p	967	625	6312	6073	-2.052	-1.450	0.003
miR-3065-5p	3	8	150	163	-3.347	-2.195	0.013
miR-3074-5p	23560	23244	1704	1514	2.677	1.268	0.000
miR-30a-5p	116002	102285	7478	9899	2.531	1.183	0.038
miR-30e-5p	678	614	188	176	1.268	0.458	0.038
miR-3152-5p	118	130	23	5	2.181	0.983	0.015
miR-31-5p	28055	31341	3196	2879	2.280	1.039	0.037
miR-3187-3p	7	3	22	19	-1.411	-1.082	0.030
miR-3188	38	41	51	53	-0.275	-0.429	0.029
miR-323b-3p	678	1076	9116	9525	-2.364	-1.630	0.001
miR-335-3p-3p	1040	1097	50556	33116	-3.667	-2.379	0.134
miR-338-3p	5	11	213	212	-3.279	-2.156	0.008
miR-339-3p	1795	1775	784	838	0.789	0.182	0.008
miR-34a-5p	12762	10534	5	3	8.041	4.351	0.061
miR-34c-5p	4599	4145	32	26	5.016	2.612	0.033
miR-363-3p	8	15	2535	2174	-5.322	-3.330	0.049
miR-363-3p	8	15	2535	2174	-5.322	-3.330	0.049
miR-365b-5p	292	327	14	13	3.132	1.529	0.038
miR-3681-5p	66	80	28	16	1.199	0.418	0.033
miR-376a-3p	370	328	917	824	-0.913	-0.796	0.028
miR-376a-5p	59	45	116	107	-0.768	-0.206	0.033

Table 7 Differentiated Skeletal Muscle Cells vs. Rh30 Cells, Continued

miRNA	U 1	U 2	D 1	D 2	ln(avg/avg)	z score	t test
miR-382-5p	1238	1264	2174	2139	-0.545	-0.584	0.001
miR-3913-3p	38	36	5	3	2.296	1.048	0.001
miR-3913-5p	38	36	5	3	2.296	1.048	0.001
miR-3916	11	13	4	3	1.350	0.505	0.043
miR-409-3p	41801	64157	199623	231206	-1.403	-1.078	0.019
miR-410	31172	56586	289272	311804	-1.924	-1.377	0.005
miR-411-3p	805	1159	7290	6767	-1.968	-1.403	0.005
miR-412	6	26	71	84	-1.578	-1.178	0.047
miR-424-5p	6241	5446	1586	741	1.614	0.657	0.015
miR-431-3p	388	653	2932	3470	-1.817	-1.316	0.030
miR-431-5p	1212	1644	47909	45967	-3.493	-2.279	0.010
miR-432-3p	19	57	252	318	-2.015	-1.429	0.038
miR-432-5p	2969	5515	14702	16655	-1.307	-1.023	0.023
miR-433	490	782	5027	4776	-2.042	-1.445	0.002
miR-454-5p	225	276	493	466	-0.651	-0.645	0.033
miR-4634	54	65	1	5	2.956	1.428	0.046
miR-4662a-5p	411	355	2	6	4.561	2.350	0.046
miR-4677-3p	531	476	138	127	1.337	0.497	0.040
miR-4687-5p	12	28	83	66	-1.312	-1.025	0.042
miR-4761-3p	5	7	40	37	-1.852	-1.336	0.003
miR-4775	275	228	54	29	1.806	0.767	0.032
miR-487a	390	410	3971	3608	-2.249	-1.564	0.034
miR-487b	1623	1980	8260	8854	-1.558	-1.167	0.006
miR-493-3p	4119	4178	13950	13245	-1.187	-0.954	0.023
miR-493-5p	4259	6407	23244	24012	-1.488	-1.127	0.021
miR-494	50	52	237	260	-1.589	-1.184	0.035
miR-496	144	215	965	793	-1.587	-1.183	0.047
miR-497-5p	716	937	14	15	4.043	2.053	0.086
miR-501-3p	2024	2543	5841	5415	-0.902	-0.790	0.011
miR-503	2195	2656	885	566	1.207	0.423	0.034
miR-508-3p	2	28	148	158	-2.322	-1.606	0.036
miR-541-3p	141	163	1485	1676	-2.339	-1.616	0.040
miR-541-5p	35	12	524	539	-3.118	-2.064	0.002
miR-550a-5p	138	176	388	339	-0.838	-0.753	0.026
miR-589-3p	171	189	509	535	-1.064	-0.883	0.003
miR-618	26	30	175	183	-1.854	-1.337	0.005
miR-624-5p	15	18	5	1	1.705	0.709	0.038
miR-652-5p	1	5	27	22	-2.100	-1.478	0.024
miR-376a-5p	59	45	116	107	-0.768	-0.206	0.033

Table 7 Differentiated Skeletal Muscle Cells vs. Rh30 Cells, Continued

miRNA	U 1	U 2	D 1	D 2	ln(avg/avg)	z score	t test
miR-708-3p	300	273	34	23	2.317	1.060	0.017
miR-758	1401	2154	16602	16088	-2.219	-1.547	0.002
miR-7-5p	51	29	190	154	-1.461	-1.111	0.037
miR-760	7	7	67	59	-2.220	-1.548	0.048
miR-770-5p	21	49	775	852	-3.146	-2.080	0.017
miR-873-3p	175	272	2	4	4.311	2.207	0.138
miR-874	2706	4669	8	7	6.192	3.288	0.166
miR-92a-1-5p	64	98	277	313	-1.293	-1.015	0.013
miR-93-5p	22555	25451	16717	14059	0.445	-0.016	0.049
miR-942	28	11	132	111	-1.831	-1.324	0.018
miR-9-5p	66	76	3055	2039	-3.579	-2.329	0.129
miR-96-5p	11	2	411	294	-3.992	-2.566	0.105
miR-99a-3p	161	169	45	63	1.115	0.370	0.023

Table 8. Differentiated Skeletal Muscle Cells vs. RD and Rh30, consensus miRNAs

let-7f-5p	miR-152	miR-22-3p	miR-31-5p
let-7g-5p	miR-181c-5p	miR-2355-5p	miR-335-3p-3p
let-7i-5p	miR-182-5p	miR-23a-5p	miR-34c-5p
miR-1	miR-183-3p	miR-24-2-5p	miR-365b-5p
miR-10a-3p	miR-183-5p	miR-24-3p	miR-424-5p
miR-132-5p	miR-1908	miR-27b-3p	miR-4775
miR-143-3p	miR-204-5p	miR-3065-5p	miR-497-5p
miR-145-5p	miR-212-3p	miR-3074-5p	miR-503
miR-146a-5p	miR-21-3p	miR-30a-5p	miR-873-3p
miR-146b-5p	miR-222-3p	miR-30e-5p	miR-96-5p

Table 9. Differentiated and Undifferentiated Skeletal Muscle vs. RD and Rh30 Consensus miRNAs

miRNA	U 1	U 2	D 1	D 2	RD 1	RD 2	Rh30 1	Rh30 2
let-7f-5p	220549	194851	408361	340052	2895	1407	2577	2504
let-7i-5p	67528	60477	131817	141237	890	499	11	19
miR-146a-5p	906	19	1549	2599	3	3	2	1
miR-204-5p	17168	569	13429	26360	29	27	4	2

Table 10. RD ERMS vs. Rh30 ARMS

miRNA	RD 1	RD 2	Rh30 1	Rh30 2	ln(avg/avg)	z score	t test
let-7a-5p	29017	27291	36893	37946	-0.285	0.032	0.021
let-7b-3p	15	13	203	204	-2.682	-1.698	0.002
let-7b-5p	309	260	2768	3175	-2.346	-1.455	0.045
let-7d-3p	29	28	1128	1013	-3.624	-2.377	0.035
let-7d-5p	156	150	3321	3559	-3.116	-2.010	0.023
let-7g-3p	3	4	9	8	-0.910	-0.419	0.020
miR-10b-5p	271226	405526	24	40	9.256	6.914	0.125
miR-1180	186	148	367	323	-0.728	-0.288	0.027
miR-1185-1-3p	35	18	530	527	-2.990	-1.919	0.009
miR-1229	4	3	2	2	0.523	0.614	0.021
miR-125a-5p	7391	6857	4834	4046	0.473	0.578	0.040
miR-1260a	23	15	83	78	-1.451	-0.809	0.012
miR-1260b	35	23	93	87	-1.125	-0.574	0.026
miR-127-3p	21985	23358	185532	171252	-2.063	-1.251	0.028
miR-127-5p	9	6	98	83	-2.466	-1.541	0.045
miR-134	110	88	1122	1152	-2.439	-1.522	0.001
miR-136-5p	5	1	101	72	-3.274	-2.125	0.107
miR-149-5p	1037	1181	1935	2042	-0.584	-0.184	0.013
miR-154-5p	5	4	28	30	-1.916	-1.145	0.002
miR-181a-3p	2990	1927	66	110	3.328	2.638	0.140
miR-181c-3p	10	6	23	22	-1.024	-0.501	0.046
miR-183-5p	25577	26393	2438	2298	2.395	1.965	0.009
miR-185-3p	11	7	28	26	-1.113	-0.565	0.020
miR-193b-3p	326	250	1591	1465	-1.669	-0.967	0.008
miR-193b-5p	6	2	35	36	-2.186	-1.340	0.028
miR-196a-5p	421	158	13	12	3.164	2.520	0.282
miR-196b-5p	627	261	10	7	3.915	3.061	0.254
miR-204-5p	29	27	4	2	2.241	1.854	0.004
miR-206	779	774	1695	1620	-0.759	-0.310	0.027
miR-2110	3	2	10	9	-1.309	-0.707	0.026
miR-23a-3p	267	230	849	885	-1.250	-0.664	0.002
miR-23a-5p	7	4	78	73	-2.645	-1.670	0.004
miR-23b-3p	579	575	197	236	0.981	0.945	0.032
miR-26a-5p	19179	11935	104194	97044	-1.867	-1.109	0.004
miR-27a-3p	592	562	1239	1244	-0.766	-0.315	0.012
miR-27a-5p	23	16	62	60	-1.113	-0.566	0.042
miR-299-3p	130	42	663	645	-2.028	-1.225	0.041
miR-3074-5p	261	237	179	161	0.383	0.513	0.039
miR-30a-3p	599	572	389	383	0.418	0.539	0.033

Table 10 . RD ERMS vs. Rh30 ARMS, Continued

miRNA	U 1	U 2	D 1	D 2	ln(avg/avg)	z score	t test
miR-376a-5p	59	45	116	107	-0.768	-0.206	0.033
miR-3180-3p	4	5	24	21	-1.595	-0.913	0.034
miR-3184-3p	1425	945	3620	3124	-1.046	-0.517	0.024
miR-3184-5p	6	5	12	11	-0.758	-0.309	0.027
miR-323b-3p	110	77	958	1012	-2.356	-1.462	0.003
miR-330-3p	9	7	17	20	-0.857	-0.381	0.044
miR-365a-5p	4	2	17	16	-1.857	-1.102	0.019
miR-3681-5p	41	22	3	2	2.601	2.114	0.202
miR-369-5p	48	28	538	546	-2.661	-1.682	0.004
miR-375	191	474	6	8	3.902	3.052	0.261
miR-376a-3p	23	10	96	88	-1.718	-1.002	0.014
miR-377-3p	12	4	49	38	-1.680	-0.975	0.046
miR-379-3p	33	31	276	241	-2.091	-1.271	0.048
miR-379-5p	86	48	365	354	-1.683	-0.977	0.028
miR-381	1638	923	36841	43468	-3.445	-2.248	0.052
miR-382-3p	4	2	16	19	-1.925	-1.151	0.011
miR-382-5p	43	33	228	227	-1.786	-1.051	0.016
miR-3909	26	10	77	64	-1.369	-0.750	0.040
miR-409-3p	1577	904	20979	24566	-2.910	-1.862	0.046
miR-409-5p	5	4	32	31	-2.003	-1.207	0.001
miR-410	3357	2467	30400	33130	-2.390	-1.486	0.018
miR-411-3p	96	68	766	719	-2.202	-1.351	0.005
miR-423-3p	3551	2176	10464	8915	-1.219	-0.642	0.023
miR-423-5p	1425	945	3620	3124	-1.046	-0.517	0.024
miR-431-5p	295	272	5035	4884	-2.861	-1.827	0.009
miR-432-5p	251	193	1545	1770	-2.011	-1.214	0.038
miR-433	72	94	528	507	-1.835	-1.086	0.001
miR-4510	7	9	14	13	-0.529	-0.144	0.048
miR-4761-3p	2	3	4	4	-0.451	-0.088	0.010
miR-487a	74	33	417	383	-2.008	-1.211	0.007
miR-487b	102	67	868	941	-2.365	-1.469	0.010
miR-493-3p	136	69	1466	1407	-2.643	-1.669	0.001
miR-493-5p	113	97	2443	2551	-3.166	-2.046	0.013
miR-495	68	57	92	102	-0.438	-0.079	0.047
miR-496	32	24	101	84	-1.194	-0.624	0.044
miR-500a-3p	1048	934	2983	2772	-1.066	-0.532	0.011
miR-504	144	162	1	1	4.975	3.826	0.038
miR-509-3p	3	2	66	53	-3.139	-2.027	0.069
miR-532-3p	182	177	744	820	-1.473	-0.825	0.039

Table 10 RD ERMS vs. Rh30 ARMS, Continued

miRNA	U 1	U 2	D 1	D 2	ln(avg/avg)	z score	t test
miR-376a-5p	59	45	116	107	-0.768	-0.206	0.033
miR-542-5p	5	3	23	22	-1.833	-1.085	0.022
miR-574-3p	186	160	392	376	-0.798	-0.339	0.009
miR-584-5p	4	1	90	92	-3.585	-2.349	0.001
miR-636	4	3	6	5	-0.465	-0.098	0.045
miR-654-3p	1841	1371	17221	16275	-2.345	-1.454	0.005
miR-654-5p	31	21	563	660	-3.167	-2.047	0.050
miR-655	15	7	50	42	-1.406	-0.777	0.025
miR-744-3p	14	11	26	23	-0.681	-0.254	0.027
miR-744-5p	286	155	1129	1028	-1.588	-0.908	0.011
miR-758	103	68	1745	1709	-3.008	-1.932	0.000
miR-99a-5p	875	1001	320	266	1.164	1.077	0.034

CHAPTER 3 - PAX3-FOXO1A ALTERS MICRORNA TRANSCRIPTOMES OF RHABDOMYOSARCOMA CELL LINES

INTRODUCTION

Pediatric rhabdomyosarcoma is commonly separated into two subtypes: embryonal rhabdomyosarcoma (ERMS) and alveolar rhabdomyosarcoma (ARMS), which confers a much poorer overall prognosis. The two subtypes have unique genetic signatures. ERMS tumors commonly exhibit loss of heterozygosity on the short arm of chromosome 11(Scrable, et al, 1987), and the majority of ARMS tumors are characterized by a translocation between chromosomes 2 and 13 that yields the fusion gene PAX3-FOXO1a(Shapiro, et al, 1993). Less often, ARMS tumors harbor an alternate translocation, PAX7-FOXO1a(Davis, et al, 1994).

The protein created as a result of the more common chromosomal translocation contains the DNA binding portion of the PAX3 protein fused to the FOXO1a transactivation domain, creating a fusion transcription factor. Normal PAX proteins are regulators of embryonic nervous system and skeletal muscle development, whereas FOXO1a is a transcription factor with multiple roles including the regulation of angiogenesis during development, cell metabolism, proliferation, and apoptosis throughout lifetime.

PAX3-FOXO1a shares some binding targets with wild type PAX3, but PAX3-FOXO1a also has unique transcriptional targets, such as *JARID2,* and *MYCN*(Mercado, et al, 2008) (Begum, et al, 2005)(Walters, et al, 2014,Mercado, et al, 2008)(Cao, et al, 2010). PAX3-FOXO1a also functions as an oncogene by binding to

tumor suppressors, leading to downstream dysregulation (Roeb, et al, 2007).PAX3-FOXO1a has also been found to inhibit immune response (Nabarro, et al, 2005). Despite these discoveries, the full functionality of PAX3-FOXO1a remains to be elucidated.

In the last decade, small, non-coding miRNAs that are responsible for critical gene regulation were discovered, as was the fact that dysregulation of miRNAs can contribute to cancer.(Cimmino, et al, 2005,Metzler, et al, 2004,Kluiver, et al, 2005). A few studies have investigated miRNA in RMS, and a few have found individual examples of miRNAs that are differentially regulated in ERMS vs. ARMS (Wang, et al, 2008), (Yan, et al, 2009), (Rao, et al, 2010), (Missiaglia, et al, 2010), (Wei, et al, 2009)(Gordon, et al, 2000), (Reichek, et al, 2011), (Ciarapica, et al, 2009), (Armeanu-Ebinger, et al, 2012) (Mayanil, et al, 2001), (Baer, et al, 2004), (Gougelet, et al, 2011). However, it is unknown if these differences are due to PAX3-FOXO1a as opposed to a separate, intrinsic property of the two subtypes.

In order to determine the role of PAX3-FOXO1a in ARMS tumorigenesis, we investigated the role of microRNA (miRNA) in PAX3-FOXO1a mediated tumorigenicity. The ability of miRNA to target multiple pathways makes them a good candidate to serve as possible downstream effectors of PAX3-FOXO1a. In this study, we investigate the miRNA profile of cells that have had their PAX3-FOXO1a expression altered. Using high throughput sequencing and qPCR analysis, we identified miRNAs that have not previously been linked to rhabdomyosarcoma, and

discovered that miRNA-495, miR-543, and miR-335-3p are upregulated in the presence of the fusion protein PAX3-FOXO1a.

RESULTS

MiRNA signatures are changed by introduction or knockdown of PAX3-FOXO1a

ARMS has a much poorer overall prognosis than ERMS. 70% of ARMS tumors contain the chromosome translocation between chromosomes 2 and 13 that results in the fusion protein transcription factor PAX3-FOXO1a. In order to investigate the effect of PAX3-FOXO1a on miRNA levels, we stably transfected PAX3-FOXO1a negative RD cells with either an empty vector or cDNA coding for HA-tagged PAX3-FOXO1a (Figure 12a). Conversely, we used siRNA targeting the fused portion of PAX3-FOXO1a to selectively knock down PAX3-FOXO1a expression in PAX3-FOXO1a positive cell line Rh30 (Figure 12b). The miRNA profiles of RD cells ± PAX3-FOXO1a-HA were compared, and yielded 46 differentially regulated miRNAs (Figure 12b, Table 11). When Rh30 cells with control siRNA were compared to cells transfected with siRNA against PAX3-FOXO1a, 37 miRNAs were found to be differentially regulated (Figure 12b, Table 12).

PAX3-FOXO1A expression upregulates three miRNAs

Between the 46 and 37 differentially regulated miRNAs, there were three in miRNAs were differentially regulated in both the RD and the RH30 models, and one that just missed significance. Out of those four, miR-3607 was discarded because the gain of function and loss of function trials both resulted in lower expression. The three

remaining miRNAs were miRNA-495, miRNA-543, and miRNA-335 (Figure 12b, Figure 13). qPCR quantification of the miRNAs confirmed their differential expression in cells with and without PAX3-FOXO1a (Figure 14). miRNA-335-3p is located in the host gene *MEST*, which activated by both PAX3 and PAX7.

miR-495 and miR-543 genes are located in non-codingRNA cluster DLK1-DIO3 *and have predicted PAX3 binding sites*

miR-495 and miR-543 are located adjacent to each other in the miRNA cluster *DLKI-DIO3* (Figure 15a). Interestingly, both miRNAs have predicted, conserved PAX3 binding sites within their genes, but it is not known if these are functional PAX3 targets. *DLK1-DIO3* is the largest miRNA cluster in the human genome with 53 miRNAs, and lies on chromosome 14. When examining the entire *DLK1-DIO3* cluster through the lens of our RNA-seq data, we found, on average, that expression of PAX3-FOXO1a in RD cells caused upregulation along chromosome 14, higher than all other miRNAs averaged over chromosomes (Figure 15b). When the analysis was limited to only those miRNAs in the *DLK1-DIO3* region, the average change in expression was even higher, suggesting that the miRNAs in the *DLK1-DIO3* cluster were responsible for the upregulation. Similarly, when comparing Rh30 with and without PAX3-FOXO1a siRNA, the average change in expression of individual miRNAs was decreased most in chromosome 14 (Figure 15c). The miRNAs in the *DLK1-DIO3* cluster had even more negative regulation, again suggesting that the *DLK1-DIO3* miRNAs were responsible for this effect.

In order to investigate the mechanism by which PAX3-FOXO1a upregulates our three candidate miRNAs, we created stable cell lines transfected with either PAX3-FOXO1a-HA or HA-tagged truncations containing only parts of the full length protein (Figure 16a). Western blot analysis of the truncated lines shows all HA-tagged constructs were similarly expressed (Figure 16b). qPCR was run on the samples to test their ability to upregulate expression of miR-495 and miR-543. Only the full length PAX3-FOXO1a was able to increase transcription of the candidate miRNAs (Figure 16c) indicating that the paired box DNA binding domain is required for regulation of these miRNAs.

DISCUSSION

Previous studies have sought to uncover the differences between ERMS and ARMS, and a few have looked at differential miRNA expression in the two subtypes (Rao, et al, 2010,Ciarapica, et al, 2009,Missiaglia, et al, 2010,Taulli, et al, 2009,Sarver, et al, 2010). In this study, we wanted to find miRNAs that were differentially regulated based solely on PAX3-FOXO1a expression. Gain and loss of function experiments yielded three interesting candidates, miR-495, miR-543, and miR-335-3p. miR-495 and miR-543 are both located in the miRNA cluster *DLK1-DIO3*, which contains 54 separate miRNAs. miRNAs in the DLK1-DIO3 cluster have been implicated in several diseases, including cancers, fibrosis, autism, lupus, and heart failure(Dixon-McIver, et al, 2008,Ueda, et al, 2010,Kriegel, et al, 2010,Abu-Elneel, et al, 2008,Eisenberg, et al, 2007,Wang, et al, 2008a) . In our previous

comparison of ERMS parental cells to ARMS parental cells, 31 out of the 54 DLK1-DIO3 miRNAs were significantly upregulated in AMRS cells, and five of those miRNAs had significance in both their 3p and 5p strands. These data echo the results from the comparison of the engineered lines (Table 10, Table 13)

miR-495 has previously been associated with cancer, but the associations vary widely. miR-495 has been found downregulated in leukemia, glioma, pancreatic cancer, and lung cancer, suggesting that miR-495 functions as a tumor suppressor(Jiang, et al, 2012,Chen, et al, 2013a,Formosa, et al, 2013,Xu, et al, 2013,Guo, et al, 2010). However, miR-495 has been found upregulated in breast cancer, adenocarcinima, and hepatocarcinoma.(Hwang-Verslues, et al, 2011,Dacic, et al, 2010,Yang, et al, 2013)

miR-543 has been found to be inversely correlated with aging, (Nidadavolu, et al, 2013), and has been suggested as a mediator of metabolic stress(Kalman, et al, 2014). miR-543 has been identified as a tumor suppressor in endometrial cancer(Bing, et al, 2014), and is downregulated in patients with chronic benzene poisoning. miR-543 has also been associated with the tumorigenic kidney phenotype of African green monkey cells(Teferedegne, et al, 2014).

miR-335 has been linked to cancer in several instances, however, the vast majority of studies have been performed on miR-335-5p, which was previously referred to as miR-335 before the change in nomenclature. At that time, miR-335* became miR-335-3p. In our analysis, expression of miR-335-5p was not correlated with PAX3-FOXO1a expression. Both miR-335-5p and miR-335-3p are upregulated

in young endothelial cells compared to their senescent counterparts (Zhang, et al, 2012). miR-335-3p was found to have higher expression in lung cancer samples than those from healthy controls, despite having very low expression overall(Ma, et al, 2013). miR-335-3p is located on chromosome 7, within the host gene *MEST*. Interestingly, PAX7 activates *MEST* in mouse myoblasts by recruiting a methyltransferase complex that results in H3K4 tri-methylation of chromatin (McKinnell, et al, 2008). PAX3 is also able to induce MEST, but to a lesser extent. (McKinnell, et al, 2008), which raises the possibility that alternate AMRS translocation PAX7-FOXO1could use this as a mechanism of tumorigenesis.

The mechanism by which PAX3-FOXO1a upregulates miRNAs 495, 543, and 335-3p remains to be found. The broad upregulation of the miRNAs in *DLK1-DIO3* suggests the upregulation is not direct, or that PAX3-FOXO1a is acting outside its canonical role as a transcription factor. DLK1-DIO3 contains two differentially methylated regions, meaning they have different methylation patterns between tissue types. This suggests that PAX3-FOXO1a may be altering the methylation of the region in order to allow for upregulation of transcription. Indeed, the fact that PAX7, and to some extent PAX3, interact with methyltransferases to increase expression adds evidence to this theory(Walters, et al, 2014). However, the conserved, predicted PAX3 binding sites located in miR-495 and miR-543 are also intriguing, as are results demonstrating the need for an intact paired box DNA binding domain in PAX3-FOXO1a for miR-495 and miR-543 upregulation.

Through this study, we have determined that PAX3-FOXO1a expression alters the miRNA transcriptome of rhabdomyosarcoma cells and specifically upregulates expression of miR-495 and miR-543. These miRNAs, located in the non-coding RNA cluster DLK1-DIO3 both have predicted PAX3 binding sites. PAX3-FOXO1a also significantly increases expression of miR-335-3p, these data suggest that PAX3-FOXO1a may exert its tumorigenic properties by modulating expression of miRNA, and nominate of miR-495, miR-543, and miR-335 as possible therapeutic targets.

METHODS

Generation of stable cell lines

RD cells were transfected with either empty pcDNA3.1 vector or pcDNA3.1 containing cDNA encoding HA-tagged fusion protein PAX3-FOXO1A using Lipofectamine 2000 (Invitrogen) and selected with Zeocin (Invitrogen). Selected cells were pooled to reduce genome integration anomalies. Each cell line was produced twice to make paired lines. Bar-coded samples were multiplexed and sequenced on Illumina's Hiseq platform. Sequences were mapped using Bowtie v. 0.12.2 (Langmead et al). Reads that mapped to over 20 loci were discarded. Two mismatches were permitted. For analysis, reads per million (RPM) were mapped for each miRNA; those with <1 RPM were discarded. The average RPM for each miRNA in the paired cell lines was compared to the average RPM of their sister lines that either did or did not express PAX3-FOXO1A. miRNAs with a z score of >1.96 or <-1.96, or with t test values >.05 were labeled as significantly different. miRNAs found to be significant

between RD cells ± PAX3FOXO1A were compared to the miRNAs found to be significantly different between Rh30 cells ± PAX3FOXO1A siRNA.

siRNA knockdown of PAX3-FOXO1A

$1x10^6$ Rh30 cells were transfected with either 30ul of 20nm nonspecific control siRNA or siRNA specifically targeting PAX3-FOXO1A using 100ul Lipofectamine RNAiMAX (Invitrogen) in 10mL of media not supplemented with penicillin or streptomycin. Control siRNA sequence: 5'-UUAGUACUGCUUACGAUACGGUTT-3', 3' TTAAUCAUGACGAAUGCUAUGCCAA5'. PAX3-FOXO1a siRNA sequence: 5' UUAUGACGAAUUGAAUUCUGAGGUG 3', 3' AAUACUGCUUAA CUUAAGACUCCAC 5'.

Western blot analysis

Cells were lysed directly in the dish by washing twice with PBS then adding RIPA buffer supplemented with a protease inhibitor cocktail. Cells were incubated at 4° C for 10 minutes. Plates were scraped and lysates was transferred to a microtube, and centrifuged at 4° for 10 minutes, 10,000 RPM to remove cell debris. Protein concentration was determined by running a BCA assay (Thermo Pierce). 20ug of protein were run on a 4-12% NuPage Bis-Tris gel (Life Technolgies) in NuPage MOPS SDS Running Buffer (Life Technologies). Gels were transferred to nitrocellulose membranes in NuPage transfer buffer (both from Life Technologies) at, 150 mV for 1.5 hours. Blots were blocked with 4% milk for 1 hour. Antibodies were

used as follows: β-actin, 1/10,000 (Santa Cruz), FOXO1 1/200 (Santa Cruz) and HA, 1/1000 (Roche). β-actin and HA antibodies were incubated with the blot at room temperature for one hour. FOXO1 antibody was incubated at 4° C over night. After washing, the FOXO1 blots were incubated with goat secondary antibody (Dako Corporation) at 1/2000, room temperature for one hour. Blots were developed with West Femto (Thermo Scientific) using either photo-sensitive film (Kodak) or Bio-Rad's ChemiDoc MP Imaging System.

RNA harvesting and extraction, and sample preparation

RNA was harvested and isolated using a standard TRIzol (Life Technologies)-chloroform protocol, and concentration and purity were tested by 260/280 optical density using a Nanodrop. Samples were prepped for sequencing using Illumina's Truseq Small RNA protocol, adapted from Lu et al, 2009. Briefly, 3' and 5' adapters were ligated to 10ug total RNA, then underwent reverse transcription and PCR amplification for 16 cycles. Unique, bar-coded PCR primers were used to identify individual samples. Small cDNAs were purified using acrylamide gel separation, and cleaned using Gel Breaker tubes and filtration.

High throughput sequencing

The barcoded samples were quality control checked using a Bioanalyzer (Agilnet Technology's chip-based capillary electrophoresis), multiplexed and

sequenced for 36 cycles using the Illumina Genome Anlayzer II, available at the UCSD sequencing core.

Processing small RNA-seq data

After standard processing through Illumina software, sequenced reads were returned in FASTA format. Linker sequences were removed from raw reads, leaving 18-25 base pair sequences that were mapped to the human genome (NCBI BUILD 36/HG18) using the algorithm Bowtie v.0.12.2 (Langmead et al). Sequences with up to two mismatches were included for miRNA expression level analysis. Reads that map to genomic repeats or more than 20 loci in the genome were excluded from the dataset.

Analysis of small RNA-seq data

For analysis, reads per million (RPM) were mapped for each miRNA; those with <1 RPM were discarded. The RPM for every miRNA was calculated for each cell line and averaged between the two paired lines. Average RPM for each paired line was compared to the average RPM of other paired lines. miRNAs with a z score of >1.96 or <-1.96, or with t test values >.05 were labeled as significantly different.

Reverse Transcription PCR and Quantitative Real-Time PCR

RNA was harvested and isolated using a standard TRIzol (Life Technologies)-chloroform protocol, quantified via Nanodrop (Thermo Scientific), and DNAse treated

(Invitrogen). Reverse Transcription was performed using Applied Biosystems' TaqMan miRNA Reverse Transcription Kit, and quantified on BioRad's CFX96 Real Time Thermocycler using Applied Biosystems' TaqMan miRNA Assays. RNU6B, an evolutionarily conserved, ubiquitous component of the spliceosome, was used as a control for RNA loading.

Determination of PAX3 binding sites

Predicted PAX3 binding sites were determined via the UCSC genome browser, as calculated by the Transfac Matrix Table, accession number M00360, Identifier V$PAX3_01, Statistical Basis: 26 sequences from oligonucleotide selection.

Generation of PAX3-FOXO1a truncations

PAX3-FOXO1a truncations were cloned into a pBABE vector with puromycin resistance. PAX3-FOXO1a (accession number U02368) truncations were made as follows: Full length clone starts at start site 58 bp. H + F only clone has sequence starting at 578 bp. F only clone has sequence starting at 997 bp. The no domain has sequence starting at 1396 bp. All truncations were HA tagged. Retrovirus was generated in 293T cells, after which RD cells were infected.

ACKNOWLEDGEMENTS

Data from this Chapter are currently being prepared for submission as a publication. Muir, Shannon; Wilbert, Melissa; Nathanson, Jason; Yeo, Gene W.; Furnari, Frank; Cavenee, Webster; Arden, Karen C. The dissertation author was the primary investigator and author of this material.

FIGURES

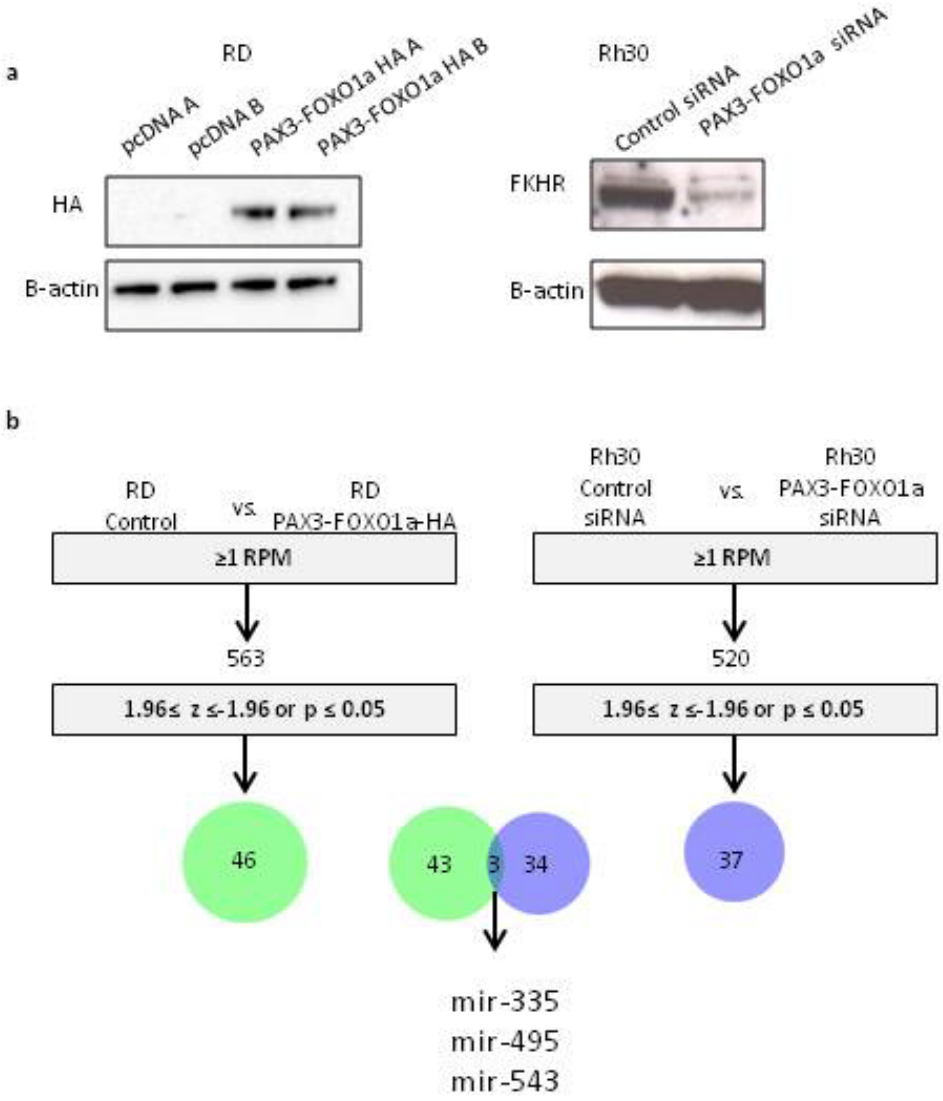

Figure 12. Creation and analysis of engineered cell lines.
a. Western blot analysis showing stable transfection of HA tagged PAX3-FOXO1a into RD cells, with two separate transfections, and transient siRNA knowckdown of endogeneous PAX3-FOXO1a in Rh30 cells. b. schematic of experimental comparisons between engineered RD cells and engineered Rh30 cells.

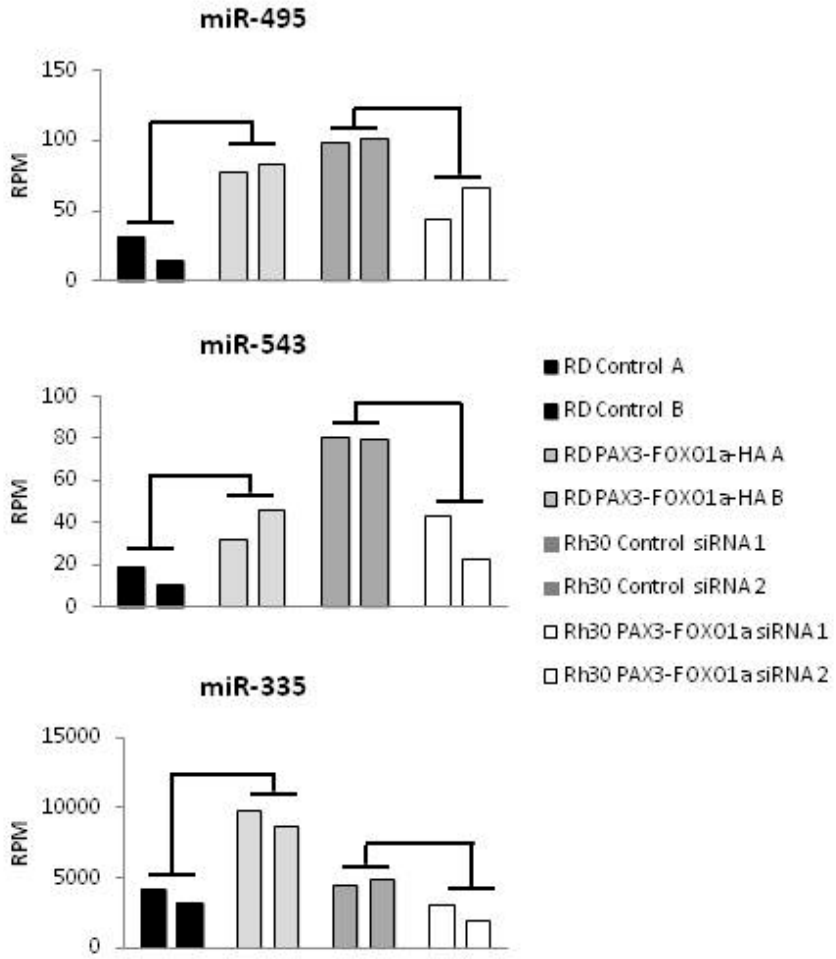

Figure 13. RNA-seq data for candidate miRNAs
In reads per million (RPM) * $p \leq 0.05$ † $-1.96 \leq z \leq 1.96$

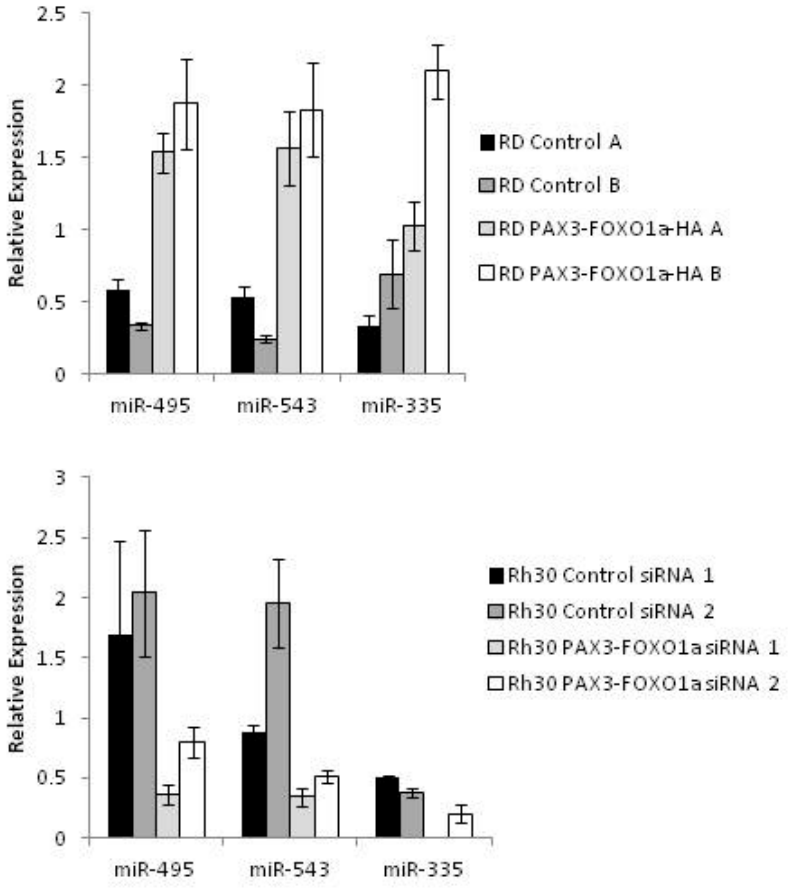

Figure 14. qPCR analysis on PAX3-FOXO1a induced miRNAs
qPCR data from the samples in Figure 11. Error bars = standard error of the mean for two technical replicates.

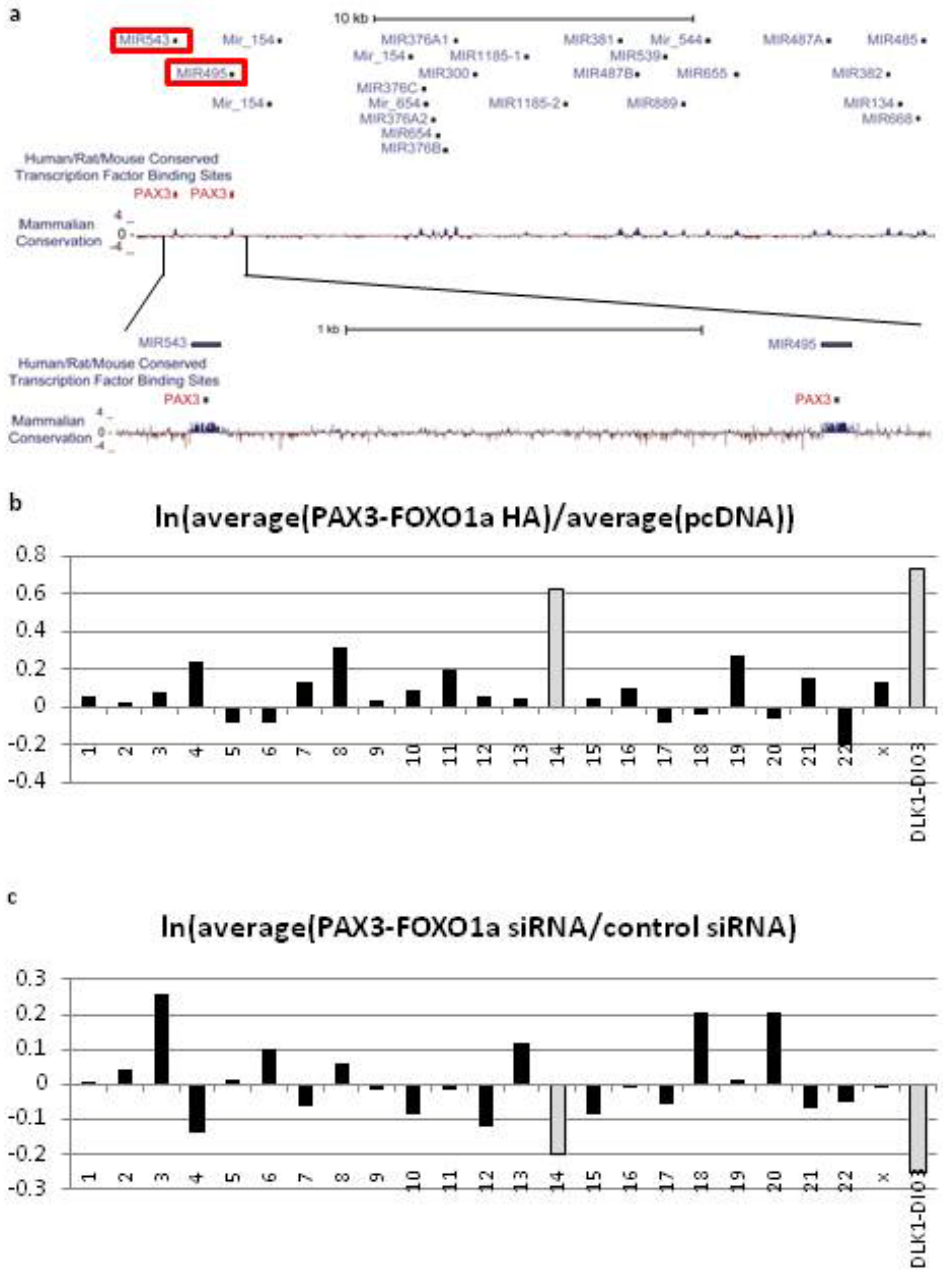

Figure 15. DLK1-DIO3 region with adjacent miR-495 and miR-543.
a. Diagram showing a portion of the DLK1-DIO3 miRNA cluster, located on chromosome 14.mir-495 and mir543 are highlighted. Inset shows conserved, predicted PAX3 binding sites located within the miR genes. b The RPM for each miRNA was averaged between the two sister cell lines. The ration was calculated between the mean RPMs in the PAX3-FOXO1a transfected cells vs. the pcDNA cells. The natural log of the ratio was calculated, and those ratios were averaged across all the miRNAs in each chromosome. Data is displayed by chromosome. c. Natural log of the ratios of the mean RPM of each miRNA, PAX3-FOXO1a siRNA vs. control siRNA, averaged over each chromosome.

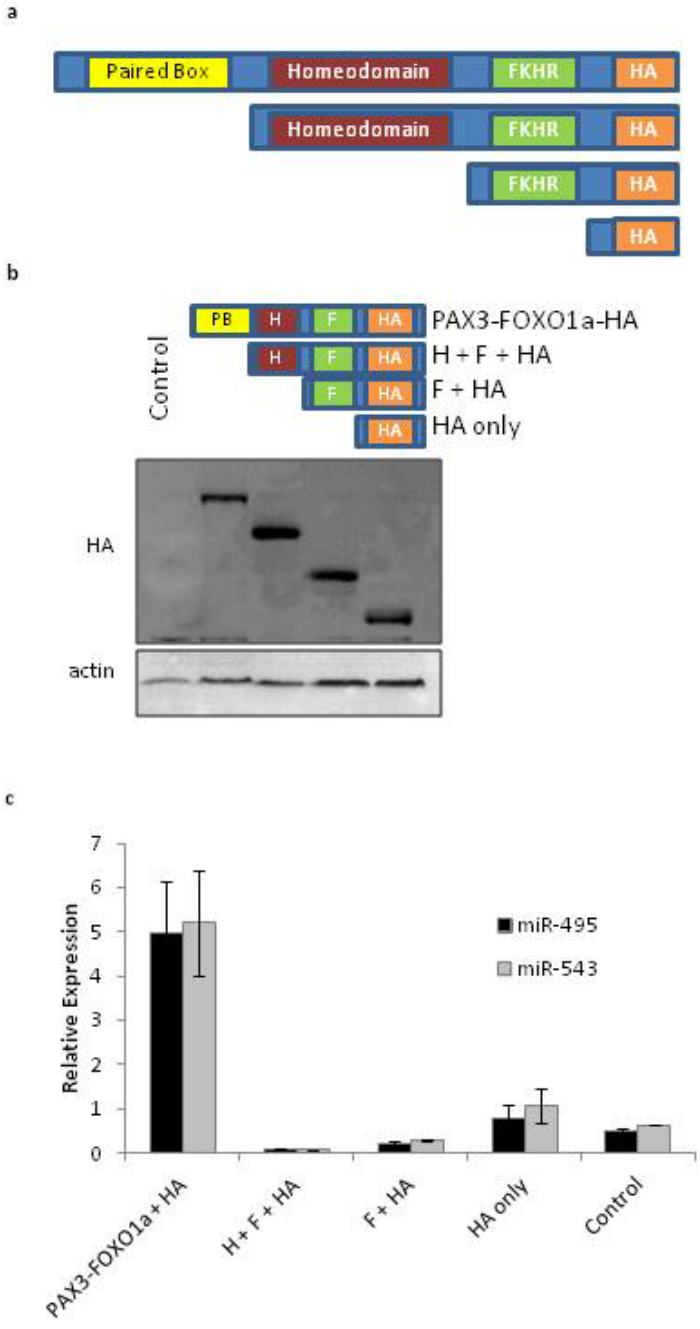

Figure 16. Effect of PAX3-FOXO1a truncation on miRNA expression
a. Diagram of PAX3-FOXO1 truncations. b. Western blot analysis of HA tagged PAX3-FOXO1 truncations. c. qPCR data showing relative expression of miR-495 and miR-543 upon stable transfection of PAX3-FOXO1 truncations into RD cells.

TABLES

Table 11. RD ERMS + Control vs. PAX3-FOXO1a

miRNA	RD Control A	RD Control B	RD PAX3-FOXO1a-HA A	RD PAX3-FOXO1a-HA B	ln(avg/avg)	z score	t test
let-7d-3p	48	47	31	33	0.402	1.228	0.018
let-7d-5p	683	586	270	356	0.706	1.930	0.040
let-7i-5p	1425	1219	489	750	0.758	2.050	0.056
miR-1	138	113	59	53	0.808	2.167	0.098
miR-1247-3p	5	5	8	7	-0.424	-0.680	0.039
miR-1271-5p	8	8	11	50	-1.340	-2.798	0.454
miR-143-3p	603	384	259	124	0.947	2.488	0.168
miR-146a-5p	5	8	18	17	-1.032	-2.084	0.032
miR-181a-5p	47335	49125	33561	32927	0.372	1.159	0.022
miR-181b-5p	9311	8741	5322	6209	0.448	1.335	0.036
miR-182-5p	126197	110094	50912	62294	0.736	2.000	0.032
miR-184	16	17	60	55	-1.215	-2.509	0.035
miR-210	115	77	51	43	0.725	1.974	0.219
miR-215	47	60	125	121	-0.838	-1.637	0.037
miR-23c	1	2	15	2	-1.551	-3.284	0.485
miR-24-3p	988	864	1455	1404	-0.434	-0.704	0.047
miR-30a-5p	2110	1537	846	900	0.737	2.001	0.184
miR-3168	1	1	2	2	-0.450	-0.741	0.004
miR-3182	2	2	4	4	-0.727	-1.380	0.009
miR-3184-3p	2324	2262	1669	1741	0.296	0.984	0.007
miR-3188	25	24	13	15	0.576	1.631	0.015
miR-329	15	7	24	42	-1.087	-2.212	0.206
miR-335-3p	4117	3228	9746	8642	-0.918	-1.821	0.018
miR-3607-3p	9	2	1	2	1.135	2.922	0.482
miR-365b-5p	14	14	12	12	0.182	0.720	0.021
miR-379-3p	26	10	41	60	-1.029	-2.078	0.122
miR-379-5p	82	68	195	203	-0.974	-1.951	0.011
miR-380-3p	35	13	58	91	-1.140	-2.334	0.142
miR-3912	5	4	1	3	0.818	2.189	0.119
miR-409-5p	2	2	4	42	-2.369	-5.175	0.463
miR-423-5p	2324	2262	1669	1741	0.296	0.984	0.007
miR-448	2	2	6	5	-1.072	-2.177	0.026
miR-4515	3	7	3	2	0.728	1.981	0.427
miR-454-5p	82	85	65	69	0.217	0.801	0.029
miR-4638-3p	5	9	2	3	0.998	2.605	0.238

Table 11 RD ERMS + Control vs. PAX3-FOXO1a, Continued

miRNA	U 1	U 2	D 1	D 2	ln(avg/avg)	z score	t test
miR-376a-5p	59	45	116	107	-0.768	-0.206	0.033
miR-489	4	5	13	22	-1.339	-2.795	0.199
miR-495	31	14	78	84	-1.286	-2.671	0.066
miR-500a-5p	14	13	21	21	-0.429	-0.693	0.006
miR-501-3p	229	291	567	869	-1.016	-2.048	0.191
miR-561-3p	1	1	3	2	-0.835	-1.631	0.046
miR-5683	7	6	19	26	-1.221	-2.521	0.134
miR-665	11	8	31	42	-1.354	-2.830	0.103
miR-708-3p	3	5	9	16	-1.195	-2.461	0.231
miR-937	32	35	25	23	0.352	1.113	0.037
miR-98	1070	1137	639	679	0.515	1.489	0.015

Table 12. Rh30 ARMS + Control siRNA vs. PAX3FOXO1a siRNA

miRNA	Rh30 Control siRNA 1	Rh30 Control siRNA 2	Rh30 PAX3-FOXO1a siRNA 1	Rh30 PAX3-FOXO1a siRNA 2	lnavg/avg	z score	t test
let-7f-5p	27170	26750	29128	28795	-0.072	-0.379	0.020
miR-100-3p	125	123	95	99	0.245	0.784	0.026
miR-10a-3p	15	14	11	5	0.573	1.987	0.306
miR-1193	3	2	7	8	-1.180	-4.449	0.032
miR-1280	3	2	4	4	-0.567	-2.197	0.212
miR-1285-3p	9	7	6	2	0.709	2.488	0.291
miR-1306-5p	14	14	10	5	0.628	2.189	0.191
miR-138-1-3p	2	3	1	2	0.608	2.115	0.111
miR-154-3p	17	13	5	5	1.129	4.028	0.137
miR-181b-3p	2	2	5	4	-0.638	-2.459	0.114
miR-185-5p	42	40	33	31	0.253	0.814	0.017
miR-196a-5p	34	33	40	39	-0.157	-0.693	0.032
miR-19a-5p	3	2	5	4	-0.586	-2.268	0.081
miR-212-5p	2	2	1	1	0.502	1.727	0.001
miR-25-3p	7773	7972	8971	8862	-0.125	-0.573	0.025
miR-27a-5p	231	212	311	326	-0.362	-1.446	0.017
miR-299-3p	1825	1688	1289	1124	0.376	1.263	0.039
miR-29b-3p	39	38	26	28	0.372	1.251	0.024
miR-30a-3p	513	546	743	693	-0.304	-1.234	0.034
miR-30c-5p	1370	1487	2562	2441	-0.560	-2.173	0.006
miR-30e-5p	64	61	77	81	-0.235	-0.979	0.025
miR-3163	3	2	1	1	0.847	2.995	0.199
miR-3176	2	1	4	3	-0.562	-2.179	0.247
miR-323a-5p	10	9	4	4	0.792	2.793	0.013
miR-335-3p-	4498	4890	3040	1953	0.631	2.202	0.123
miR-3607-3p	9	6	5	2	0.672	2.351	0.273
miR-3609	1	2	4	2	-0.925	-3.512	0.260
miR-362-3p	22	20	176	191	-2.172	-8.090	0.026
miR-432-3p	16	18	9	11	0.532	1.839	0.029
miR-4511	2	4	2	2	0.659	2.304	0.252
miR-485-3p	167	150	71	62	0.866	3.064	0.022
miR-495	98	101	44	66	0.595	2.070	0.141
miR-539-3p	417	430	301	302	0.338	1.125	0.034
miR-543	80	79	43	22	0.895	3.170	0.135
miR-573	2	2	4	3	-0.543	-2.109	0.117
miR-625-5p	1	1	2	2	-0.509	-1.983	0.059
miR-758	1382	1305	1017	959	0.308	1.014	0.022

Table 13. Significantly Different DLK1-DIO3 miRNAs, ERMS vs. ARMS

miRNA	RD 1	RD 2	Rh30 1	Rh30 2	lnavg/avg	zscore	ttest
miR-493-5p	113	97	2443	2551	3.166	2.046	0.013
miR-493-3p	136	69	1466	1407	2.643	1.669	0.001
miR-431-5p	295	272	5035	4884	2.861	1.827	0.009
miR-433	72	94	528	507	1.835	1.086	0.001
miR-127-5p	9	6	98	83	2.466	1.541	0.045
miR-127-3p	21985	23358	185532	171252	2.063	1.251	0.028
miR-432-5p	251	193	1545	1770	2.011	1.214	0.038
miR-136-5p	5	1	101	72	3.274	2.125	0.107
miR-379-5p	86	48	365	354	1.683	0.977	0.028
miR-379-3p	33	31	276	241	2.091	1.271	0.048
miR-411-3p	96	68	766	719	2.202	1.351	0.005
miR-299-3p	130	42	663	645	2.028	1.225	0.041
miR-758	103	68	1745	1709	3.008	1.932	0.000
miR-495	68	57	92	102	0.438	0.079	0.047
miR-654-5p	31	21	563	660	3.167	2.047	0.050
miR-654-3p	1841	1371	17221	16275	2.345	1.454	0.005
miR-376a-3p	23	10	96	88	1.718	1.002	0.014
miR-1185-1-3p	35	18	530	527	2.990	1.919	0.009
miR-381	1638	923	36841	43468	3.445	2.248	0.052
miR-487b	102	67	868	941	2.365	1.469	0.010
miR-539-5p	4	4	22	22	1.665	0.964	0.001
miR-889	681	295	3214	2482	1.764	1.035	0.053
miR-655	15	7	50	42	1.406	0.777	0.025
miR-487a	74	33	417	383	2.008	1.211	0.007
miR-382-5p	43	33	228	227	1.786	1.051	0.016
miR-382-3p	4	2	16	19	1.925	1.151	0.011
miR-134	110	88	1122	1152	2.439	1.522	0.001
miR-323b-3p	110	77	958	1012	2.356	1.462	0.003
miR-154-5p	5	4	28	30	1.916	1.145	0.002
miR-496	32	24	101	84	1.194	0.624	0.044
miR-377-3p	12	4	49	38	1.680	0.975	0.046
miR-409-5p	5	4	32	31	2.003	1.207	0.001
miR-409-3p	1577	904	20979	24566	2.910	1.862	0.046
miR-412	2	1	7	9	1.801	1.061	0.051
miR-369-5p	48	28	538	546	2.661	1.682	0.004
miR-410	3357	2467	30400	33130	2.390	1.486	0.018

CHAPTER 4 - MANIPULATION OF MICRORNAS

INTRODUCTION

A chromosomal translocation resulting in the fusion protein PAX3-FOXO1a correlates with a much poorer prognosis in rhabdomyosarcoma patients (Ries, et al, 1999b). We have shown that PAX3-FOXO1a upregulates specific miRNAs, including miR-335, miR-543, and miR-495. However, the biological significance of this regulation has yet to be determined. The three PAX3-FOXO1a effected miRNAs have been associated with cancer in other models. miR-335-3p has higher expression in lung cancer tissue than in normal cancer tissue(Ma, et al, 2013). miR-543 is a regulator of metabolic stress (Kalman, et al, 2014), and miR-495 has been associated with adherens junctions and the extracellular matrix (Hwang-Verslues, et al, 2011). Adherens junctions connect the actin cytoskeleton of the cell with its microenvironment to aid in mechanical cell migration (for review, see (Friedl and Wolf, 2009). In normal tissues, cell migration is vital for embryogenesis as well as wound healing and tissue renewal. However, if cells fail to bind sufficiently to the extracelluar matrix, uncontrolled migration can lead to invasion and metastasis of cancer cells. PAX3-FOXO1a positive rhabdomyosarcoma has been shown to metastasize more often than the fusion negative disease (Ries, et al, 1999b).

Here we investigate the biological effect of PAX3-FOXO1a-regulated miRNAs on cell phenotype. Given the possible link between miR-495, adherens junctions, PAX3-FOXO1a, migration, and metastasis, we studied the ability of miR-

495 to regulate migration through a permeable membrane. Additionally, the overall implications of the project, as well as future directions, are discussed.

RESULTS

Inhibition of miRNA-543 increases miR-495

To study the affect of miR-495 on migration, we used loss of function experiments in which miR-495 was selectively inhibited using single stranded inhibitory RNA. Use of the inhibitor successfully decreased miR-495 expression (Figure 17a). An inhibitor against miR-543 was used to test inhibitor specificity. Interestingly, inhibition of miR-543 increased the expression of miR-495 to levels much higher than in the scramble inhibitor sample. Dual transfection of inhibitors against both miR-495 and miR-543 brought miR-495 expression back to control levels (Figure 17a). The mechanism by which a miR-543 inhibitor causes increased expression is not known. One possibility is that miR-543 may lead to feedback inhibition of miR-495 transcription, so inhibition of miR-543 would derepress miR-495. It is also possible that miR-543 inhibits miR-495 degradation, meaning that decreased miR-543 expression would lead to a net increase of miR-495.

Effect of miRNA inhibition on migration

When miRNAs 495 and 543 were inhibited in stably transfected PAX3-FOXO1a RD cells, the ability of the cells to migrate through a permeable membrane was diminished. Figure 17b shows stained cells from the lower transwell compartment. Fewer cells are present on the membrane when miR-495 and miR-543

are inhibited, both alone and in combination. Stained cells were dissolved in SDS, and absorbance was measured to quantify relative numbers of migrated cells. Cells transfected with the control inhibitor had a higher absorbance reading, indicating increased migration compared to cells transfected with inhibitors against miR-495 and miR-543 (Figure 17c). These data support the notion that miR-495 and miR-543 may contribute to cancer cell migration.

The inhibition of migration by miR-495 and miR-543 inhibitors does not appear to be additive or synergistic, which agrees with the qPCR data showing an increase in miR-495 when cells are tranfected with inhibitors agains miR-543 (Figure 17a).

METHODS

Knockdown of miRNAs

Inhibition of microRNAs was performed using Life Technologies' miRVana miRNA inhibition kits. Briefly, single stranded RNA inhibitors were forward transfected into cells using RNAiMAX (Life Technologies). Cells were plated at a density that yielded 70% confluency after 24 hours. Cells were plated in the transwell and assayed for miRNA expression 24 hours post transfection.

RNA analysis

RNA analysis was performed using Life Technologies Cells to Ct RNA processing kit. $1x10^5$ cells were counted from each sample and resuspended in 5 µl phosphate buffered saline. Cells were treated with 50 µl of Lysis solution with DNAse

for 8 minutes, after which 5 μl of stop solution was applied. Following cell lysis, RNA samples were reverse transcribed using Applied Biosystems' TaqMan miRNA Assays which utilizes primers specific to each miRNA. Samples were then quantified on BioRad's CFX96 Real Time. RNU6B, an evolutionarily conserved, ubiquitous component of the spliceosome, was used as a control for RNA loading.

Migration assay

Migration assays were performed using Corning's transwell permeable supports. $6x10^4$ cells were placed in the upper chamber of the transwell with 100 μl 1% FBS DMEM. 600 μl 10% FBS DMEM was placed in the bottom chamber. After 24 hours, cells from the top chamber were removed, as was the media from the lower chamber. Cells on the permeable membrane in the lower chamber were stained with 600 μl 25% methanol and 0.5% crystal violet for 30 minutes, then washed twice in water. Images were taken using an inverted brighfield at 20X. For quantification of results, transwells were placed in 600ul 1% SDS solution for 1 hour, followed by absorbance analysis at 590 nm.

FUTURE DIRECTIONS

The motivation to study the effect of PAX3-FOXO1a on miRNA expression stems from a need to develop new treatments for patients with fusion protein positive RMS. The data herein reveal some information about the interaction between PAX3-FOXO1a and miRNA, but an enormous amount of additional research lies between

these studies and a cure for pediatric RMS. The most obvious limitation of this data is that it is restricted to a small number of cultured cell lines, and experimentation on other cell lines as well as patient samples is vital. In addition to increasing the number of samples, there are several possible next steps. We discuss these below, as well as the rationale behind them.

What is the mechanism by which PAX3-FOXO1A alters expression of miRNAs?

Identification of novel therapeutic targets is a major strategy for the invention of new drugs. The individual miRNAs that were upregulated by the fusion protein can be considered therapeutic candidates, but knowing the mechanism of PAX3-FOXO1 would provide additional avenues of combating the effect of the fusion protein. PAX3-FOXO1a significantly downregulated some miRNAs while upregulated others (Table 11, Table 12). PAX3-FOXO1a may alter miRNA expression through its canonical role as a transcription factor. Evidence for this mechanism includes the existence of conserved predicted PAX3 binding sites within two of the significantly upregulated miRNAs (Figure 15a), as well as the data showing their upregulation to be contingent on the PAX3 binding domain. Conversely, it is conceivable that PAX3-FOXO1a could downregulate expression of miRNAs by inhibiting normal binding of activating transcription factors. Investigation into the role of DNA binding in PAX3-FOXO1a-induced miRNA expression can be achieved using mutations to the DNA binding domains of the fusion protein and concordant chromatin immunoprecipitation studies.

Additional data demonstrates that PAX3-FOXO1a causes broad upregulation of entire regions or the genome, as opposed to individual miRNAs (Figure 15a and b). To test if this regional activation is achieved through the increase of activating methylation or decrease of inhibitory methylation, gain and loss of function of studies could be performed on methytransferases, as could experiments that mutate the differentially methylated regions in DLK1-DIO3.

PAX3-FOXO1a also upregulates miR-335, which contains neither a DNA binding domain nor a nearby differentially methylated region. It does however, lie in host gene *MEST*, which is known to be directly upregulated by members of the PAX family. It is therefore pertinent to determine if direct PAX3-FOXO1a regulation of MEST explains changes in miR-335 expression. Simple gene expression studies could readily answer this question.

Is PAX3-FOXO1a regulation of miRNAs clinically significant?

Correlation studies between gene expression and clinical outcome have long been used to identify possible causes of disease. Correlation studies rely on clinical data from a large number of patients, and a critical mass must be achieved before reliable data can be recovered. Although the rarity of pediatric RMS is positive from a public health perspective, it means fewer patients and fewer clinical data points. A concerted effort by the RMS community to gather clinical data and sequence the transcriptomes of RMS samples is necessary before the significance of our candidate miRNAs can be determined. In the meantime, inhibition of individual miRNAs and

miRNA processing machinery in both *in vitro* and *in vivo* models will have to suffice. Besides migration, other relevant cellular phenotypes include invasion, apoptosis, tumorigenicity, immune response, longevity, metastasis, drug resistance, and recurrence

CONCLUSIONS

Although the implications of the data may be wide spread, the data must be considered in a conservative fashion. The experiments in this dissertation suggest the following:

1. Small miRNA-seq is able to identify known markers of skeletal muscle cells and distinguish between primary cultured differentiated and undifferentiated skeletal muscle cells.
2. Primary cultured differentiated and undifferentiated skeletal muscle cells have unique miRNA signatures.
3. Primary cultured normal skeletal muscle cells have miRNA profiles that differ from cultured rhabdomyosarcoma cell lines RD and Rh30.
4. The embryonal rhabdomyosarcoma cell line RD and the alveolar rhabdomyosarcoma cell line Rh30 have different miRNA expression.
5. Exogenous expression and inhibition of PAX3-FOXO1a is able to alter miRNA expression in rhabdomyosarcoma cell lines RD and Rh30, respectively.

6. PAX3-FOXO1a increases expression of miR-335, miR-495, and miR-543.
7. PAX3-FOXO1a broadly increases expression of miRNAs in the DLK1-DIO3 cluster.
8. Upregulation of miR-495 and miR-543 is dependent on the paired box DNA binding domain of PAX3-FOXO1a.
9. Inhibition of miR-495 and miR-543 mitigates the ability of rhabdomyosarcoma cells to migrate through a permeable membrane along and FBS gradient.

ACKNOWLEDGEMENTS

Data from this Chapter are currently being prepared for submission as a publication. Muir, Shannon E.; Wilbert, Melissa; Nathanson, Jason; Yeo, Gene W.; Furnari, Frank; Cavenee, Webster; Arden, Karen C. The dissertation author was the primary investigator and author of this material.

FIGURES

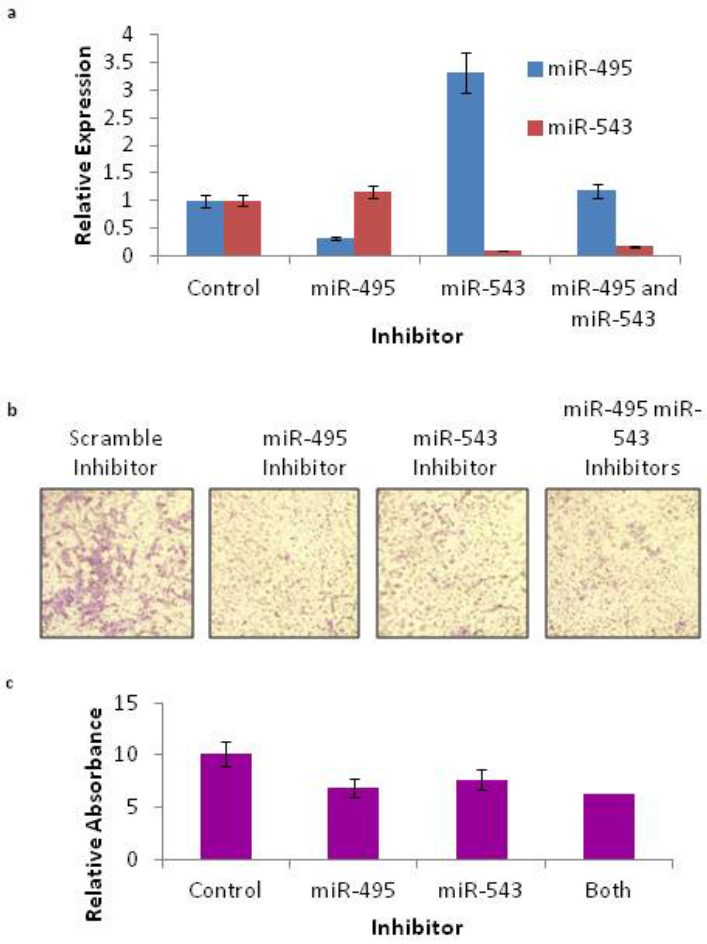

Figure 17. Migration of RMC cells with miRNA inhibition.
a. Relative expression of miRNAs after treatment with mirVANA miRNA inhibitors., as measured by qPCR. b. Brightfield images of lower side of transwell permeable membrane, 20x. c. Relative absorbance of stained cells treated with SDS.

REFERENCES

Abu-Elneel, K., Liu, T., Gazzaniga, F.S., Nishimura, Y., Wall, D.P., Geschwind, D.H., Lao, K., and Kosik, K.S. 2008. Heterogeneous dysregulation of microRNAs across the autism spectrum. *Neurogenetics* 9, 153-161.

Adessi, C., Matton, G., Ayala, G., Turcatti, G., Mermod, J.J., Mayer, P., and Kawashima, E. 2000. Solid phase DNA amplification: characterisation of primer attachment and amplification mechanisms. *Nucleic Acids Res.* 28, E87.

Anderson, C., Catoe, H., and Werner, R. 2006. MIR-206 regulates connexin43 expression during skeletal muscle development. *Nucleic Acids Res.* 34, 5863-5871.

Anderson, J., Ramsay, A., Gould, S., and Pritchard-Jones, K. 2001a. PAX3-FKHR induces morphological change and enhances cellular proliferation and invasion in rhabdomyosarcoma. *Am.J.Pathol.* 159, 1089-1096.

Anderson, M.J., Shelton, G.D., Cavenee, W.K., and Arden, K.C. 2001b. Embryonic expression of the tumor-associated PAX3-FKHR fusion protein interferes with the developmental functions of Pax3. *Proc.Natl.Acad.Sci.U.S.A.* 98, 1589-1594.

Anderson, M.J., Viars, C.S., Czekay, S., Cavenee, W.K., and Arden, K.C. 1998. Cloning and characterization of three human forkhead genes that comprise an FKHR-like gene subfamily. *Genomics* 47, 187-199.

Andreoli, S.C., Gasparini, N.J., Carvalho, G.P., Garicochea, B., Pogue, R.E., and Andrade, R.V. 2014. Use of microRNAs in directing therapy and evaluating treatment response in colorectal cancer. *Einstein (Sao.Paulo)* 12, 256-258.

Arden, K.C., and Biggs, W.H.,3rd. 2002. Regulation of the FoxO family of transcription factors by phosphatidylinositol-3 kinase-activated signaling. *Arch.Biochem.Biophys.* 403, 292-298.

Armeanu-Ebinger, S., Herrmann, D., Bonin, M., Leuschner, I., Warmann, S.W., Fuchs, J., and Seitz, G. 2012. Differential expression of miRNAs in rhabdomyosarcoma and malignant rhabdoid tumor. *Exp.Cell Res.* 318, 2567-2577.

Baer, C., Nees, M., Breit, S., Selle, B., Kulozik, A.E., Schaefer, K.L., Braun, Y., Wai, D., and Poremba, C. 2004. Profiling and functional annotation of mRNA gene expression in pediatric rhabdomyosarcoma and Ewing's sarcoma. *Int.J.Cancer* 110, 687-694.

Bajard, L., Relaix, F., Lagha, M., Rocancourt, D., Daubas, P., and Buckingham, M.E. 2006. A novel genetic hierarchy functions during hypaxial myogenesis: Pax3 directly activates Myf5 in muscle progenitor cells in the limb. *Genes Dev.* 20, 2450-2464.

Bao, W., Wang, H.H., Tian, F.J., He, X.Y., Qiu, M.T., Wang, J.Y., Zhang, H.J., Wang, L.H., and Wan, X.P. 2013. A TrkB-STAT3-miR-204-5p regulatory circuitry controls proliferation and invasion of endometrial carcinoma cells. *Mol.Cancer.* 12, 155-4598-12-155.

Bao, Y., Guo, Y., Li, Z., Fang, W., Yang, Y., Li, X., Li, Z., Xiong, B., Chen, Z., Wang, J., Kang, K., Gou, D., and Yang, W. 2014. MicroRNA profiling in Muc2 knockout mice of colitis-associated cancer model reveals epigenetic alterations during chronic colitis malignant transformation. *PLoS One* 9, e99132.

Bearfoot, J.L., Choong, D.Y., Gorringe, K.L., and Campbell, I.G. 2008. Genetic analysis of cancer-implicated MicroRNA in ovarian cancer. *Clin.Cancer Res.* 14, 7246-7250.

Begum, S., Emami, N., Cheung, A., Wilkins, O., Der, S., and Hamel, P.A. 2005. Cell-type-specific regulation of distinct sets of gene targets by Pax3 and Pax3/FKHR. *Oncogene* 24, 1860-1872.

Behm-Ansmant, I., Rehwinkel, J., Doerks, T., Stark, A., Bork, P., and Izaurralde, E. 2006. mRNA degradation by miRNAs and GW182 requires both CCR4:NOT deadenylase and DCP1:DCP2 decapping complexes. *Genes Dev.* 20, 1885-1898.

Bennicelli, J.L., Edwards, R.H., and Barr, F.G. 1996. Mechanism for transcriptional gain of function resulting from chromosomal translocation in alveolar rhabdomyosarcoma. *Proc.Natl.Acad.Sci.U.S.A.* 93, 5455-5459.

Bentzinger, C.F., Wang, Y.X., and Rudnicki, M.A. 2012. Building muscle: molecular regulation of myogenesis. *Cold Spring Harb Perspect.Biol.* 4, 10.1101/cshperspect.a008342.

Berber, U., Yilmaz, I., Narli, G., Haholu, A., Kucukodaci, Z., and Demirel, D. 2014. miR-205 and miR-200c: Predictive Micro RNAs for Lymph Node Metastasis in Triple Negative Breast Cancer. *J.Breast Cancer.* 17, 143-148.

Bernstein, E., Caudy, A.A., Hammond, S.M., and Hannon, G.J. 2001. Role for a bidentate ribonuclease in the initiation step of RNA interference. *Nature* 409, 363-366.

Berry, F.B., Skarie, J.M., Mirzayans, F., Fortin, Y., Hudson, T.J., Raymond, V., Link, B.A., and Walter, M.A. 2008. FOXC1 is required for cell viability and resistance to oxidative stress in the eye through the transcriptional regulation of FOXO1A. *Hum.Mol.Genet.* 17, 490-505.

Bing, L., Hong, C., Li-Xin, S., and Wei, G. 2014. MicroRNA-543 suppresses endometrial cancer oncogenicity via targeting FAK and TWIST1 expression. *Arch.Gynecol.Obstet.*

Bober, E., Franz, T., Arnold, H.H., Gruss, P., and Tremblay, P. 1994. Pax-3 is required for the development of limb muscles: a possible role for the migration of dermomyotomal muscle progenitor cells. *Development* 120, 603-612.

BOHANNON, R.A., MILLER, D.G., and DIAMOND, H.D. 1963. Vincristine in the treatment of lymphomas and leukemias. *Cancer Res.* 23, 613-621.

Bopp, D., Burri, M., Baumgartner, S., Frigerio, G., and Noll, M. 1986. Conservation of a large protein domain in the segmentation gene paired and in functionally related genes of Drosophila. *Cell* 47, 1033-1040.

Braun, T., and Arnold, H.H. 1991. The four human muscle regulatory helix-loop-helix proteins Myf3-Myf6 exhibit similar hetero-dimerization and DNA binding properties. *Nucleic Acids Res.* 19, 5645-5651.

Cai, X., Hagedorn, C.H., and Cullen, B.R. 2004. Human microRNAs are processed from capped, polyadenylated transcripts that can also function as mRNAs. *RNA* 10, 1957-1966.

Calin, G.A., Dumitru, C.D., Shimizu, M., Bichi, R., Zupo, S., Noch, E., Aldler, H., Rattan, S., Keating, M., Rai, K., Rassenti, L., Kipps, T., Negrini, M., Bullrich, F., and Croce, C.M. 2002. Frequent deletions and down-regulation of micro- RNA genes miR15 and miR16 at 13q14 in chronic lymphocytic leukemia. *Proc.Natl.Acad.Sci.U.S.A.* 99, 15524-15529.

Calin, G.A., Ferracin, M., Cimmino, A., Di Leva, G., Shimizu, M., Wojcik, S.E., Iorio, M.V., Visone, R., Sever, N.I., Fabbri, M., Iuliano, R., Palumbo, T., Pichiorri, F., Roldo, C., Garzon, R., Sevignani, C., Rassenti, L., Alder, H., Volinia, S., Liu, C.G., Kipps, T.J., Negrini, M., and Croce, C.M. 2005. A MicroRNA signature associated with prognosis and progression in chronic lymphocytic leukemia. *N.Engl.J.Med.* 353, 1793-1801.

Calin, G.A., Sevignani, C., Dumitru, C.D., Hyslop, T., Noch, E., Yendamuri, S., Shimizu, M., Rattan, S., Bullrich, F., Negrini, M., and Croce, C.M. 2004. Human

microRNA genes are frequently located at fragile sites and genomic regions involved in cancers. *Proc.Natl.Acad.Sci.U.S.A.* 101, 2999-3004.

Cao, L., Yu, Y., Bilke, S., Walker, R.L., Mayeenuddin, L.H., Azorsa, D.O., Yang, F., Pineda, M., Helman, L.J., and Meltzer, P.S. 2010. Genome-wide identification of PAX3-FKHR binding sites in rhabdomyosarcoma reveals candidate target genes important for development and cancer. *Cancer Res.* 70, 6497-6508.

Cardinali, B., Castellani, L., Fasanaro, P., Basso, A., Alema, S., Martelli, F., and Falcone, G. 2009. Microrna-221 and microrna-222 modulate differentiation and maturation of skeletal muscle cells. *PLoS One* 4, e7607.

Chalepakis, G., Goulding, M., Read, A., Strachan, T., and Gruss, P. 1994. Molecular basis of splotch and Waardenburg Pax-3 mutations. *Proc.Natl.Acad.Sci.U.S.A.* 91, 3685-3689.

Chalepakis, G., and Gruss, P. 1995. Identification of DNA recognition sequences for the Pax3 paired domain. *Gene* 162, 267-270.

Chan, J.A., Krichevsky, A.M., and Kosik, K.S. 2005. MicroRNA-21 is an antiapoptotic factor in human glioblastoma cells. *Cancer Res.* 65, 6029-6033.

Chang, T.C., Wentzel, E.A., Kent, O.A., Ramachandran, K., Mullendore, M., Lee, K.H., Feldmann, G., Yamakuchi, M., Ferlito, M., Lowenstein, C.J., Arking, D.E., Beer, M.A., Maitra, A., and Mendell, J.T. 2007. Transactivation of miR-34a by p53 broadly influences gene expression and promotes apoptosis. *Mol.Cell* 26, 745-752.

Chemaitilly, W., Mertens, A.C., Mitby, P., Whitton, J., Stovall, M., Yasui, Y., Robison, L.L., and Sklar, C.A. 2006. Acute ovarian failure in the childhood cancer survivor study. *J.Clin.Endocrinol.Metab.* 91, 1723-1728.

Chen, J.F., Mandel, E.M., Thomson, J.M., Wu, Q., Callis, T.E., Hammond, S.M., Conlon, F.L., and Wang, D.Z. 2006. The role of microRNA-1 and microRNA-133 in skeletal muscle proliferation and differentiation. *Nat.Genet.* 38, 228-233.

Chen, S.M., Chen, H.C., Chen, S.J., Huang, C.Y., Chen, P.Y., Wu, T.W., Feng, L.Y., Tsai, H.C., Lui, T.N., Hsueh, C., and Wei, K.C. 2013a. MicroRNA-495 inhibits proliferation of glioblastoma multiforme cells by downregulating cyclin-dependent kinase 6. *World J.Surg.Oncol.* 11, 87-7819-11-87.

Chen, Z., Sangwan, V., Banerjee, S., Mackenzie, T., Dudeja, V., Li, X., Wang, H., Vickers, S.M., and Saluja, A.K. 2013b. miR-204 mediated loss of Myeloid cell

leukemia-1 results in pancreatic cancer cell death. *Mol.Cancer.* 12, 105-4598-12-105.

Chien, C.H., Sun, Y.M., Chang, W.C., Chiang-Hsieh, P.Y., Lee, T.Y., Tsai, W.C., Horng, J.T., Tsou, A.P., and Huang, H.D. 2011. Identifying transcriptional start sites of human microRNAs based on high-throughput sequencing data. *Nucleic Acids Res.* 39, 9345-9356.

Chu, H., Chen, X., Wang, H., Du, Y., Wang, Y., Zang, W., Li, P., Li, J., Chang, J., Zhao, G., and Zhang, G. 2014. MiR-495 regulates proliferation and migration in NSCLC by targeting MTA3. *Tumour Biol.* 35, 3487-3494.

Ciafre, S.A., Galardi, S., Mangiola, A., Ferracin, M., Liu, C.G., Sabatino, G., Negrini, M., Maira, G., Croce, C.M., and Farace, M.G. 2005. Extensive modulation of a set of microRNAs in primary glioblastoma. *Biochem.Biophys.Res.Commun.* 334, 1351-1358.

Ciarapica, R., Russo, G., Verginelli, F., Raimondi, L., Donfrancesco, A., Rota, R., and Giordano, A. 2009. Deregulated expression of miR-26a and Ezh2 in rhabdomyosarcoma. *Cell.Cycle* 8, 172-175.

Cimmino, A., Calin, G.A., Fabbri, M., Iorio, M.V., Ferracin, M., Shimizu, M., Wojcik, S.E., Aqeilan, R.I., Zupo, S., Dono, M., Rassenti, L., Alder, H., Volinia, S., Liu, C.G., Kipps, T.J., Negrini, M., and Croce, C.M. 2005. miR-15 and miR-16 induce apoptosis by targeting BCL2. *Proc.Natl.Acad.Sci.U.S.A.* 102, 13944-13949.

Clark, K.L., Halay, E.D., Lai, E., and Burley, S.K. 1993. Co-crystal structure of the HNF-3/fork head DNA-recognition motif resembles histone H5. *Nature* 364, 412-420.

Cloonan, N., Forrest, A.R., Kolle, G., Gardiner, B.B., Faulkner, G.J., Brown, M.K., Taylor, D.F., Steptoe, A.L., Wani, S., Bethel, G., Robertson, A.J., Perkins, A.C., Bruce, S.J., Lee, C.C., Ranade, S.S., Peckham, H.E., Manning, J.M., McKernan, K.J., and Grimmond, S.M. 2008. Stem cell transcriptome profiling via massive-scale mRNA sequencing. *Nat.Methods* 5, 613-619.

Cornett, A.L., and Lutz, C.S. 2014. Regulation of COX-2 expression by miR-146a in lung cancer cells. *RNA.*

Crippa, S., Cassano, M., Messina, G., Galli, D., Galvez, B.G., Curk, T., Altomare, C., Ronzoni, F., Toelen, J., Gijsbers, R., Debyser, Z., Janssens, S., Zupan, B., Zaza, A., Cossu, G., and Sampaolesi, M. 2011. miR669a and miR669q prevent skeletal

muscle differentiation in postnatal cardiac progenitors. *J.Cell Biol.* 193, 1197-1212.

Crist, W., Gehan, E.A., Ragab, A.H., Dickman, P.S., Donaldson, S.S., Fryer, C., Hammond, D., Hays, D.M., Herrmann, J., and Heyn, R. 1995. The Third Intergroup Rhabdomyosarcoma Study. *J.Clin.Oncol.* 13, 610-630.

Dacic, S., Kelly, L., Shuai, Y., and Nikiforova, M.N. 2010. miRNA expression profiling of lung adenocarcinomas: correlation with mutational status. *Mod.Pathol.* 23, 1577-1582.

d'Adhemar, C.J., Spillane, C.D., Gallagher, M.F., Bates, M., Costello, K.M., Barry-O'Crowley, J., Haley, K., Kernan, N., Murphy, C., Smyth, P.C., O'Byrne, K., Pennington, S., Cooke, A.A., Ffrench, B., Martin, C.M., O'Donnell, D., Hennessy, B., Stordal, B., Finn, S., McCann, A., Gleeson, N., D'Arcy, T., Flood, B., O'Neill, L.A., Sheils, O., O'Toole, S., and O'Leary, J.J. 2014. The MyD88+ phenotype is an adverse prognostic factor in epithelial ovarian cancer. *PLoS One* 9, e100816.

Dagher, R., and Helman, L. 1999. Rhabdomyosarcoma: an overview. *Oncologist* 4, 34-44.

Davis, R.J., D'Cruz, C.M., Lovell, M.A., Biegel, J.A., and Barr, F.G. 1994. Fusion of PAX7 to FKHR by the variant t(1;13)(p36;q14) translocation in alveolar rhabdomyosarcoma. *Cancer Res.* 54, 2869-2872.

De Sarkar, N., Roy, R., Mitra, J.K., Ghose, S., Chakraborty, A., Paul, R.R., Mukhopadhyay, I., and Roy, B. 2014. A Quest for miRNA Bio-Marker: A Track Back Approach from Gingivo Buccal Cancer to Two Different Types of Precancers. *PLoS One* 9, e104839.

Deacon, D.C., Nevis, K.R., Cashman, T.J., Zhou, Y., Zhao, L., Washko, D., Guner-Ataman, B., Burns, C.G., and Burns, C.E. 2010. The miR-143-adducin3 pathway is essential for cardiac chamber morphogenesis. *Development* 137, 1887-1896.

Demontis, F., and Perrimon, N. 2010. FOXO/4E-BP signaling in Drosophila muscles regulates organism-wide proteostasis during aging. *Cell* 143, 813-825.

Dey, B.K., Gagan, J., and Dutta, A. 2011. miR-206 and -486 induce myoblast differentiation by downregulating Pax7. *Mol.Cell.Biol.* 31, 203-214.

Dias, P., Chen, B., Dilday, B., Palmer, H., Hosoi, H., Singh, S., Wu, C., Li, X., Thompson, J., Parham, D., Qualman, S., and Houghton, P. 2000. Strong

immunostaining for myogenin in rhabdomyosarcoma is significantly associated with tumors of the alveolar subclass. *Am.J.Pathol.* 156, 399-408.

Dixon-McIver, A., East, P., Mein, C.A., Cazier, J.B., Molloy, G., Chaplin, T., Andrew Lister, T., Young, B.D., and Debernardi, S. 2008. Distinctive patterns of microRNA expression associated with karyotype in acute myeloid leukaemia. *PLoS One* 3, e2141.

Dressman, D., Yan, H., Traverso, G., Kinzler, K.W., and Vogelstein, B. 2003. Transforming single DNA molecules into fluorescent magnetic particles for detection and enumeration of genetic variations. *Proc.Natl.Acad.Sci.U.S.A.* 100, 8817-8822.

Eisenberg, I., Eran, A., Nishino, I., Moggio, M., Lamperti, C., Amato, A.A., Lidov, H.G., Kang, P.B., North, K.N., Mitrani-Rosenbaum, S., Flanigan, K.M., Neely, L.A., Whitney, D., Beggs, A.H., Kohane, I.S., and Kunkel, L.M. 2007. Distinctive patterns of microRNA expression in primary muscular disorders. *Proc.Natl.Acad.Sci.U.S.A.* 104, 17016-17021.

El-Badry, O.M., Minniti, C., Kohn, E.C., Houghton, P.J., Daughaday, W.H., and Helman, L.J. 1990. Insulin-like growth factor II acts as an autocrine growth and motility factor in human rhabdomyosarcoma tumors. *Cell Growth Differ.* 1, 325-331.

Epstein, J.A., Shapiro, D.N., Cheng, J., Lam, P.Y., and Maas, R.L. 1996. Pax3 modulates expression of the c-Met receptor during limb muscle development. *Proc.Natl.Acad.Sci.U.S.A.* 93, 4213-4218.

Eulalio, A., Huntzinger, E., Nishihara, T., Rehwinkel, J., Fauser, M., and Izaurralde, E. 2009. Deadenylation is a widespread effect of miRNA regulation. *RNA* 15, 21-32.

Eulalio, A., Rehwinkel, J., Stricker, M., Huntzinger, E., Yang, S.F., Doerks, T., Dorner, S., Bork, P., Boutros, M., and Izaurralde, E. 2007. Target-specific requirements for enhancers of decapping in miRNA-mediated gene silencing. *Genes Dev.* 21, 2558-2570.

Fabbri, M., Garzon, R., Cimmino, A., Liu, Z., Zanesi, N., Callegari, E., Liu, S., Alder, H., Costinean, S., Fernandez-Cymering, C., Volinia, S., Guler, G., Morrison, C.D., Chan, K.K., Marcucci, G., Calin, G.A., Huebner, K., and Croce, C.M. 2007. MicroRNA-29 family reverts aberrant methylation in lung cancer by targeting DNA methyltransferases 3A and 3B. *Proc.Natl.Acad.Sci.U.S.A.* 104, 15805-15810.

Faller, M., and Guo, F. 2008. MicroRNA biogenesis: there's more than one way to skin a cat. *Biochim.Biophys.Acta* 1779, 663-667.

Fan, X., and Wu, Z. 2014. Effects of four single nucleotide polymorphisms in microRNA-coding genes on lung cancer risk. *Tumour Biol.*

Fassina, A., Cappellesso, R., and Fassan, M. 2011. Classification of non-small cell lung carcinoma in transthoracic needle specimens using microRNA expression profiling. *Chest* 140, 1305-1311.

Fedurco, M., Romieu, A., Williams, S., Lawrence, I., and Turcatti, G. 2006. BTA, a novel reagent for DNA attachment on glass and efficient generation of solid-phase amplified DNA colonies. *Nucleic Acids Res.* 34, e22.

Ferrari, A., Dileo, P., Casanova, M., Bertulli, R., Meazza, C., Gandola, L., Navarria, P., Collini, P., Gronchi, A., Olmi, P., Fossati-Bellani, F., and Casali, P.G. 2003. Rhabdomyosarcoma in adults. A retrospective analysis of 171 patients treated at a single institution. *Cancer* 98, 571-580.

Finckenstein, F.G., Davicioni, E., Osborn, K.G., Cavenee, W.K., Arden, K.C., and Anderson, M.J. 2006. Transgenic mice expressing PAX3-FKHR have multiple defects in muscle development, including ectopic skeletal myogenesis in the developing neural tube. *Transgenic Res.* 15, 595-614.

Formosa, A., Markert, E.K., Lena, A.M., Italiano, D., Finazzi-Agro', E., Levine, A.J., Bernardini, S., Garabadgiu, A.V., Melino, G., and Candi, E. 2013. MicroRNAs, miR-154, miR-299-5p, miR-376a, miR-376c, miR-377, miR-381, miR-487b, miR-485-3p, miR-495 and miR-654-3p, mapped to the 14q32.31 locus, regulate proliferation, apoptosis, migration and invasion in metastatic prostate cancer cells. *Oncogene*.

Fortin, A.S., Underhill, D.A., and Gros, P. 1997. Reciprocal effect of Waardenburg syndrome mutations on DNA binding by the Pax-3 paired domain and homeodomain. *Hum.Mol.Genet.* 6, 1781-1790.

Frankel, L.B., Christoffersen, N.R., Jacobsen, A., Lindow, M., Krogh, A., and Lund, A.H. 2008. Programmed cell death 4 (PDCD4) is an important functional target of the microRNA miR-21 in breast cancer cells. *J.Biol.Chem.* 283, 1026-1033.

Franz, T. 1993. The Splotch (Sp1H) and Splotch-delayed (Spd) alleles: differential phenotypic effects on neural crest and limb musculature. *Anat.Embryol.(Berl)* 187, 371-377.

Fredericks, W.J., Galili, N., Mukhopadhyay, S., Rovera, G., Bennicelli, J., Barr, F.G., and Rauscher, F.J.,3rd. 1995. The PAX3-FKHR fusion protein created by the t(2;13) translocation in alveolar rhabdomyosarcomas is a more potent transcriptional activator than PAX3. *Mol.Cell.Biol.* 15, 1522-1535.

Friedl, P., and Wolf, K. 2009. Proteolytic interstitial cell migration: a five-step process. *Cancer Metastasis Rev.* 28, 129-135.

Friedman, O., and Seligman, A. 1954. **Preparation of Secondary Amine Mustards with High Toxicity1a**. *Journal of the American Chemical Society* 76, 658.

Fulci, V., Chiaretti, S., Goldoni, M., Azzalin, G., Carucci, N., Tavolaro, S., Castellano, L., Magrelli, A., Citarella, F., Messina, M., Maggio, R., Peragine, N., Santangelo, S., Mauro, F.R., Landgraf, P., Tuschl, T., Weir, D.B., Chien, M., Russo, J.J., Ju, J., Sheridan, R., Sander, C., Zavolan, M., Guarini, A., Foa, R., and Macino, G. 2007. Quantitative technologies establish a novel microRNA profile of chronic lymphocytic leukemia. *Blood* 109, 4944-4951.

Galili, N., Davis, R.J., Fredericks, W.J., Mukhopadhyay, S., Rauscher, F.J.,3rd, Emanuel, B.S., Rovera, G., and Barr, F.G. 1993. Fusion of a fork head domain gene to PAX3 in the solid tumour alveolar rhabdomyosarcoma. *Nat.Genet.* 5, 230-235.

Garzon, R., Garofalo, M., Martelli, M.P., Briesewitz, R., Wang, L., Fernandez-Cymering, C., Volinia, S., Liu, C.G., Schnittger, S., Haferlach, T., Liso, A., Diverio, D., Mancini, M., Meloni, G., Foa, R., Martelli, M.F., Mecucci, C., Croce, C.M., and Falini, B. 2008a. Distinctive microRNA signature of acute myeloid leukemia bearing cytoplasmic mutated nucleophosmin. *Proc.Natl.Acad.Sci.U.S.A.* 105, 3945-3950.

Garzon, R., Volinia, S., Liu, C.G., Fernandez-Cymering, C., Palumbo, T., Pichiorri, F., Fabbri, M., Coombes, K., Alder, H., Nakamura, T., Flomenberg, N., Marcucci, G., Calin, G.A., Kornblau, S.M., Kantarjian, H., Bloomfield, C.D., Andreeff, M., and Croce, C.M. 2008b. MicroRNA signatures associated with cytogenetics and prognosis in acute myeloid leukemia. *Blood* 111, 3183-3189.

Ge, W., Yu, D.C., Li, Q.G., Chen, X., Zhang, C.Y., and Ding, Y.T. 2014. Expression of serum miR-16, let-7f, and miR-21 in patients with hepatocellular carcinoma and their clinical significances. *Clin.Lab.* 60, 427-434.

Ge, Y., Sun, Y., and Chen, J. 2011. IGF-II is regulated by microRNA-125b in skeletal myogenesis. *J.Cell Biol.* 192, 69-81.

Gebeshuber, C.A., Zatloukal, K., and Martinez, J. 2009. miR-29a suppresses tristetraprolin, which is a regulator of epithelial polarity and metastasis. *EMBO Rep.* 10, 400-405.

Goldhamer, D.J., Brunk, B.P., Faerman, A., King, A., Shani, M., and Emerson, C.P.,Jr. 1995. Embryonic activation of the myoD gene is regulated by a highly conserved distal control element. *Development* 121, 637-649.

Goljanek-Whysall, K., Sweetman, D., Abu-Elmagd, M., Chapnik, E., Dalmay, T., Hornstein, E., and Munsterberg, A. 2011. MicroRNA regulation of the paired-box transcription factor Pax3 confers robustness to developmental timing of myogenesis. *Proc.Natl.Acad.Sci.U.S.A.* 108, 11936-11941.

Gordon, A.T., Brinkschmidt, C., Anderson, J., Coleman, N., Dockhorn-Dworniczak, B., Pritchard-Jones, K., and Shipley, J. 2000. A novel and consistent amplicon at 13q31 associated with alveolar rhabdomyosarcoma. *Genes Chromosomes Cancer* 28, 220-226.

Gougelet, A., Perez, J., Pissaloux, D., Besse, A., Duc, A., Decouvelaere, A.V., Ranchere-Vince, D., Blay, J.Y., and Alberti, L. 2011. miRNA Profiling: How to Bypass the Current Difficulties in the Diagnosis and Treatment of Sarcomas. *Sarcoma* 2011, 460650.

Green, D.M., Kawashima, T., Stovall, M., Leisenring, W., Sklar, C.A., Mertens, A.C., Donaldson, S.S., Byrne, J., and Robison, L.L. 2010. Fertility of male survivors of childhood cancer: a report from the Childhood Cancer Survivor Study. *J.Clin.Oncol.* 28, 332-339.

Gregory, R.I., Chendrimada, T.P., and Shiekhattar, R. 2006. MicroRNA biogenesis: isolation and characterization of the microprocessor complex. *Methods Mol.Biol.* 342, 33-47.

Gripp, K.W., Scott, C.I.,Jr, Nicholson, L., McDonald-McGinn, D.M., Ozeran, J.D., Jones, M.C., Lin, A.E., and Zackai, E.H. 2002. Five additional Costello syndrome patients with rhabdomyosarcoma: proposal for a tumor screening protocol. *Am.J.Med.Genet.* 108, 80-87.

Gruss, P., and Walther, C. 1992. Pax in development. *Cell* 69, 719-722.

Guo, L., Liu, Y., Bai, Y., Sun, Y., Xiao, F., and Guo, Y. 2010. Gene expression profiling of drug-resistant small cell lung cancer cells by combining microRNA and cDNA expression analysis. *Eur.J.Cancer* 46, 1692-1702.

He, L., He, X., Lim, L.P., de Stanchina, E., Xuan, Z., Liang, Y., Xue, W., Zender, L., Magnus, J., Ridzon, D., Jackson, A.L., Linsley, P.S., Chen, C., Lowe, S.W., Cleary, M.A., and Hannon, G.J. 2007. A microRNA component of the p53 tumour suppressor network. *Nature* 447, 1130-1134.

Heerema-McKenney, A., Wijnaendts, L.C., Pulliam, J.F., Lopez-Terrada, D., McKenney, J.K., Zhu, S., Montgomery, K., Mitchell, J., Marinelli, R.J., Hart, A.A., van de Rijn, M., and Linn, S.C. 2008. Diffuse myogenin expression by immunohistochemistry is an independent marker of poor survival in pediatric rhabdomyosarcoma: a tissue microarray study of 71 primary tumors including correlation with molecular phenotype. *Am.J.Surg.Pathol.* 32, 1513-1522.

Heyn, R., Haeberlen, V., Newton, W.A., Ragab, A.H., Raney, R.B., Tefft, M., Wharam, M., Ensign, L.G., and Maurer, H.M. 1993. Second malignant neoplasms in children treated for rhabdomyosarcoma. Intergroup Rhabdomyosarcoma Study Committee. *J.Clin.Oncol.* 11, 262-270.

Hollenbach, A.D., Sublett, J.E., McPherson, C.J., and Grosveld, G. 1999. The Pax3-FKHR oncoprotein is unresponsive to the Pax3-associated repressor hDaxx. *EMBO J.* 18, 3702-3711.

Housby, J.N., and Southern, E.M. 1998. Fidelity of DNA ligation: a novel experimental approach based on the polymerisation of libraries of oligonucleotides. *Nucleic Acids Res.* 26, 4259-4266.

Hu, Q., Yuan, Y., and Wang, C. 2013. Structural and functional studies of FKHR-PAX3, a reciprocal fusion gene of the t(2;13) chromosomal translocation in alveolar rhabdomyosarcoma. *PLoS One* 8, e68065.

Huang, H., Regan, K.M., Lou, Z., Chen, J., and Tindall, D.J. 2006. CDK2-dependent phosphorylation of FOXO1 as an apoptotic response to DNA damage. *Science* 314, 294-297.

Huang, M.B., Xu, H., Xie, S.J., Zhou, H., and Qu, L.H. 2011. Insulin-like growth factor-1 receptor is regulated by microRNA-133 during skeletal myogenesis. *PLoS One* 6, e29173.

Huang, S., He, R., Rong, M., Dang, Y., and Chen, G. 2014. Synergistic effect of MiR-146a mimic and cetuximab on hepatocellular carcinoma cells. *Biomed.Res.Int.* 2014, 384121.

Hullinger, T.G., Montgomery, R.L., Seto, A.G., Dickinson, B.A., Semus, H.M., Lynch, J.M., Dalby, C.M., Robinson, K., Stack, C., Latimer, P.A., Hare, J.M.,

Olson, E.N., and van Rooij, E. 2012. Inhibition of miR-15 protects against cardiac ischemic injury. *Circ.Res.* 110, 71-81.

Huse, J.T., Brennan, C., Hambardzumyan, D., Wee, B., Pena, J., Rouhanifard, S.H., Sohn-Lee, C., le Sage, C., Agami, R., Tuschl, T., and Holland, E.C. 2009. The PTEN-regulating microRNA miR-26a is amplified in high-grade glioma and facilitates gliomagenesis in vivo. *Genes Dev.* 23, 1327-1337.

Hutvagner, G., McLachlan, J., Pasquinelli, A.E., Balint, E., Tuschl, T., and Zamore, P.D. 2001. A cellular function for the RNA-interference enzyme Dicer in the maturation of the let-7 small temporal RNA. *Science* 293, 834-838.

Hwang-Verslues, W.W., Chang, P.H., Wei, P.C., Yang, C.Y., Huang, C.K., Kuo, W.H., Shew, J.Y., Chang, K.J., Lee, E.Y., and Lee, W.H. 2011. miR-495 is upregulated by E12/E47 in breast cancer stem cells, and promotes oncogenesis and hypoxia resistance via downregulation of E-cadherin and REDD1. *Oncogene* 30, 2463-2474.

Iorio, M.V., Ferracin, M., Liu, C.G., Veronese, A., Spizzo, R., Sabbioni, S., Magri, E., Pedriali, M., Fabbri, M., Campiglio, M., Menard, S., Palazzo, J.P., Rosenberg, A., Musiani, P., Volinia, S., Nenci, I., Calin, G.A., Querzoli, P., Negrini, M., and Croce, C.M. 2005. MicroRNA gene expression deregulation in human breast cancer. *Cancer Res.* 65, 7065-7070.

Janssen, H.L., Reesink, H.W., Lawitz, E.J., Zeuzem, S., Rodriguez-Torres, M., Patel, K., van der Meer, A.J., Patick, A.K., Chen, A., Zhou, Y., Persson, R., King, B.D., Kauppinen, S., Levin, A.A., and Hodges, M.R. 2013. Treatment of HCV infection by targeting microRNA. *N.Engl.J.Med.* 368, 1685-1694.

Jia, W., Wu, Y., Zhang, Q., Gao, G., Zhang, C., and Xiang, Y. 2013. Identification of four serum microRNAs from a genome-wide serum microRNA expression profile as potential non-invasive biomarkers for endometrioid endometrial cancer. *Oncol.Lett.* 6, 261-267.

Jiang, X., Huang, H., Li, Z., He, C., Li, Y., Chen, P., Gurbuxani, S., Arnovitz, S., Hong, G.M., Price, C., Ren, H., Kunjamma, R.B., Neilly, M.B., Salat, J., Wunderlich, M., Slany, R.K., Zhang, Y., Larson, R.A., Le Beau, M.M., Mulloy, J.C., Rowley, J.D., and Chen, J. 2012. MiR-495 is a tumor-suppressor microRNA down-regulated in MLL-rearranged leukemia. *Proc.Natl.Acad.Sci.U.S.A.* 109, 19397-19402.

Kalman, S., Garbett, K.A., Vereczkei, A., Shelton, R.C., Korade, Z., and Mirnics, K. 2014. Metabolic stress-induced microRNA and mRNA expression profiles of human fibroblasts. *Exp.Cell Res.* 320, 343-353.

Kamei, Y., Miura, S., Suzuki, M., Kai, Y., Mizukami, J., Taniguchi, T., Mochida, K., Hata, T., Matsuda, J., Aburatani, H., Nishino, I., and Ezaki, O. 2004. Skeletal muscle FOXO1 (FKHR) transgenic mice have less skeletal muscle mass, down-regulated Type I (slow twitch/red muscle) fiber genes, and impaired glycemic control. *J.Biol.Chem.* 279, 41114-41123.

Kassar-Duchossoy, L., Gayraud-Morel, B., Gomes, D., Rocancourt, D., Buckingham, M., Shinin, V., and Tajbakhsh, S. 2004. Mrf4 determines skeletal muscle identity in Myf5:Myod double-mutant mice. *Nature* 431, 466-471.

Kenney, L.B., Laufer, M.R., Grant, F.D., Grier, H., and Diller, L. 2001. High risk of infertility and long term gonadal damage in males treated with high dose cyclophosphamide for sarcoma during childhood. *Cancer* 91, 613-621.

KERSTEN, W., KERSTEN, H., and RAUEN, H.M. 1960. Action of nucleic acids on the inhibition of growth by actinomycin of Neurospora crassa. *Nature* 187, 60-61.

Kim, H.K., Lee, Y.S., Sivaprasad, U., Malhotra, A., and Dutta, A. 2006. Muscle-specific microRNA miR-206 promotes muscle differentiation. *J.Cell Biol.* 174, 677-687.

Kluiver, J., Poppema, S., de Jong, D., Blokzijl, T., Harms, G., Jacobs, S., Kroesen, B.J., and van den Berg, A. 2005. BIC and miR-155 are highly expressed in Hodgkin, primary mediastinal and diffuse large B cell lymphomas. *J.Pathol.* 207, 243-249.

Kota, J., Chivukula, R.R., O'Donnell, K.A., Wentzel, E.A., Montgomery, C.L., Hwang, H.W., Chang, T.C., Vivekanandan, P., Torbenson, M., Clark, K.R., Mendell, J.R., and Mendell, J.T. 2009. Therapeutic microRNA delivery suppresses tumorigenesis in a murine liver cancer model. *Cell* 137, 1005-1017.

Kozakowska, M., Ciesla, M., Stefanska, A., Skrzypek, K., Was, H., Jazwa, A., Grochot-Przeczek, A., Kotlinowski, J., Szymula, A., Bartelik, A., Mazan, M., Yagensky, O., Florczyk, U., Lemke, K., Zebzda, A., Dyduch, G., Nowak, W., Szade, K., Stepniewski, J., Majka, M., Derlacz, R., Loboda, A., Dulak, J., and Jozkowicz, A. 2012. Heme oxygenase-1 inhibits myoblast differentiation by targeting myomirs. *Antioxid.Redox Signal.* 16, 113-127.

Kozubek, J., Ma, Z., Fleming, E., Duggan, T., Wu, R., Shin, D.G., and Dadras, S.S. 2013. In-depth characterization of microRNA transcriptome in melanoma. *PLoS One* 8, e72699.

Krasin, M.J., Wiese, K.M., Spunt, S.L., Hua, C.H., Daw, N., Navid, F., Davidoff, A.M., McGregor, L., Merchant, T.E., Kun, L.E., McCrarey, L., Hoth, K.A., Yan,

X., and Xiong, X. 2012. Jaw dysfunction related to pterygoid and masseter muscle dosimetry after radiation therapy in children and young adults with head-and-neck sarcomas. *Int.J.Radiat.Oncol.Biol.Phys.* 82, 355-360.

Kriegel, A.J., Fang, Y., Liu, Y., Tian, Z., Mladinov, D., Matus, I.R., Ding, X., Greene, A.S., and Liang, M. 2010. MicroRNA-target pairs in human renal epithelial cells treated with transforming growth factor beta 1: a novel role of miR-382. *Nucleic Acids Res.* 38, 8338-8347.

Kuang, W., Tan, J., Duan, Y., Duan, J., Wang, W., Jin, F., Jin, Z., Yuan, X., and Liu, Y. 2009. Cyclic stretch induced miR-146a upregulation delays C2C12 myogenic differentiation through inhibition of Numb. *Biochem.Biophys.Res.Commun.* 378, 259-263.

Kumar, M.S., Erkeland, S.J., Pester, R.E., Chen, C.Y., Ebert, M.S., Sharp, P.A., and Jacks, T. 2008. Suppression of non-small cell lung tumor development by the let-7 microRNA family. *Proc.Natl.Acad.Sci.U.S.A.* 105, 3903-3908.

Lagos-Quintana, M., Rauhut, R., Yalcin, A., Meyer, J., Lendeckel, W., and Tuschl, T. 2002. Identification of tissue-specific microRNAs from mouse. *Curr.Biol.* 12, 735-739.

Lagutina, I., Conway, S.J., Sublett, J., and Grosveld, G.C. 2002. Pax3-FKHR knock-in mice show developmental aberrations but do not develop tumors. *Mol.Cell.Biol.* 22, 7204-7216.

Lam, P.Y., Sublett, J.E., Hollenbach, A.D., and Roussel, M.F. 1999. The oncogenic potential of the Pax3-FKHR fusion protein requires the Pax3 homeodomain recognition helix but not the Pax3 paired-box DNA binding domain. *Mol.Cell.Biol.* 19, 594-601.

Landgraf, P., Rusu, M., Sheridan, R., Sewer, A., Iovino, N., Aravin, A., Pfeffer, S., Rice, A., Kamphorst, A.O., Landthaler, M., Lin, C., Socci, N.D., Hermida, L., Fulci, V., Chiaretti, S., Foa, R., Schliwka, J., Fuchs, U., Novosel, A., Muller, R.U., Schermer, B., Bissels, U., Inman, J., Phan, Q., Chien, M., Weir, D.B., Choksi, R., De Vita, G., Frezzetti, D., Trompeter, H.I., Hornung, V., Teng, G., Hartmann, G., Palkovits, M., Di Lauro, R., Wernet, P., Macino, G., Rogler, C.E., Nagle, J.W., Ju, J., Papavasiliou, F.N., Benzing, T., Lichter, P., Tam, W., Brownstein, M.J., Bosio, A., Borkhardt, A., Russo, J.J., Sander, C., Zavolan, M., and Tuschl, T. 2007. A mammalian microRNA expression atlas based on small RNA library sequencing. *Cell* 129, 1401-1414.

Lee, R.C., Feinbaum, R.L., and Ambros, V. 1993. The C. elegans heterochronic gene lin-4 encodes small RNAs with antisense complementarity to lin-14. *Cell* 75, 843-854.

Lee, S., Yoon, D.S., Paik, S., Lee, K.M., Jang, Y., and Lee, J.W. 2014. microRNA-495 Inhibits Chondrogenic Differentiation in Human Mesenchymal Stem Cells by Targeting Sox9. *Stem Cells Dev.*

Lee, S.T., Chu, K., Oh, H.J., Im, W.S., Lim, J.Y., Kim, S.K., Park, C.K., Jung, K.H., Lee, S.K., Kim, M., and Roh, J.K. 2011. Let-7 microRNA inhibits the proliferation of human glioblastoma cells. *J.Neurooncol.* 102, 19-24.

Lee, Y., Kim, M., Han, J., Yeom, K.H., Lee, S., Baek, S.H., and Kim, V.N. 2004. MicroRNA genes are transcribed by RNA polymerase II. *EMBO J.* 23, 4051-4060.

Li, W., Jin, X., Zhang, Q., Zhang, G., Deng, X., and Ma, L. 2014. Decreased expression of miR-204 is associated with poor prognosis in patients with breast cancer. *Int.J.Clin.Exp.Pathol.* 7, 3287-3292.

Liu, B., Wu, X., Liu, B., Wang, C., Liu, Y., Zhou, Q., and Xu, K. 2012. MiR-26a enhances metastasis potential of lung cancer cells via AKT pathway by targeting PTEN. *Biochim.Biophys.Acta* 1822, 1692-1704.

Liu, J., Luo, X.J., Xiong, A.W., Zhang, Z.D., Yue, S., Zhu, M.S., and Cheng, S.Y. 2010. MicroRNA-214 promotes myogenic differentiation by facilitating exit from mitosis via down-regulation of proto-oncogene N-ras. *J.Biol.Chem.* 285, 26599-26607.

Liu, P., Kao, T.P., and Huang, H. 2008. CDK1 promotes cell proliferation and survival via phosphorylation and inhibition of FOXO1 transcription factor. *Oncogene* 27, 4733-4744.

Lu, J., Getz, G., Miska, E.A., Alvarez-Saavedra, E., Lamb, J., Peck, D., Sweet-Cordero, A., Ebert, B.L., Mak, R.H., Ferrando, A.A., Downing, J.R., Jacks, T., Horvitz, H.R., and Golub, T.R. 2005. MicroRNA expression profiles classify human cancers. *Nature* 435, 834-838.

Lui, W.O., Pourmand, N., Patterson, B.K., and Fire, A. 2007. Patterns of known and novel small RNAs in human cervical cancer. *Cancer Res.* 67, 6031-6043.

Ma, J., Li, N., Guarnera, M., and Jiang, F. 2013. Quantification of Plasma miRNAs by Digital PCR for Cancer Diagnosis. *Biomark Insights* 8, 127-136.

Ma, L., Deng, X., Wu, M., Zhang, G., and Huang, J. 2014. Down-regulation of miRNA-204 by LMP-1 enhances CDC42 activity and facilitates invasion of EBV-associated nasopharyngeal carcinoma cells. *FEBS Lett.* 588, 1562-1570.

Margue, C.M., Bernasconi, M., Barr, F.G., and Schafer, B.W. 2000. Transcriptional modulation of the anti-apoptotic protein BCL-XL by the paired box transcription factors PAX3 and PAX3/FKHR. *Oncogene* 19, 2921-2929.

Margulies, M., Egholm, M., Altman, W.E., Attiya, S., Bader, J.S., Bemben, L.A., Berka, J., Braverman, M.S., Chen, Y.J., Chen, Z., Dewell, S.B., Du, L., Fierro, J.M., Gomes, X.V., Godwin, B.C., He, W., Helgesen, S., Ho, C.H., Irzyk, G.P., Jando, S.C., Alenquer, M.L., Jarvie, T.P., Jirage, K.B., Kim, J.B., Knight, J.R., Lanza, J.R., Leamon, J.H., Lefkowitz, S.M., Lei, M., Li, J., Lohman, K.L., Lu, H., Makhijani, V.B., McDade, K.E., McKenna, M.P., Myers, E.W., Nickerson, E., Nobile, J.R., Plant, R., Puc, B.P., Ronan, M.T., Roth, G.T., Sarkis, G.J., Simons, J.F., Simpson, J.W., Srinivasan, M., Tartaro, K.R., Tomasz, A., Vogt, K.A., Volkmer, G.A., Wang, S.H., Wang, Y., Weiner, M.P., Yu, P., Begley, R.F., and Rothberg, J.M. 2005. Genome sequencing in microfabricated high-density picolitre reactors. *Nature* 437, 376-380.

Maurer, H.M., Gehan, E.A., Beltangady, M., Crist, W., Dickman, P.S., Donaldson, S.S., Fryer, C., Hammond, D., Hays, D.M., and Herrmann, J. 1993. The Intergroup Rhabdomyosarcoma Study-II. *Cancer* 71, 1904-1922.

Mayanil, C.S., George, D., Freilich, L., Miljan, E.J., Mania-Farnell, B., McLone, D.G., and Bremer, E.G. 2001. Microarray analysis detects novel Pax3 downstream target genes. *J.Biol.Chem.* 276, 49299-49309.

McCarthy, J.J. 2008. MicroRNA-206: the skeletal muscle-specific myomiR. *Biochim.Biophys.Acta* 1779, 682-691.

McKernan, K., Blanchard, A., Kotler, L., and Costa, G. 2011. Reagents, Methods, and Libraries for Bead-Based Sequencing.

McKinnell, I.W., Ishibashi, J., Le Grand, F., Punch, V.G., Addicks, G.C., Greenblatt, J.F., Dilworth, F.J., and Rudnicki, M.A. 2008. Pax7 activates myogenic genes by recruitment of a histone methyltransferase complex. *Nat.Cell Biol.* 10, 77-84.

Meng, F., Henson, R., Wehbe-Janek, H., Ghoshal, K., Jacob, S.T., and Patel, T. 2007. MicroRNA-21 regulates expression of the PTEN tumor suppressor gene in human hepatocellular cancer. *Gastroenterology* 133, 647-658.

Mercado, G.E., Xia, S.J., Zhang, C., Ahn, E.H., Gustafson, D.M., Lae, M., Ladanyi, M., and Barr, F.G. 2008. Identification of PAX3-FKHR-regulated genes

differentially expressed between alveolar and embryonal rhabdomyosarcoma: focus on MYCN as a biologically relevant target. *Genes Chromosomes Cancer* 47, 510-520.

Metzler, M., Wilda, M., Busch, K., Viehmann, S., and Borkhardt, A. 2004. High expression of precursor microRNA-155/BIC RNA in children with Burkitt lymphoma. *Genes Chromosomes Cancer* 39, 167-169.

Missiaglia, E., Shepherd, C.J., Patel, S., Thway, K., Pierron, G., Pritchard-Jones, K., Renard, M., Sciot, R., Rao, P., Oberlin, O., Delattre, O., and Shipley, J. 2010. MicroRNA-206 expression levels correlate with clinical behaviour of rhabdomyosarcomas. *Br.J.Cancer* 102, 1769-1777.

Mott, J.L., Kobayashi, S., Bronk, S.F., and Gores, G.J. 2007. mir-29 regulates Mcl-1 protein expression and apoptosis. *Oncogene* 26, 6133-6140.

Muller, S., and Nowak, K. 2014. Exploring the miRNA-mRNA regulatory network in clear cell renal cell carcinomas by next-generation sequencing expression profiles. *Biomed.Res.Int.* 2014, 948408.

Munari, E., Marchionni, L., Chitre, A., Hayashi, M., Martignoni, G., Brunelli, M., Gobbo, S., Argani, P., Allaf, M., Hoque, M.O., and Netto, G.J. 2014. Clear cell papillary renal cell carcinoma: micro-RNA expression profiling and comparison with clear cell renal cell carcinoma and papillary renal cell carcinoma. *Hum.Pathol.* 45, 1130-1138.

Nabarro, S., Himoudi, N., Papanastasiou, A., Gilmour, K., Gibson, S., Sebire, N., Thrasher, A., Blundell, M.P., Hubank, M., Canderan, G., and Anderson, J. 2005. Coordinated oncogenic transformation and inhibition of host immune responses by the PAX3-FKHR fusion oncoprotein. *J.Exp.Med.* 202, 1399-1410.

Naguibneva, I., Ameyar-Zazoua, M., Polesskaya, A., Ait-Si-Ali, S., Groisman, R., Souidi, M., Cuvellier, S., and Harel-Bellan, A. 2006. The microRNA miR-181 targets the homeobox protein Hox-A11 during mammalian myoblast differentiation. *Nat.Cell Biol.* 8, 278-284.

Nakae, J., Kitamura, T., Kitamura, Y., Biggs, W.H.,3rd, Arden, K.C., and Accili, D. 2003. The forkhead transcription factor Foxo1 regulates adipocyte differentiation. *Dev.Cell.* 4, 119-129.

Nakamura, T., Canaani, E., and Croce, C.M. 2007. Oncogenic All1 fusion proteins target Drosha-mediated microRNA processing. *Proc.Natl.Acad.Sci.U.S.A.* 104, 10980-10985.

Napoli, C., Lemieux, C., and Jorgensen, R. 1990. Introduction of a Chimeric Chalcone Synthase Gene into Petunia Results in Reversible Co-Suppression of Homologous Genes in trans. *Plant Cell* 2, 279-289.

Nasarre, P., Gemmill, R.M., Potiron, V.A., Roche, J., Lu, X., Baron, A.E., Korch, C., Garrett-Mayer, E., Lagana, A., Howe, P.H., and Drabkin, H.A. 2013. Neuropilin-2 Is upregulated in lung cancer cells during TGF-beta1-induced epithelial-mesenchymal transition. *Cancer Res.* 73, 7111-7121.

Ng, P., Wei, C.L., Sung, W.K., Chiu, K.P., Lipovich, L., Ang, C.C., Gupta, S., Shahab, A., Ridwan, A., Wong, C.H., Liu, E.T., and Ruan, Y. 2005. Gene identification signature (GIS) analysis for transcriptome characterization and genome annotation. *Nat.Methods* 2, 105-111.

Nidadavolu, L.S., Niedernhofer, L.J., and Khan, S.A. 2013. Identification of microRNAs dysregulated in cellular senescence driven by endogenous genotoxic stress. *Aging (Albany NY)* 5, 460-473.

O'Rourke, J.R., Georges, S.A., Seay, H.R., Tapscott, S.J., McManus, M.T., Goldhamer, D.J., Swanson, M.S., and Harfe, B.D. 2007. Essential role for Dicer during skeletal muscle development. *Dev.Biol.* 311, 359-368.

Ota, A., Tagawa, H., Karnan, S., Tsuzuki, S., Karpas, A., Kira, S., Yoshida, Y., and Seto, M. 2004. Identification and characterization of a novel gene, C13orf25, as a target for 13q31-q32 amplification in malignant lymphoma. *Cancer Res.* 64, 3087-3095.

Ouyang, W., Liao, W., Luo, C.T., Yin, N., Huse, M., Kim, M.V., Peng, M., Chan, P., Ma, Q., Mo, Y., Meijer, D., Zhao, K., Rudensky, A.Y., Atwal, G., Zhang, M.Q., and Li, M.O. 2012. Novel Foxo1-dependent transcriptional programs control T(reg) cell function. *Nature* 491, 554-559.

Pallante, P., Visone, R., Ferracin, M., Ferraro, A., Berlingieri, M.T., Troncone, G., Chiappetta, G., Liu, C.G., Santoro, M., Negrini, M., Croce, C.M., and Fusco, A. 2006. MicroRNA deregulation in human thyroid papillary carcinomas. *Endocr.Relat.Cancer* 13, 497-508.

PALMER, C.G., WARREN, A.K., and SIMPSON, P.J. 1963. A Comparison of Cytologic Effects of Leurosine Methiodide and Vinblastine in the Tissue Culture. *Cancer Chemother.Rep.* 31, 1-2.

Pardini, B., Rosa, F., Barone, E., Di Gaetano, C., Slyskova, J., Novotny, J., Levy, M., Garritano, S., Vodickova, L., Buchler, T., Gemignani, F., Landi, S., Vodicka, P., and Naccarati, A. 2013. Variation within 3'-UTRs of base excision repair genes

and response to therapy in colorectal cancer patients: A potential modulation of microRNAs binding. *Clin.Cancer Res.* 19, 6044-6056.

Parham, D.M., Qualman, S.J., Teot, L., Barr, F.G., Morotti, R., Sorensen, P.H., Triche, T.J., Meyer, W.H., and Soft Tissue Sarcoma Committee of the Children's Oncology Group. 2007. Correlation between histology and PAX/FKHR fusion status in alveolar rhabdomyosarcoma: a report from the Children's Oncology Group. *Am.J.Surg.Pathol.* 31, 895-901.

Pastore, G., Peris-Bonet, R., Carli, M., Martinez-Garcia, C., Sanchez de Toledo, J., and Steliarova-Foucher, E. 2006. Childhood soft tissue sarcomas incidence and survival in European children (1978-1997): report from the Automated Childhood Cancer Information System project. *Eur.J.Cancer* 42, 2136-2149.

Paulino, A.C. 2004. Late effects of radiotherapy for pediatric extremity sarcomas. *Int.J.Radiat.Oncol.Biol.Phys.* 60, 265-274.

Paulino, A.C., Simon, J.H., Zhen, W., and Wen, B.C. 2000. Long-term effects in children treated with radiotherapy for head and neck rhabdomyosarcoma. *Int.J.Radiat.Oncol.Biol.Phys.* 48, 1489-1495.

Pekarsky, Y., Santanam, U., Cimmino, A., Palamarchuk, A., Efanov, A., Maximov, V., Volinia, S., Alder, H., Liu, C.G., Rassenti, L., Calin, G.A., Hagan, J.P., Kipps, T., and Croce, C.M. 2006. Tcl1 expression in chronic lymphocytic leukemia is regulated by miR-29 and miR-181. *Cancer Res.* 66, 11590-11593.

PHILIPS, F.S., SCHWARTZ, H.S., STERNBERG, S.S., and TAN, C.T. 1960. The toxicity of actinomycin D. *Ann.N.Y.Acad.Sci.* 89, 348-360.

Prevot, P.P., Augereau, C., Simion, A., Van den Steen, G., Dauguet, N., Lemaigre, F.P., and Jacquemin, P. 2013. Let-7b and miR-495 stimulate differentiation and prevent metaplasia of pancreatic acinar cells by repressing HNF6. *Gastroenterology* 145, 668-78.e3.

Punyko, J.A., Mertens, A.C., Baker, K.S., Ness, K.K., Robison, L.L., and Gurney, J.G. 2005. Long-term survival probabilities for childhood rhabdomyosarcoma. A population-based evaluation. *Cancer* 103, 1475-1483.

Qiu, Y.H., Wei, Y.P., Shen, N.J., Wang, Z.C., Kan, T., Yu, W.L., Yi, B., and Zhang, Y.J. 2013. miR-204 inhibits epithelial to mesenchymal transition by targeting slug in intrahepatic cholangiocarcinoma cells. *Cell.Physiol.Biochem.* 32, 1331-1341.

Raney, R.B., Anderson, J.R., Barr, F.G., Donaldson, S.S., Pappo, A.S., Qualman, S.J., Wiener, E.S., Maurer, H.M., and Crist, W.M. 2001. Rhabdomyosarcoma and undifferentiated sarcoma in the first two decades of life: a selective review of intergroup rhabdomyosarcoma study group experience and rationale for Intergroup Rhabdomyosarcoma Study V. *J.Pediatr.Hematol.Oncol.* 23, 215-220.

Raney, R.B., Anderson, J.R., Kollath, J., Vassilopoulou-Sellin, R., Klein, M.J., Heyn, R., Glicksman, A.S., Wharam, M., Crist, W.M., and Maurer, H.M. 2000. Late effects of therapy in 94 patients with localized rhabdomyosarcoma of the orbit: Report from the Intergroup Rhabdomyosarcoma Study (IRS)-III, 1984-1991. *Med.Pediatr.Oncol.* 34, 413-420.

Raney, R.B., Asmar, L., Vassilopoulou-Sellin, R., Klein, M.J., Donaldson, S.S., Green, J., Heyn, R., Wharam, M., Glicksman, A.S., Gehan, E.A., Anderson, J., and Maurer, H.M. 1999. Late complications of therapy in 213 children with localized, nonorbital soft-tissue sarcoma of the head and neck: A descriptive report from the Intergroup Rhabdomyosarcoma Studies (IRS)-II and - III. IRS Group of the Children's Cancer Group and the Pediatric Oncology Group. *Med.Pediatr.Oncol.* 33, 362-371.

Rao, P.K., Missiaglia, E., Shields, L., Hyde, G., Yuan, B., Shepherd, C.J., Shipley, J., and Lodish, H.F. 2010. Distinct roles for miR-1 and miR-133a in the proliferation and differentiation of rhabdomyosarcoma cells. *FASEB J.* 24, 3427-3437.

Raver-Shapira, N., Marciano, E., Meiri, E., Spector, Y., Rosenfeld, N., Moskovits, N., Bentwich, Z., and Oren, M. 2007. Transcriptional activation of miR-34a contributes to p53-mediated apoptosis. *Mol.Cell* 26, 731-743.

Rayner, K.J., Esau, C.C., Hussain, F.N., McDaniel, A.L., Marshall, S.M., van Gils, J.M., Ray, T.D., Sheedy, F.J., Goedeke, L., Liu, X., Khatsenko, O.G., Kaimal, V., Lees, C.J., Fernandez-Hernando, C., Fisher, E.A., Temel, R.E., and Moore, K.J. 2011. Inhibition of miR-33a/b in non-human primates raises plasma HDL and lowers VLDL triglycerides. *Nature* 478, 404-407.

Reichek, J.L., Duan, F., Smith, L.M., Gustafson, D.M., O'Connor, R.S., Zhang, C., Dunlevy, M.J., Gastier-Foster, J.M., and Barr, F.G. 2011. Genomic and clinical analysis of amplification of the 13q31 chromosomal region in alveolar rhabdomyosarcoma: a report from the Children's Oncology Group. *Clin.Cancer Res.* 17, 1463-1473.

Relaix, F., Polimeni, M., Rocancourt, D., Ponzetto, C., Schafer, B.W., and Buckingham, M. 2003. The transcriptional activator PAX3-FKHR rescues the defects of Pax3 mutant mice but induces a myogenic gain-of-function phenotype

with ligand-independent activation of Met signaling in vivo. *Genes Dev.* 17, 2950-2965.

Ren, H., Orozco, I.J., Su, Y., Suyama, S., Gutierrez-Juarez, R., Horvath, T.L., Wardlaw, S.L., Plum, L., Arancio, O., and Accili, D. 2012. FoxO1 target Gpr17 activates AgRP neurons to regulate food intake. *Cell* 149, 1314-1326.

Rena, G., Guo, S., Cichy, S.C., Unterman, T.G., and Cohen, P. 1999. Phosphorylation of the transcription factor forkhead family member FKHR by protein kinase B. *J.Biol.Chem.* 274, 17179-17183.

Rena, G., Prescott, A.R., Guo, S., Cohen, P., and Unterman, T.G. 2001. Roles of the forkhead in rhabdomyosarcoma (FKHR) phosphorylation sites in regulating 14-3-3 binding, transactivation and nuclear targetting. *Biochem.J.* 354, 605-612.

Ridgeway, A.G., and Skerjanc, I.S. 2001. Pax3 is essential for skeletal myogenesis and the expression of Six1 and Eya2. *J.Biol.Chem.* 276, 19033-19039.

Ries, L.A.G., Percy, C.L., and Bunin, G.R. 1999a. Introduction, 1. *In* Ries, L.A.G., Smith, M.A., Gurney, J.G., Linet, M., Tamra, T., Young, J.L., and Bunin, G.R. eds., *Cancer Incidence and Survival among Children and Adolescents: United States SEER Program 1975-1995*. National Cancer Institute, SEER Program, Bethesda, MD.

Ries, L.A.G., Smith, M.A., Gurney, J.G., Linet, M., Tamra, T., Young, J.L., and Bunin, G.R. 1999b. *Cancer Incidence and Survival among Children and Adolescents: United States SEER Program 1975-1995*. 99-4649.

Rodriguez, A., Griffiths-Jones, S., Ashurst, J.L., and Bradley, A. 2004. Identification of mammalian microRNA host genes and transcription units. *Genome Res.* 14, 1902-1910.

Roeb, W., Boyer, A., Cavenee, W.K., and Arden, K.C. 2007. PAX3-FOXO1 controls expression of the p57Kip2 cell-cycle regulator through degradation of EGR1. *Proc.Natl.Acad.Sci.U.S.A.* 104, 18085-18090.

Ronaghi, M., Karamohamed, S., Pettersson, B., Uhlen, M., and Nyren, P. 1996. Real-time DNA sequencing using detection of pyrophosphate release. *Anal.Biochem.* 242, 84-89.

Sandhu, R., Rein, J., D'Arcy, M., Herschkowitz, J.I., Hoadley, K.A., and Troester, M.A. 2014. Over-expression of miR-146a in basal-like breast cancer cells confers enhanced tumorigenic potential in association with altered p53 status. *Carcinogenesis*.

Santoro, I.M., Yi, T.M., and Walsh, K. 1991. Identification of single-stranded-DNA-binding proteins that interact with muscle gene elements. *Mol.Cell.Biol.* 11, 1944-1953.

Sarver, A.L., Li, L., and Subramanian, S. 2010. MicroRNA miR-183 functions as an oncogene by targeting the transcription factor EGR1 and promoting tumor cell migration. *Cancer Res.* 70, 9570-9580.

Scheidler, S., Fredericks, W.J., Rauscher, F.J.,3rd, Barr, F.G., and Vogt, P.K. 1996. The hybrid PAX3-FKHR fusion protein of alveolar rhabdomyosarcoma transforms fibroblasts in culture. *Proc.Natl.Acad.Sci.U.S.A.* 93, 9805-9809.

Schwarz, D.S., Hutvagner, G., Du, T., Xu, Z., Aronin, N., and Zamore, P.D. 2003. Asymmetry in the assembly of the RNAi enzyme complex. *Cell* 115, 199-208.

Scrable, H.J., Witte, D.P., Lampkin, B.C., and Cavenee, W.K. 1987. Chromosomal localization of the human rhabdomyosarcoma locus by mitotic recombination mapping. *Nature* 329, 645-647.

Shapiro, D.N., Sublett, J.E., Li, B., Downing, J.R., and Naeve, C.W. 1993. Fusion of PAX3 to a member of the forkhead family of transcription factors in human alveolar rhabdomyosarcoma. *Cancer Res.* 53, 5108-5112.

Shell, S., Park, S.M., Radjabi, A.R., Schickel, R., Kistner, E.O., Jewell, D.A., Feig, C., Lengyel, E., and Peter, M.E. 2007. Let-7 expression defines two differentiation stages of cancer. *Proc.Natl.Acad.Sci.U.S.A.* 104, 11400-11405.

Shendure, ,Jay, and Ji, ,Hanlee. Next-generation DNA sequencing.

Shendure, J., Porreca, G.J., Reppas, N.B., Lin, X., McCutcheon, J.P., Rosenbaum, A.M., Wang, M.D., Zhang, K., Mitra, R.D., and Church, G.M. 2005. Accurate multiplex polony sequencing of an evolved bacterial genome. *Science* 309, 1728-1732.

Smith, A.C., Squire, J.A., Thorner, P., Zielenska, M., Shuman, C., Grant, R., Chitayat, D., Nishikawa, J.L., and Weksberg, R. 2001. Association of alveolar rhabdomyosarcoma with the Beckwith-Wiedemann syndrome. *Pediatr.Dev.Pathol.* 4, 550-558.

Solnica-Krezel, L., and Sepich, D.S. 2012. Gastrulation: making and shaping germ layers. *Annu.Rev.Cell Dev.Biol.* 28, 687-717.

Sorensen, P.H., Lynch, J.C., Qualman, S.J., Tirabosco, R., Lim, J.F., Maurer, H.M., Bridge, J.A., Crist, W.M., Triche, T.J., and Barr, F.G. 2002. PAX3-FKHR and

PAX7-FKHR gene fusions are prognostic indicators in alveolar rhabdomyosarcoma: a report from the children's oncology group. *J.Clin.Oncol.* 20, 2672-2679.

Spunt, S.L., Sweeney, T.A., Hudson, M.M., Billups, C.A., Krasin, M.J., and Hester, A.L. 2005. Late effects of pelvic rhabdomyosarcoma and its treatment in female survivors. *J.Clin.Oncol.* 23, 7143-7151.

Sudour, H., Chastagner, P., Claude, L., Desandes, E., Klein, M., Carrie, C., and Bernier, V. 2010. Fertility and pregnancy outcome after abdominal irradiation that included or excluded the pelvis in childhood tumor survivors. *Int.J.Radiat.Oncol.Biol.Phys.* 76, 867-873.

Sultan, I., Qaddoumi, I., Yaser, S., Rodriguez-Galindo, C., and Ferrari, A. 2009. Comparing adult and pediatric rhabdomyosarcoma in the surveillance, epidemiology and end results program, 1973 to 2005: an analysis of 2,600 patients. *J.Clin.Oncol.* 27, 3391-3397.

Sun, Q., Zhang, Y., Yang, G., Chen, X., Zhang, Y., Cao, G., Wang, J., Sun, Y., Zhang, P., Fan, M., Shao, N., and Yang, X. 2008. Transforming growth factor-beta-regulated miR-24 promotes skeletal muscle differentiation. *Nucleic Acids Res.* 36, 2690-2699.

Sun, Y., Ge, Y., Drnevich, J., Zhao, Y., Band, M., and Chen, J. 2010. Mammalian target of rapamycin regulates miRNA-1 and follistatin in skeletal myogenesis. *J.Cell Biol.* 189, 1157-1169.

Sun, Y., Wu, J., Wu, S.H., Thakur, A., Bollig, A., Huang, Y., and Liao, D.J. 2009. Expression profile of microRNAs in c-Myc induced mouse mammary tumors. *Breast Cancer Res.Treat.* 118, 185-196.

Suspitsin, E.N., Kashyap, A., Shelekhova, K.V., Sokolenko, A.P., Kuligina, E.S., Iyevleva, A.G., Kornilov, A.V., Ehemann, V., Yanus, G.A., Aleksakhina, S.N., Preobrazhenskaya, E.V., Zaitseva, O.A., Yatsuk, O.S., Klimashevsky, V.F., Togo, A.V., and Imyanitov, E.N. 2013. Evidence for angiogenesis-independent contribution of VEGFR1 (FLT1) in gastric cancer recurrence. *Med.Oncol.* 30, 644-013-0644-2. Epub 2013 Jun 26.

Sutow, W.W., Sullivan, M.P., Ried, H.L., Taylor, H.G., and Griffith, K.M. 1970. Prognosis in childhood rhabdomyosarcoma. *Cancer* 25, 1384-1390.

Tajbakhsh, S., Rocancourt, D., Cossu, G., and Buckingham, M. 1997. Redefining the genetic hierarchies controlling skeletal myogenesis: Pax-3 and Myf-5 act upstream of MyoD. *Cell* 89, 127-138.

Taulli, R., Bersani, F., Foglizzo, V., Linari, A., Vigna, E., Ladanyi, M., Tuschl, T., and Ponzetto, C. 2009. The muscle-specific microRNA miR-206 blocks human rhabdomyosarcoma growth in xenotransplanted mice by promoting myogenic differentiation. *J.Clin.Invest.* 119, 2366-2378.

Teferedegne, B., Macauley, J., Foseh, G., Dragunsky, E., Chumakov, K., Murata, H., Peden, K., and Lewis, A.M.,Jr. 2014. MicroRNAs as potential biomarkers for VERO cell tumorigenicity. *Vaccine.*

Teixeira, C.C., Liu, Y., Thant, L.M., Pang, J., Palmer, G., and Alikhani, M. 2010. Foxo1, a novel regulator of osteoblast differentiation and skeletogenesis. *J.Biol.Chem.* 285, 31055-31065.

Tomari, Y., Du, T., Haley, B., Schwarz, D.S., Bennett, R., Cook, H.A., Koppetsch, B.S., Theurkauf, W.E., and Zamore, P.D. 2004. RISC assembly defects in the Drosophila RNAi mutant armitage. *Cell* 116, 831-841.

Tomizawa, J., and Itoh, T. 1981. Plasmid ColE1 incompatibility determined by interaction of RNA I with primer transcript. *Proc.Natl.Acad.Sci.U.S.A.* 78, 6096-6100.

Tothova, Z., Kollipara, R., Huntly, B.J., Lee, B.H., Castrillon, D.H., Cullen, D.E., McDowell, E.P., Lazo-Kallanian, S., Williams, I.R., Sears, C., Armstrong, S.A., Passegue, E., DePinho, R.A., and Gilliland, D.G. 2007. FoxOs are critical mediators of hematopoietic stem cell resistance to physiologic oxidative stress. *Cell* 128, 325-339.

Trang, P., Wiggins, J.F., Daige, C.L., Cho, C., Omotola, M., Brown, D., Weidhaas, J.B., Bader, A.G., and Slack, F.J. 2011. Systemic delivery of tumor suppressor microRNA mimics using a neutral lipid emulsion inhibits lung tumors in mice. *Mol.Ther.* 19, 1116-1122.

Turcatti, G., Romieu, A., Fedurco, M., and Tairi, A.P. 2008. A new class of cleavable fluorescent nucleotides: synthesis and optimization as reversible terminators for DNA sequencing by synthesis. *Nucleic Acids Res.* 36, e25.

Ueda, T., Volinia, S., Okumura, H., Shimizu, M., Taccioli, C., Rossi, S., Alder, H., Liu, C.G., Oue, N., Yasui, W., Yoshida, K., Sasaki, H., Nomura, S., Seto, Y., Kaminishi, M., Calin, G.A., and Croce, C.M. 2010. Relation between microRNA expression and progression and prognosis of gastric cancer: a microRNA expression analysis. *Lancet Oncol.* 11, 136-146.

van Dalen, E.C., van der Pal, H.J., Kok, W.E., Caron, H.N., and Kremer, L.C. 2006. Clinical heart failure in a cohort of children treated with anthracyclines: a long-term follow-up study. *Eur.J.Cancer* 42, 3191-3198.

Venturini, L., Battmer, K., Castoldi, M., Schultheis, B., Hochhaus, A., Muckenthaler, M.U., Ganser, A., Eder, M., and Scherr, M. 2007. Expression of the miR-17-92 polycistron in chronic myeloid leukemia (CML) CD34+ cells. *Blood* 109, 4399-4405.

Volinia, S., Calin, G.A., Liu, C.G., Ambs, S., Cimmino, A., Petrocca, F., Visone, R., Iorio, M., Roldo, C., Ferracin, M., Prueitt, R.L., Yanaihara, N., Lanza, G., Scarpa, A., Vecchione, A., Negrini, M., Harris, C.C., and Croce, C.M. 2006. A microRNA expression signature of human solid tumors defines cancer gene targets. *Proc.Natl.Acad.Sci.U.S.A.* 103, 2257-2261.

Wachtel, M., Runge, T., Leuschner, I., Stegmaier, S., Koscielniak, E., Treuner, J., Odermatt, B., Behnke, S., Niggli, F.K., and Schafer, B.W. 2006. Subtype and prognostic classification of rhabdomyosarcoma by immunohistochemistry. *J.Clin.Oncol.* 24, 816-822.

Walters, Z.S., Villarejo-Balcells, B., Olmos, D., Buist, T.W., Missiaglia, E., Allen, R., Al-Lazikani, B., Garrett, M.D., Blagg, J., and Shipley, J. 2014. JARID2 is a direct target of the PAX3-FOXO1 fusion protein and inhibits myogenic differentiation of rhabdomyosarcoma cells. *Oncogene* 33, 1148-1157.

Wang, H., Garzon, R., Sun, H., Ladner, K.J., Singh, R., Dahlman, J., Cheng, A., Hall, B.M., Qualman, S.J., Chandler, D.S., Croce, C.M., and Guttridge, D.C. 2008. NF-kappaB-YY1-miR-29 regulatory circuitry in skeletal myogenesis and rhabdomyosarcoma. *Cancer.Cell.* 14, 369-381.

Wang, H., Hertlein, E., Bakkar, N., Sun, H., Acharyya, S., Wang, J., Carathers, M., Davuluri, R., and Guttridge, D.C. 2007. NF-kappaB regulation of YY1 inhibits skeletal myogenesis through transcriptional silencing of myofibrillar genes. *Mol.Cell.Biol.* 27, 4374-4387.

Wang, L., Chen, X., Zheng, Y., Li, F., Lu, Z., Chen, C., Liu, J., Wang, Y., Peng, Y., Shen, Z., Gao, J., Zhu, M., and Chen, H. 2012. MiR-23a inhibits myogenic differentiation through down regulation of fast myosin heavy chain isoforms. *Exp.Cell Res.* 318, 2324-2334.

Wang, Q., Wang, Y., Minto, A.W., Wang, J., Shi, Q., Li, X., and Quigg, R.J. 2008a. MicroRNA-377 is up-regulated and can lead to increased fibronectin production in diabetic nephropathy. *FASEB J.* 22, 4126-4135.

Wang, X., Tang, S., Le, S.Y., Lu, R., Rader, J.S., Meyers, C., and Zheng, Z.M. 2008b. Aberrant expression of oncogenic and tumor-suppressive microRNAs in cervical cancer is required for cancer cell growth. *PLoS One* 3, e2557.

Wei, J.S., Johansson, P., Chen, Q.R., Song, Y.K., Durinck, S., Wen, X., Cheuk, A.T., Smith, M.A., Houghton, P., Morton, C., and Khan, J. 2009. microRNA Profiling Identifies Cancer-Specific and Prognostic Signatures in Pediatric Malignancies. *Clin.Cancer Res.*

Wiggan, O., Fadel, M.P., and Hamel, P.A. 2002. Pax3 induces cell aggregation and regulates phenotypic mesenchymal-epithelial interconversion. *J.Cell.Sci.* 115, 517-529.

Wong, C.F., and Tellam, R.L. 2008. MicroRNA-26a targets the histone methyltransferase Enhancer of Zeste homolog 2 during myogenesis. *J.Biol.Chem.* 283, 9836-9843.

Xu, Y., Ohms, S.J., Li, Z., Wang, Q., Gong, G., Hu, Y., Mao, Z., Shannon, M.F., and Fan, J.Y. 2013. Changes in the expression of miR-381 and miR-495 are inversely associated with the expression of the MDR1 gene and development of multi-drug resistance. *PLoS One* 8, e82062.

Yan, D., Dong Xda, E., Chen, X., Wang, L., Lu, C., Wang, J., Qu, J., and Tu, L. 2009. MicroRNA-1/206 targets c-Met and inhibits rhabdomyosarcoma development. *J.Biol.Chem.* 284, 29596-29604.

Yan, L.X., Huang, X.F., Shao, Q., Huang, M.Y., Deng, L., Wu, Q.L., Zeng, Y.X., and Shao, J.Y. 2008. MicroRNA miR-21 overexpression in human breast cancer is associated with advanced clinical stage, lymph node metastasis and patient poor prognosis. *RNA* 14, 2348-2360.

Yanaihara, N., Caplen, N., Bowman, E., Seike, M., Kumamoto, K., Yi, M., Stephens, R.M., Okamoto, A., Yokota, J., Tanaka, T., Calin, G.A., Liu, C.G., Croce, C.M., and Harris, C.C. 2006. Unique microRNA molecular profiles in lung cancer diagnosis and prognosis. *Cancer.Cell.* 9, 189-198.

Yang, H., Cho, M.E., Li, T.W., Peng, H., Ko, K.S., Mato, J.M., and Lu, S.C. 2013. MicroRNAs regulate methionine adenosyltransferase 1A expression in hepatocellular carcinoma. *J.Clin.Invest.* 123, 285-298.

Yi, R., Qin, Y., Macara, I.G., and Cullen, B.R. 2003. Exportin-5 mediates the nuclear export of pre-microRNAs and short hairpin RNAs. *Genes Dev.* 17, 3011-3016.

Yuan, H., Qin, F., Movassagh, M., Park, H., Golden, W., Xie, Z., Zhang, P., Sklar, J., and Li, H. 2013. A chimeric RNA characteristic of rhabdomyosarcoma in normal myogenesis process. *Cancer.Discov.* 3, 1394-1403.

Zhan, S., Shapiro, D.N., and Helman, L.J. 1994. Activation of an imprinted allele of the insulin-like growth factor II gene implicated in rhabdomyosarcoma. *J.Clin.Invest.* 94, 445-448.

Zhang, J.B., Zhu, X.N., Cui, J., Chen, P., Wang, S.M., and Wang, J.S. 2012. Differential expressions of microRNA between young and senescent endothelial cells. *Zhonghua Yi Xue Za Zhi* 92, 2205-2209.

Zhang, L., Wang, X., and Chen, P. 2013. MiR-204 down regulates SIRT1 and reverts SIRT1-induced epithelial-mesenchymal transition, anoikis resistance and invasion in gastric cancer cells. *BMC Cancer* 13, 290-2407-13-290.

Zhang, X., Yalcin, S., Lee, D.F., Yeh, T.Y., Lee, S.M., Su, J., Mungamuri, S.K., Rimmele, P., Kennedy, M., Sellers, R., Landthaler, M., Tuschl, T., Chi, N.W., Lemischka, I., Keller, G., and Ghaffari, S. 2011. FOXO1 is an essential regulator of pluripotency in human embryonic stem cells. *Nat.Cell Biol.* 13, 1092-1099.

Zhou, X., Li, L., Su, J., and Zhang, G. 2014. Decreased miR-204 in H. pylori-associated gastric cancer promotes cancer cell proliferation and invasion by targeting SOX4. *PLoS One* 9, e101457.

Zhu, S., Si, M.L., Wu, H., and Mo, Y.Y. 2007. MicroRNA-21 targets the tumor suppressor gene tropomyosin 1 (TPM1). *J.Biol.Chem.* 282, 14328-14336.